Advanced Mesoporous Particles for Colon-targeted Delivery: Insights into Enhanced Delivery of Proteolysis-targeting Chimeras

Shouq J H H Sh Alshatti

Doctor of Philosophy

Aston University

March 2025

Aston University

Advanced Mesoporous Particles for Colon-targeted Delivery: Insights into Enhanced Delivery of Proteolysis-targeting Chimeras

Shouq J H H Sh Alshatti
Doctor of Philosophy
March 2025

Thesis Abstract

Proteolysis-targeting Chimeras (PROTACs) are revolutionary molecules that induce target protein degradation and, therefore, are suited for intractable drug targets. However, they challenge traditional delivery methods for small molecules via the oral route due to their complex physiochemical properties. Delivery using mesoporous carriers emerge as an advanced strategy that could address PROTACs challenges and aid their delivery to target sites. The colon is one such site with promise for oral delivery of these molecules due to low degradative capacity and efflux compared to other regions. This thesis aims to engineer a novel mesoporous carrier to enhance the delivery of small and mid-sized molecules to the colon. The work investigated the effects of different atomisation nozzles and process parameters on physical properties of the novel carrier. This was followed by assessment of its ability to accommodate complex molecules like PROTACs and loading characterisation. Finally, colonic targeting of loaded carrier with different molecules was investigated.

Optimising atomisation and spray drying parameters led to carrier particles which retained their porosity and solubility-enhancing function but acquired spherical, non-deflated morphology with uniform size distribution. The poorly soluble model PROTAC, MZ1, was loaded into the engineered carrier leading to significant dissolution enhancement. However, imaging techniques revealed the loaded drug was mainly located within the larger pores near the periphery of the carrier, possibly due to difficulty to diffuse deeper. The carrier was also tested for its targeted colonic release using a capping material incorporated within Felodipine-loaded and MZ1-loaded formulations, respectively. *In vitro* dissolution tests in simulated media demonstrated selective colonic release upon exposure to colonic enzymes. This work demonstrated the capability of mesoporous carriers to improve the dissolution profile and simultaneously deliver drugs, like PROTACs, into colonic environment where absorption could occur. The work paves the way for translation of challenging molecules into oral dosage forms.

Keywords: mesoporous particles, atomisation, PROTAC, MZ1, colon-targeted delivery, colon-specific

Acknowledgements

With immense gratitude, I begin with praising God, the almighty, whose mercy and infinite grace has surrounded us throughout the toughest times of this journey.

I would like to express my deepest gratitude to my supervisors, Dr. Ali Al-Khattawi and Dr. Daniel Kirby, for their valuable insights and continuous guidance. To all the hours spent in sharing your knowledge and all the times you welcomed me when I reached out with questions and doubts, I would like to express my greatest appreciation, as this did not only help me navigate through this journey but also boosted my confidence in approaching challenges.

I would also like to sincerely thank National Physical Laboratory for their collaboration in conducting Raman spectroscopy analysis.

To my greatest blessing in this life, my husband and daughter: Thank you for your patience and boundless support over the past four years. Thank you for being around and for being my emotional support team. Dalal– I hope that one day, when you reflect back on this journey, you realise how you contributed to the ease that came with this hardship. Dr. Saleh– you have witnessed my everyday crisis, endless hours of theoretical explanations, and perhaps been my personal research assistant, and for that, you are immensely thanked.

I thankfully acknowledge the assistance and helpful advice provided by all my colleagues in MB328, particularly: Abdulkhaliq, Kyprianos, Shital, Rhys, Amr, Mohammad, Marwah, and Tatiana.

I am sincerely grateful to my friends, Lulu, Wafa, Mona, Ameena, Fatima, Jehney, and Ohood, who made this city home, far away from home. Thank you for your continuous support. I am thankful for all our gatherings, coffee runs, and the moments we spent comforting each other and sharing our journeys. I cannot underestimate how these little breaks had kept me going through the very difficult times.

Last but not least, I am forever indebted to my parents, siblings (Hamad, Nouf, and Ghala), family, family-in-law, and friends (Monya, Shareefa, Shaima, and Fatima) for their profound belief in my abilities and for keeping me in their prayers. My parents and siblings, in particular, are to be deeply appreciated for their endless sacrifice and care offered to both, my daughter and I. I am truly thankful for the support and encouragement that they offered. Special thanks go to my mother-in-law, may her soul rest in peace, who had always been proud of my success and was eager to witness the completion of this degree but is, unfortunately, no longer with us today. Her encouragement, love, and warmth had always been inspirational and provided a sense of security and strength.

Table of Contents

[Entire chapter text and table of contents headings redacted from open access version]

Abbreviations List

˚C	Degree Celsius
ASA	Aminosalicylic acid
API	Active pharmaceutical ingredient
ASDs	Amorphous solid dispersions
BET	Bromodomain and extra-terminal
BET	Brunauer–Emmett–Teller
BJH	Barrett–Joyner–Halenda
BRD4	Bromodomain containing protein 4
BSA	Bovine serum albumin
CAB	Cellulose acetate butyrate
cc	Cubic centimetre
cm	Centimetre
CRBN	Cereblon
Da	Daltons
DCAF15	CUL4 associated factor 15
DDB1	DNA damage binding protein 1
DNA	Deoxyribonucleic acid
DSC	Differential scanning calorimetry
F-PEI	Fluorinated polyethyleneimine
g	Gram
GIT	Gastrointestinal
GRAS	Generally recognised s safe
HMP	High methoxy pectin
HPLC	High performance liquid chromatography
HPMC	Hydroxypropylmethylcelluose
HPMCAS	Hydroxypropyl methylcellulose acetate succinate
hr	Hour
IAP	Inhibitor of apoptosis
IBD	Irritable bowel disease
ICH	International Conference on Harmonization
K	Kelvin
KEAP1	Kelch-like ECH-associated protein-1
kHz	Kilohertz
kV	Kilo Volts
L	Litres
LOD	Limit of detection
Log P	Logarithm of the partition coefficient
Log S	10 based logarithm of solubility
LOQ	Limit of quantification
m	Metres
M	Molar
m²	Cubic metre
m3	Cubic metre
mA	Milliampere
MDM2	Mouse double minute 2 homologue
MESOPAC	CAB mesoporous particles
mg	Milligram
MHz	Megahertz
Min	minutes
mL	Millilitre
mm	Millimetre

mol	Moles
MSN	Mesoporous silica nanoparticles
mV.s	Millivolt-seconds
N	Normality
NF	National formulary
nm	Nanometre
P-gp	P-glycoprotein
P/P0	Pressure over saturation pressure
Pa.s	Pascal-second
PAA	Polyacrylic acid
Pe	Péclet number
PEG	Polyethylene glycol
PLGA	Polylactide-co-glycolide
PROTACs	Proteolysis-targeting chimeras
PTEN	Phosphatase and tensin homolog
R2	Correlation coefficient
RNA	Ribonucleic acid
Ro5	Lipinski's rule of 5
RSD	Relative standard deviation
s	Seconds
SD	Standard deviation
SEM	Scanning electron microscopy
SiRNA	Small interfering RNA
SLS	Sodium lauryl sulfate
SMIs	Small molecule inhibitors
SRS	Stimulated Raman scattering
Tg	Glass transition
U/mL	Units per millilitre
UK	United Kingdom
UPS	Ubiquitin-proteasome system
USP	United States Pharmacopeia
UV	Ultraviolet
VHL	Von Hippel-Lindau
VMD	Volume mean diameter
W	Watts
w/v	Weight per volume
w/w	Weight per weight
XRD	X-ray diffraction
µg	Micrograms
µL	Micro litre
µm	Micro metre

List of Figures

Figure 2.8. *[redacted]*

Figure 2.9. *[redacted]*

Figure 2.10. *[redacted]*

Figure 2.11. *[redacted]*

Figure 2.12. *[redacted]*

Figure 2.13. *[redacted]*

Figure 2.14. *[redacted]*

Figure 2.15. *[redacted]*

Figure 2.16. *[redacted]*

Figure 2.17. *[redacted]*

Figure 2.18. *[redacted]*

Figure 2.19. *[redacted]*

Figure 2.20. *[redacted]*

Figure 2.21. *[redacted]*

Figure 2.22. *[redacted]*

Figure 2.23. *[redacted]*

Figure 2.24. *[redacted]*

Figure 2.25. *[redacted]*

List of Tables

Chapter 1

Introduction

Recent scientific breakthroughs have revealed a deep understanding of the molecular mechanisms driving a number of diseases. This has motivated scientists to explore and modulate the molecular targets with enhanced precision, reshaping the field of targeted therapy (Martín-Acosta & Xiao, 2021). The discovery of new therapeutic modalities has, thus, been the focus of the pharmaceutical industry, but, despite these advancements, its progress is impeded by intractable molecular targets that cannot be tackled by traditional small molecules. Unfortunately, only 20% of pathogenic protein targets have been identified as being effectively targeted by pharmaceutical agents (Sun et al., 2019). The remaining majority are classified as “undruggable” by conventional therapies.

Accordingly, the scientific community and pharmaceutical industry have shifted their focus from developing and modifying small molecules to genuinely discovering new targeted therapies. This comes with the fact that the pipeline of developing small molecules has entered a bottleneck stage with escalating barriers, such as evolving resistance, toxicity, and reduced activity against drug targets (Liang et al., 2020).

To overcome the challenges posed by small molecule therapeutics, proteolysis-targeting chimeras (PROTACs) have emerged with promising potential to induce degradation of targets that were previously thought to be unreachable. PROTACs are considered bifunctional, mid-sized molecules that bring together a disease-causing protein and an E3 ligase. This close interaction forms a ternary complex that initiates protein degradation by activating the cell’s proteasome system (Békés et al., 2022). In fact, their discovery has led to the recognition of new drug targets, particularly in oncology (Yan et al., 2024). Unlike small molecules which merely inhibit protein function, PROTACs trigger the degradation of disease-driving targets by using the body’s inherent protein clearance machinery, providing an opportunity to modulate a wide array of targets and minimise drug resistance (Sun et al., 2019; Wang et al., 2023). However, PROTACs do not contribute to the evolving field of drug development without being accompanied by challenges. Their structural complexity places them in a chemical space beyond the rule of five, which affects their physiochemical and pharmacokinetic properties (Madan et al., 2022; Pike et al., 2020). In general, poor water solubility and reduced cell permeability of PROTACs that lead to low oral bioavailability represent the greatest obstacle to their fast clinical translation (Moon et al., 2023). This indeed creates a burden on the pharmaceutical industry to design innovate technologies to overcome these hurdles. The demand of the current era lies in the need for formulation strategies that can encompass the complexity of these molecules while addressing their delivery challenges.

Scientific research does not thoroughly discuss the delivery strategies of PROTACs. The field, thus, remains relatively unexplored, with very scarce literature body approaching this concept. Early insights into the delivery strategies adopted to improve the physiochemical properties,

particularly solubility of PROTACs, mainly revolved around traditional formulation designs, such as amorphous solid dispersions (ASDs).

Four key contributions to enhance the solubility of model PROTACs using ASDs were reported in literature, advancing our understanding from a formulation design perspective. Studies by Pöstges and colleagues (2023), Hofmann and co-workers (2024), Mareczek et al. (2024), and Zhang et al. (2025a) reinforced the dissolution enhancement function of ASDs beyond small molecules to include PROTACs. Whether the PROTACs were crystalline or amorphous in binary or ternary ASDs, enhanced dissolution performances compared to raw forms were noticed. Different mechanisms contributed to these observations such as improved wettability, supersaturation and molecular interactions that stabilise the amorphous forms, and formation of reservoirs. Altogether, these findings indicate that with several preparation methods and proper polymer selection, ASDs can successfully accommodate PROTACs with different E3 ligase recruiting capacities (Hofmann et al., 2024; Mareczek et al., 2024; Pöstges et al., 2023; Zhang et al., 2025a).

Another conventional strategy employed to enhance the pharmacokinetic performance of PROTACs was lipid-based systems (Gong et al., 2024a; Saraswat et al., 2024). It is noteworthy to mention that traditional delivery formulations, such as amorphous solid dispersions, are at risk of losing their stability and homogeneity (Al-Japairai et al., 2023). The thermodynamic advantage that is imparted by solid dispersions can be compromised by the tendency of amorphous drugs to recrystallise (Al-Japairai et al., 2023). Stability upon storage is another issue associated with ASDs that concerns the industry, with phase separation representing one form of storage instability (Meere et al., 2019). Consequently, limitations related to drug loading come into play, with increased tendency to lose stability upon high drug loadings (Anane-Adjei et al., 2022). Scalability of ASDs to large-scale productions is another concern (He & Ho, 2015). Although traditional ASDs gained prominent recognition in literature and demonstrated robust solubility enhancement of conventional and innovative molecules, the identified limitations call for an improved alternative and more complex delivery system to meet the rapidly evolving field of drug development. Mesoporous particles, thus, stand out as advanced and refined forms of ASDs (Le, 2021), while still retaining the solubility enhancement effect. The fundamental distinguishing factor between the two is the amorphisation strategy (Schittny et al., 2020; Zhang et al., 2022a). With mesoporous particles, stabilisation of the amorphous form is achieved through confinement within pores, whose nanoscale prevents recrystallisation (Zhang et al., 2022a). The superiority of amorphous formulations based on mesoporous silica over solid dispersions in terms of enhanced stability and dissolution performance was demonstrated in literature (Zhang et al., 2022a).

Several techniques have been employed to engineer the structure of ASDs and mesoporous particles, with spray drying being a cornerstone for both strategies. Scalability and fine tuning

of the properties of the produced particles make spray drying an appealing method for particle engineering (Wang et al., 2021). These advantages become even more pronounced when ultrasonic atomisation is employed in spray drying. Particle size and uniformity can be carefully controlled, for example, with ultrasonic atomisation, whose fine mist and droplet formation mechanism account for better product and process outcomes (Khaire & Gogate, 2020). Thus, spray drying via ultrasonic atomisation is considered a viable technique to generate and optimise mesoporous particles.

The clinical implementation of this novel delivery technology that combines PROTAC molecules with ultrasonic-assisted spray drying to generate polymeric mesoporous particles becomes essential to validate its therapeutic potential in addressing the gap between laboratory research and clinical practice. In this context, one form of clinical application is exploring the targeting capability of the mesoporous system to release drugs, such as PROTACs, in a specific site. The colon, thus, is a region that holds great promise due to its stable environment that allows tailored drug release in response to characteristic features, notably the diverse microbiome, favourable pH, and extended transit time (Awad et al., 2022). It is, however, the colon's lower expression of efflux transporters, namely P-gp, that could be exploited to circumvent the low permeability of PROTACs (McCoubrey et al., 2023).

The research carried out in this thesis explores the untapped potential of advanced mesoporous carriers optimised by ultrasonic atomisation to address the delivery challenges of next-generation molecules and explore their selective targeting to the colon. The novelty of this work lies in investigating the functionality of CAB (cellulose acetate butyrate)-based mesoporous particles to accommodate a variety of molecules, improving the loading and solubility of PROTACs, and targeting the whole system to the colon as a site for selective therapeutic applications. The next sections of this chapter will provide a comprehensive overview of spray drying via ultrasonic atomisation, PROTACs, and colon-targeted delivery. This will, indeed, clarify and strengthen the understanding of the concepts and discussions presented in the upcoming experimental chapters.

1.1. Emergence of Next-generation Molecules, Associated Challenges, and Current Delivery Strategies

It was not until nowadays that complete eradication of pathogenic protein targets was made possible, namely by the advent of PROTACs. These new frontiers in targeted therapy have been identified as the pillars of the modern pharmacological era, owing to their ability to tackle protein targets that were previously categorised as “undruggable” by conventional therapy.

1.1.1. Structure of PROTACs

These molecules are known for being heterobifunctional, possessing two functional ends. At one end is a ligand that connects to an E3 ligase while the other end is a different ligand that brings a protein of interest into degradation. The two ligands are connected by a linker to create a ternary complex, which upon forming initiates the degradation mechanism (Békés et al., 2022). **Figure 1.1** illustrates what PROTACs are composed of.

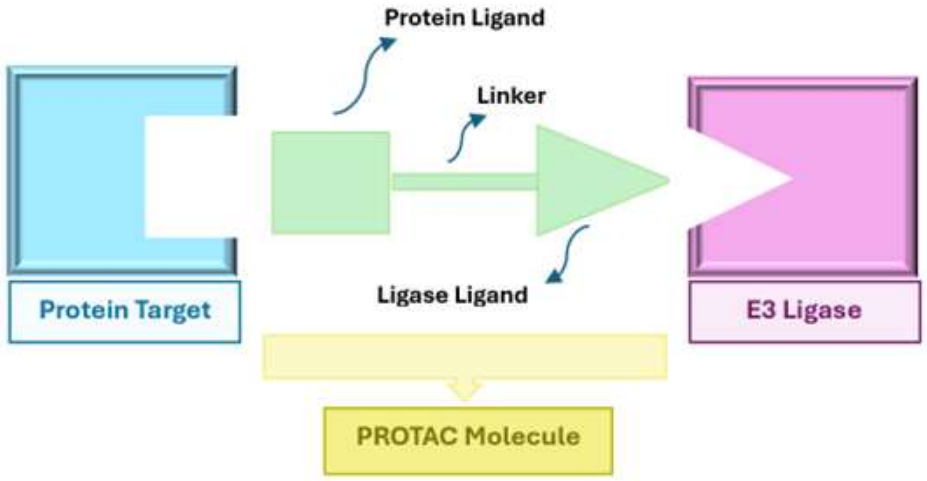

Figure 1.1. *Schematic diagram of PROTAC structure*

With regards to the functionality of the PROTAC molecule, each component of the structure is as crucial as the other. Yet, ligands binding to E3 ligases serve as key elements as they are responsible for recruiting the ligase and initiating the degradation process (Liu et al., 2023). The ability of a PROTAC molecule to tag a protein target for degradation is greatly influenced by the choice of the ligase. For example, Sobierajski and colleagues (2024) stated that some E3 ligases are present in abundancy in certain tumours, varying in their intracellular expression. Others favour certain protein targets and possess higher affinities to them. Altogether, these preferences highlight the role of E3 ligases in determining the selectivity of the PROTAC (Sobierajski et al, 2024). While the human genome harbours more than 600 known E3 ligases, only few (approximately 2%) have been harnessed in the design of PROTACs (Liu et al., 2023). So far, the synthesised PROTACs have been mainly designed but are not limited to recruit von Hippel-Lindau (VHL), cereblon (CRBN), and mouse double minute 2 homologue (MDM2) E3 ligases (Sobierajski et al, 2024). Other less common ligases

that were studied via experimentation include DDB1 (DNA damage binding protein 1), CUL4 associated factor 15 (DCAF15), inhibitor of apoptosis (IAP), and kelch-like ECH-associated protein-1 (KEAP1) (Bricelj et al., 2021). Despite this diverse selection, only VHL and cereblon-based PROTACs have currently progressed into clinical trials to facilitate protein degradation, mainly due to their ease of synthesis, vast expression in human body, and widely available ligands (Bricelj et al., 2021; Lee et al. 2022; Sobierajski et al, 2024). This restriction in the clinical application of E3 ligases presents a scientific opportunity to investigate a largely unexplored set of E3 ligases and discover new candidates that could add to the versatility of PROTACs.

While the affinity of the ligands to their substrates remains important in determining the bioactivity of PROTACs, it is not the sole determinant as the role of linkers come into play. The ability of the linker to pair the ligands together and form a ternary complex is recognised as crucial for the degradative function (Troup et al., 2020). Hence, the optimisation of the linker in terms of its length, functional group composition, and attachment points is deemed necessary yet challenging (Troup et al., 2020). Previous studies showed that the formation of the ternary structure is governed by the length of the linker, which can either weaken or strengthen the interaction of the E3 ligase with the protein of interest and affect the assembly into a ternary complex (Dong et al., 2024). For example, a group of researchers investigated the impact of linker length of the proposed PROTAC on the degradation of KEAP1 protein (Chen et al., 2023). It was found that the activity of the PROTAC was higher when the linker consisted of 8 to 13 atoms. Shortening the linker length to 7 atoms or less reduces the degradation potency of the PROTAC against KEAP1 (Chen et al., 2023). Conversely, another group of researchers investigated the effect of linker length on the potency of a model degrader with ethylene glycol linker (Zhou et al., 2022). The length of the linker was varied between one, two, and four ethylene glycol units. Results showed that the shortest linker (i.e. with one ethylene glycol unit) proved to be of highest degradative potency, which otherwise decreased when the linker was elongated (Zhou et al., 2022). Altogether, these findings highlight the importance of determining the optimal linker length to achieve a stable ternary complex with the highest degradation activity.

1.1.2. Mechanism of Action of PROTAC Molecules

A PROTAC induces the degradation of pathogenic proteins by utilising the body's natural protein disposal machinery known as ubiquitin-proteasome system, or UPS (Wang et al., 2023). The process of degrading the target protein via UPS consists of a series of sequential steps, starting with ubiquitination of a protein followed by proteasomal-mediated degradation (Xie & Zhang, 2024).

Ubiquitination is a vital process for maintaining cellular homeostasis and regulating cellular processes. In fact, it is an enzymatic cascade carried out by three ubiquitin ligases, E1, E2, and E3. It involves the activation, conjugation, and ligation of ubiquitin, the transfer of which to an end substrate modifies a plethora of protein-related activities (Sincere et al., 2023; Xie & Zhang, 2024). The process of ubiquitin activation is initiated by E1 enzyme forming a thioester bond with the ubiquitin molecule to activate it. Once activated, ubiquitin is passed on to an E2 enzyme as part of the multi-step degradation process. The E2 enzyme cannot trigger degradation without cooperating with the E3 enzyme. The latter identifies the protein to destroy and bridges the transfer of ubiquitin molecule from an E2 enzyme to the protein substrate (Xie & Zhang, 2024). As the process repeats itself, the target protein gets tagged with several ubiquitin moieties such that it becomes recognisable by the proteasome system (Li & Crews, 2022).

Within the 26S proteasome, ubiquitin receptors recognise the protein that is then deubiquitinated, unfolded, and sent to the catalytic core for degradation into its constituent peptides and amino acid fragments (Xie & Zhang, 2024). It can be understood that the activation of this proteasome-based degradation is thus driven by the engagement of an E2-E3-ubiquitin complex with a protein of interest. The role of a PROTAC molecule comes into play as it brings the two in close proximity via its ligands, forming a ternary complex (Li & Crews, 2022). The formation of the latter mediates the transfer of ubiquitin and initiates degradation (Li & Crews, 2022). **Figure 1.2** shows the mechanism of ubiquitination and the role of PROTACs in recruiting the E3 ligase.

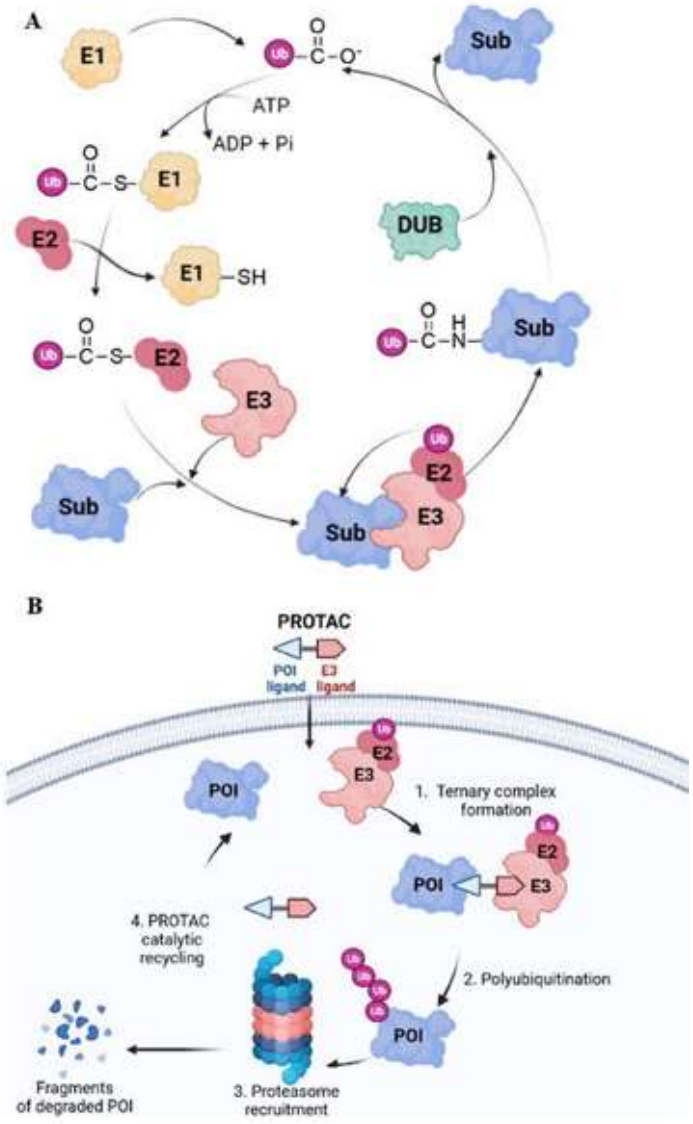

Figure 1.2. *A) An illustration of the proteasome ubiquitin system within the human body. B) The PROTAC molecule induces the formation of a ternary complex that mediates proteasome-dependent protein degradation (adapted from Pichlack et al., 2023)*

1.1.3. Advantages and Limitations of PROTACs

Years of research have not yet unravelled the dilemma associated with drug resistance and selectivity of anticancer treatment. Despite the success achieved with targeted therapy, namely small molecule inhibitors (SMIs) and monoclonal antibodies, scientists still face shortcomings with both traditional and targeted cancer therapy (Qi et al., 2021). In fact, there is a need for more effective targeted therapeutic options, where PROTACs come into play with their unique mode of action that distinguishes them from other therapeutic modalities like SMIs. The inhibitory pharmacological effect of the latter can only be seen with physical occupation of the protein's active pocket site. Nevertheless, some disease-driving proteins, for example transcription factors, cannot be tackled due to mutations or the lack of an active binding site, rendering them "undruggable". PROTACs can unlock the undruggable space as

they behave in a catalytic manner that is based on a transient interaction rather than constant, sustained binding. The degradative activity can be induced through proximity-based recruitment of the protein target by the ligand that can attach anywhere on the protein without the need for high affinity blocking of the protein's active site (Ma et al., 2022; Neklesa et al., 2017; Paiva & Crews, 2019).

With their unique mechanism of action, PROTACs are capable of eradicating the entire protein of interest directly rather than merely blocking an active site to inhibit its activity as it is the case with SMI or intervening at the genetic level as with DNA (Deoxyribonucleic acid)- or RNA (Ribonucleic acid)-targeted therapies (Gao et al., 2020; Graham, 2022). This mechanism allows the PROTAC to detach easily from the complex and engage in another degradative cycle (Ma et al., 2022). Because of this recycling activity, PROTACs tend to knockdown the target at lower doses compared to SMIs, thus minimising dose-related toxicity and increasing the therapeutic window (Békés et al., 2022; Chen et al., 2023).

Moreover, because of this proximity-based mechanism, it is unlikely for mutations to arise because the target is exposed to the PROTAC molecule for a brief period of time that is only sufficient enough to induce the ubiquitin transfer and activate the degradation process. The exposure is not long enough to trigger mutations and, therefore, PROTACs can minimise the likelihood of drug resistance emergence that occur due to mutations in the active pocket site as seen with other drug modalities (Graham, 2022).

In addition, PROTACs have superior selectivity due to their interaction with specific ligases, which can selectively identify the protein of interest from other closely related proteins within the family (Liu et al., 2022; Neklesa et al., 2017). This is achievable by combining different ligands of E3 enzyme and the protein target in addition to optimising linker composition to achieve enhanced specificity (Graham, 2022). Not only that, but they can also degrade intracellular protein targets that reside inside the cell rather than the surfaces. These intracellular targets were, thus, once considered unreachable by conventional therapies (Rutherford & McManus, 2024).

It should be noted that the binding of SMIs to a target protein can result in overexpression, accumulation, and subsequent resistance due to compensatory mechanism. While this remains an issue with SMIs, PROTACs, with their unique mechanism, can surmount that and eliminate proteins that show reduced sensitivity as a result of overexpression (Neklesa et al., 2017). Collectively, PROTACs show considerable promise for overcoming the limitations associated with anticancer drugs.

While there is no silver bullet, the journey of developing a PROTAC is full of hurdles. Although PROTACs can combat the issue of resistance associated with conventional drug therapies because of their unique mechanism of action, tumour cells can always exploit biological loopholes to evade new drugs and develop resistance. It was found that cancer cells targeted

with PROTACs over a long period of time can develop resistance, however, by different means compared to conventional treatments (Graham, 2022). Resistance is mediated with the latter by mutations within the protein that hinder the binding process. Meanwhile, with PROTACs, resistance is triggered at the genomic level through deletion or loss of the genes encoding for E3 ligase machinery involved in the ternary complexes (Graham, 2022). It is noteworthy to emphasise that cells can easily signal the deletion of such ligases, whose loss would not affect the viability of cells (Békés et al., 2022).

The ability of PROTACs to tackle membrane proteins is another questionable limitation. Because the UPS is localised within the cytoplasm, PROTAC molecules cannot degrade those targets that are beyond the reach of the UPS such as cell-surface proteins (Békés et al., 2022).

Among all the shortcomings of PROTAC molecules, poor physiochemical properties that hinder their oral administration stand out as the challenge with great relevancy to the scope of this thesis. PROTACs possess challenging physiochemical properties as they fall in a chemical space beyond the rule of five (Madan et al., 2022). Such molecules violate the well-known Lipinski's rule of 5 (Ro5) that predicts the oral solubility and permeability of a drug. For a drug to exert its therapeutic effect orally, it needs to have a molecular mass less than 500 Da, calculated Log P of less than five, and no more than five and ten hydrogen bond donors and acceptors, respectively (Madan et al., 2022). Protein degraders, on the other hand, do not meet this rule and possess unfavourable physiochemical properties, owing mainly to their large molecular mass and high lipophilicity (Madan et al., 2022). From a drug delivery perspective, the challenge with PROTACs lies in their inferior oral bioavailability and low solubility and cell permeability.

Yet, some PROTACs can be potentially taken orally and are currently in clinical trials, with CRBN-based PROTACs being more promising candidates for oral delivery than VHL-based molecules. This is mainly due to the lower molecular weight that molecules with CRBN E3 ligase possess (Apprato et al., 2024). Thus, the type of E3 ligase incorporated into the structure can dictate the physiochemical properties of the PROTAC.

However, not only extrinsic factors such as the type of E3 ligase being recruited affect the physiochemical properties of a PROTAC molecule, but also the intrinsic factors represented by the design of the PROTAC structure that is inclusive of its warhead, linker, and ligands. For example, García Jiménez and colleagues (2022) investigated whether the solubility of PROTACs can be predicted from their warhead, linker, and ligand design. Two PROTACs, MZ1 and MZP-54, shared the same structure that differed only in the type of warhead incorporated. JQ1 was the warhead employed with MZ1 while I-BET726 was the one associated with MZP-54. Both PROTACs experienced inferior solubility; yet, MZP-54 showed poorer solubility compared to MZ1 because its warhead was less soluble. This highlights how the structure of a PROTAC can determine the physiochemical properties including solubility

and identifies the need for solubility enhancement technologies. In another study conducted by Apprato and colleagues (2024) on PROTACs with reported oral bioavailability in mice, 36.36% of their data set showed extremely low oral bioavailability in animals, further emphasising the need to optimise the performance and properties of PROTACs via utilising drug delivery platforms. It would be more feasible to utilise drug delivery technologies to enhance the bioavailability and solubility issues of PROTACs than revisiting the chemical synthesis processes. Despite that, the majority of the work done in literature focused on the synthetic approach, and only few articles tackled the targeting efficiency and properties that affect the oral bioavailability of these molecules.

1.1.4. Optimising Drug Delivery of PROTACs

While PROTACs present a breakthrough in the field of targeted medicine and offer new exciting possibilities, their translation from bench to bedside is being hindered by their biopharmaceutical properties. In fact, poor solubility, permeability, and bioavailability cause suboptimal therapeutic effects as PROTACs fail to present with an effective concentration. Their practical implementation can be made possible by the use of drug delivery systems that alter the targeting efficacy and biopharmaceutical behaviour of these molecules towards a more promising delivery profile and therapeutic outcome. Several strategies, namely polymeric and lipid-based nanoparticles, prodrugs, and amorphous solid dispersions, are being employed in an attempt to expedite the transition of PROTACs from preclinical studies to clinical application.

a. Polymeric Nanoparticles

Among the different types of nanoparticles available, polymeric nanoparticles emerge as a technology for effective targeting. Saraswat and co-workers (2020) demonstrated that polymeric nanoparticles can be employed to achieve this goal. The PROTAC molecule investigated in their study was ARV-825, which shows poor pharmacokinetic profile, such as low aqueous solubility and rapid metabolism. The incorporation of this PROTAC into a biodegradable, targeted moiety through the utilisation of polylactide-co-glycolide (PLGA) and polyethylene glycol (PEG), respectively, addressed some of the issues associated with the PROTAC. The nanoparticle system minimised degradation by enzymes, protecting the drug load from rapid metabolism. Meanwhile, surface modification with PEG conjugation enhanced the targeting efficiency to the tumour site by enabling the PROTAC to evade destruction by the immune system and accumulate at the target site. The nano formulation was not only able enhance the cytotoxic activity compared to raw drug but also achieve controlled drug release (Minko, 2020; Saraswat et al., 2020).

b. Lipid-based Carriers

A variety of lipid-based platforms have been used to enhance the stability and targeted delivery of PROTACs within and beyond the field of oncology. For example, Gong and colleagues (2024a) developed a novel nanocomplex of lipidoids. The complex was created to destroy Tau aggregates that were potentially thought to contribute to the pathophysiology of Alzheimer's disease. The free PROTAC molecule, peptide 1, experienced poor stability in the serum and difficulty in penetrating the blood brain barrier. When the PROTAC was loaded into the neurotransmitter-derived lipidoids to form nanocomplexes, a relatively high encapsulation efficiency of 60% was obtained, and the complex demonstrated good penetration across the blood brain barrier, delivering the PROTAC to the neuronal cells. This finding highlighted how drug delivery systems can help with the permeability and stability of PROTACs (Gong et al., 2024a). Their work demonstrated that the delivery of PROTAC molecules is spanning into areas beyond oncology.

Despite that, cancer treatment remains the cornerstone of the PROTAC modality. Therefore, another attempt was made by Saraswat and colleagues (2024) using lipid nanocarriers to simultaneously deliver PROTACs and plasmids to treat resistant melanoma. A number of molecular pathways that include BRAF mutations and activation of c-MYC oncogene drive skin malignancy. BRAF inhibitors like vemurafenib have been developed, yet with resistance emerging shortly over prolonged use. BRAF resistant melanoma tissues have shown upregulation in BRD4 (Bromodomain containing protein 4), a protein target, in addition to a loss in a tumour suppressor gene known as PTEN (phosphatase and tensin homolog). Therefore, the group focused on co-delivering a PROTAC molecule that targets BRD4 and a PTEN plasmid as synergetic therapy to overcome the resistance associated with melanoma. However, the two differ in their physiochemical properties and hence were delivered separately but under the same delivery approach of lipid-based carrier. Because the PROTAC they used suffers from several physiochemical challenges such as poor solubility and permeability in addition to encapsulation difficulty, it was loaded into nanoliposomes to address these delivery challenges (Saraswat et al., 2024).

The lipid bilayer of the liposomal structure helped with the entrapment of such a large lipophilic molecule, increasing its stability. Moreover, this incorporation helped with overcoming the PROTAC’s poor aqueous solubility. It also assisted in cellular uptake due its resemblance to cell membranes, thus enhancing the permeability of the PROTAC. This work illustrated the potential use of lipid-based platforms to address the delivery challenges of PROTACs in cancer therapy.

A similar investigation was carried out by Zhang and co-workers (2025b) to enhance the degradative and delivery efficiency of PROTACs. Given the poor aqueous solubility of the PROTAC DT2216, the researchers formulated a liposomal nano-delivery system to

incorporate DT2216, which is otherwise not soluble without the addition of a minimum of 10% (v/v) of dimethyl sulfoxide. The addition of such a harsh solvent raises safety concerns, and the resistance to PROTACs acquired by tumours necessitate a novel delivery vehicle to degrade the protein targets.

From this perspective, Zhang and colleagues (2025b) prepared a cationic liposomal carrier for the co-delivery of a PROTAC molecule and SiRNA (small interfering RNA) to target the protein BCL-XL at the protein and gene level, respectively. They managed to successfully encapsulate the poorly soluble DT2216 into the liposome's cationic core and bind the SiRNA to the surface with fluorinated polyethyleneimine (F-PEI) added on top as a protective shell. Altogether, the delivery system showed enhanced solubility of the PROTAC, promoted the cellular uptake and endocytosis of both payloads, and improved target degradation when compared to each therapeutic modality alone. The co-delivery system showed improved anti-cancer effects in mice while maintaining good safety profile (Zhang et al., 2025b). This study proved that the degradative efficiency of a PROTAC can be enhanced via liposomal formulations that address its solubility and permeability challenges.

Two other studies utilised lipid-based nanoscale delivery systems to deliver PROTACs to their target sites more effectively by overcoming the delivery issues that hinder their clinical efficacy. The research group of Wang et al. (2024) targeted KRAS protein target, which was previously thought undruggable, via a surface modified liposomal vehicle. The delivery challenge that the researchers were facing was related to the permeability and targeting of the PROTAC molecule, LC-2. Thus, engineering a liposomal formulation with cell-penetrating peptide R8 and PEG conjugated on the surface not only enhanced the cellular uptake of LC-2 but also showed improved anti-cancer effects in KRAS-mutant models of lung cancer (Wang et al., 2024). This anti-cancer effect was only achieved because the liposomal formulation was able to enhance the bioavailability of the PROTAC compared to its raw form.

While Wang et al. (2024) discussed the potential of liposomal formulations in the PROTAC field, Xu et al. (2024) expanded on the concept of lipid-based nanoscale carriers by additionally sensitising the tumour cells to radiation to eradicate BRD4 target. In their work, Xu and researchers (2024) conjugated the PROTAC, MZ1, to PEG to form self-assembled, stimuli-responsive nanomicelles. The nanomicelles did not release the payload in the circulation unless X-ray radiation was applied, providing a control over the PROTAC delivery and off-target effects. Both formulations, whether liposomal or radio-responsive micelles, are nanoscale strategies that could potentially improve PROTAC delivery. Another group of scientists attempted to improve the water solubility of an Epidermal Growth Factor Receptor-targeting PROTAC and enhance its targeting efficiency via conjugating the PROTAC with folate and PEG that then self-assembled into micelles and tested in mice (Ma et al., 2024). PEGylation was introduced to the delivery system to improve the PROTAC's water solubility

by acting as the hydrophilic component. Similarly, Saraswat et al. (2022) explored the selective targeting capability of ARV-825 through surface modification of nanoliposomes with galactose to specifically target asialoglycoprotein receptors on hepatocellular carcinoma. Because of this galactose moiety, the formulation was able to accumulate in hepatocellular tissues, assisting the PROTAC to achieve more efficient degradation of BRD4 compared to the free form of the PROTAC (Saraswat et al., 2022).

c. Prodrugs

Prodrugs are inactive forms of medicinal compounds intended to improve the shortcomings associated with active ingredients such as poor physiochemical properties and off-target effects. Because of their selective activation, prodrugs have found their way in enhancing the delivery of PROTACs, whose cellular uptake and distribution is hindered. Recently, researchers showed an interest in innovative prodrug approaches, utilising both endogenous and exogenous stimuli, to effectively and selectively deliver PROTACs and ensure on-demand activation in target cells.

Gao et al. (2024) attempted to advance the pharmacokinetics of a PROTAC molecule, ARV-771, particularly its stability in the circulation and susceptibility to degradation. By merging the concept of nanotechnology and dual-activated prodrugs to generate a sophisticated delivery system, the group also aimed at enhancing the specificity of the proposed technology, ensuring accumulation within the tumour microenvironment, rather than in healthy tissues, and efficient cellular uptake.

The researchers shielded ARV-771 within the nanoparticles that were decorated with PEG corona. Altogether, this shielding effect protected the PROTAC from the immune system and delivered it to the tumour site. To allow for tumour penetration, the cleavage of PEG shielding was triggered by the action of matrix metalloproteinase-2 enzyme, and the disassembly of the nanoparticle was initiated intratumorally by the acidic environment. Upon entry to the tumour cell, the dormant PROTAC was activated depending on the tumour region it resided in. If the region was normoxic, reactive oxygen species that were highly abundant in cells subjected to photodynamic therapy activated the PROTAC. In hypoxic regions of the tumour such as those regions where stem cells were located, nitroreductase present within the oxygen-deprived regions activated the PROTAC molecule (Gao et al., 2024).

Collectively, these techniques, namely the use of nanotechnology, PEG shielding, and double-stimuli activation, provided the PROTAC with protection against degradation, recognition, and clearance in circulation, promote preferential delivery of the PROTAC to and into the tumour regions, and ensured no activation is initiated prior to reaching the tumour site. The technology, therefore, claimed to offer enhanced pharmacokinetics and specificity of PROTACs to cancerous regions with minimal off-target effects.

Some other articles discussed PROTAC prodrugs but mainly focused on either endogenous stimuli, such as enzymes and oxygen status within the cell, or exogenous stimuli, such as ultrasound and phototherapy, to activate PROTAC prodrugs (Huang et al., 2023). The former type may present with diminished selectivity while the latter may require heavy and advanced external equipment to run the process. From this argument, Huang et al. (2023) decided to use a simple exogenous stimulus of bioorthogonal bond cleaved by tetrazine to activate a PROTAC in the prodrug form. They engineered a prodrug of MZ1 to limit off-target BRD4 degradation during circulation and in healthy cells. The inactive prodrug (MZ1-O) was created by caging the PROTAC with 4-(vinyloxy) benzyl carbonate moiety, which was then altogether encapsulated into PLGA nanoparticles conjugated with peptide for additional cell targeting. The nanoparticles provided protection for the PROTAC and ensured its delivery and entry into target cancerous cells. Meanwhile, the caged PROTAC molecule can be only activated via a bioorthogonal reaction mediated by the presence of 3,6-dimethyl-1,2,4,5-tetrazine. This exogenous activator was introduced into the cells via dissolvable microneedles that were administered locally to ensure that bond cleavage occurs at the desired tumour site specifically (Huang et al., 2023).

It can be inferred from the study that off-target toxicity of PROTACs can be minimised by using the prodrug approach, particularly if using an external activator to trigger a cleavage reaction that does exist genuinely in the body and does not interfere with biological processes. This maximises specificity and offers a degree of control, ultimately reducing off-target effects of PROTACs.

d. Amorphous Solid Dispersions (ASDs)

Despite the promising application of lipid-based nanocarriers in the field of PROTAC delivery, namely in enhancing the targeting efficiency and bioavailability, the stability of such carriers remains a concern for oral delivery (He et al., 2018). Thus, ASDs emerge as an alternative approach offering benefits in improving oral delivery, specifically with regards to enhancing solubility and dissolution rate.

To date, only four attempts were published to incorporate PROTAC molecules into ASDs, focusing on solubility enhancement (Hofmann et al., 2024; Mareczek et al., 2024; Pöstges et al., 2023; Zhang et al., 2025a).

First is the work done by Pöstges et al. (2023), who formulated liquisolid formulations of a poorly soluble PROTAC, ARCC-4, in comparison to ASDs through vacuum compression molding using two polymers: Hydroxypropyl methylcellulose acetate succinate (HPMCAS) or Eudragit. Dissolution profiles of raw PROTAC and all liquisolid formulations showed less than 1 µg/mL of drug released over the predetermined period. This indicated that pure drug exhibited poor solubility, and liquisolid technology failed to enhance the solubility of PROTACs.

In contrast, ASDs were promising in enhancing the solubility of the PROTAC regardless of the polymer used. The dissolution of ARCC-4 jumped from less than 0.4 µg/mL with the raw form to 31.8 ± 0.6 µg/mL with 10% HPMCAS ASD and 35.8 ± 0.4 µg/mL with 10% Eudragit ASD. This finding demonstrated the potential of ASDs in improving the dissolution of PROTACs.

To expand on this work, Hofmann et al. (2024) also explored ASDs to tackle the poor solubility and slow dissolution of PROTACs, however, using another widely known approach which is spray drying via conventional nozzle and a different PROTAC category that recruits CRBN instead of VHL. The spray-dried ASDs demonstrated a substantial increase in supersaturation—exceeding a 70-fold rise compared to the pure PROTAC. This solubility enhancement was attributed to the homogenous distribution of the PROTAC within the polymeric matrix and increased wettability achieved with one of the polymers used. Altogether, this resulted in enhanced stabilisation of the supersaturated state without any precipitation noticed (Hofmann et al., 2024).

Delving deeper into the use of ASDs in PROTAC delivery, Mareczek and co-workers (2024) investigated the poor solubility of two PROTACs (ARV-110 and SelDeg51). They embedded the crystalline PROTAC, ARV-110, and the amorphous PROTAC, SelDeg51, into ASDs via spray drying using three-fluid nozzle. Results showed that the pure forms of the PROTACs were undetectable when performing dissolution studies as their solubilities were too low. Regardless of the original solid state of the PROTAC, a significant enhancement in dissolution and maintenance of supersaturation were reported with the ASDs compared to the crude forms (Mareczek et al., 2024).

Recently, drug amorphisation techniques have evolved to include advanced and more refined forms of ASDs, such as mesoporous particles that emerge as an alternative strategy. Both formulation strategies transform crystalline drugs into amorphous forms, in an attempt to enhance solubility and dissolution performance (Zhang et al., 2022a). However, they differ in the way by which the active pharmaceutical ingredient (API) is loaded and its amorphous form is stabilised. **Figure 1.3** is a schematic diagram of how ASDs and mesoporous particles share the drug amorphisation phenomenon but differ in the mechanism of drug loading and stabilising. It is noteworthy to mention that while ASDs have been explored, no attempts were made to date to utilise mesoporous particles for addressing the solubility of PROTACs.

In conclusion, ASDs act as a promising strategy to address the poor solubility of different PROTACs and improve their dissolution profile, which should ultimately enhance their oral bioavailability. The scientific work discussed above proves the versatility of ASDs in accommodating different PROTAC categories, from VHL-based to CRBN-based molecules, using multiple polymeric matrices, such as polyvinyl alcohol and Soluplus, and various preparation techniques that include spray drying. However, as with lipid-based systems, stability remains an issue with the tendency of recrystallisation becoming high upon storage.

Also, *in vivo* studies are indeed needed to validate whether the current solubility enhancement translate into pronounced oral bioavailability. Hence, mesoporous particles present as an advanced form of ASDs, achieving the same function but with enhanced stability.

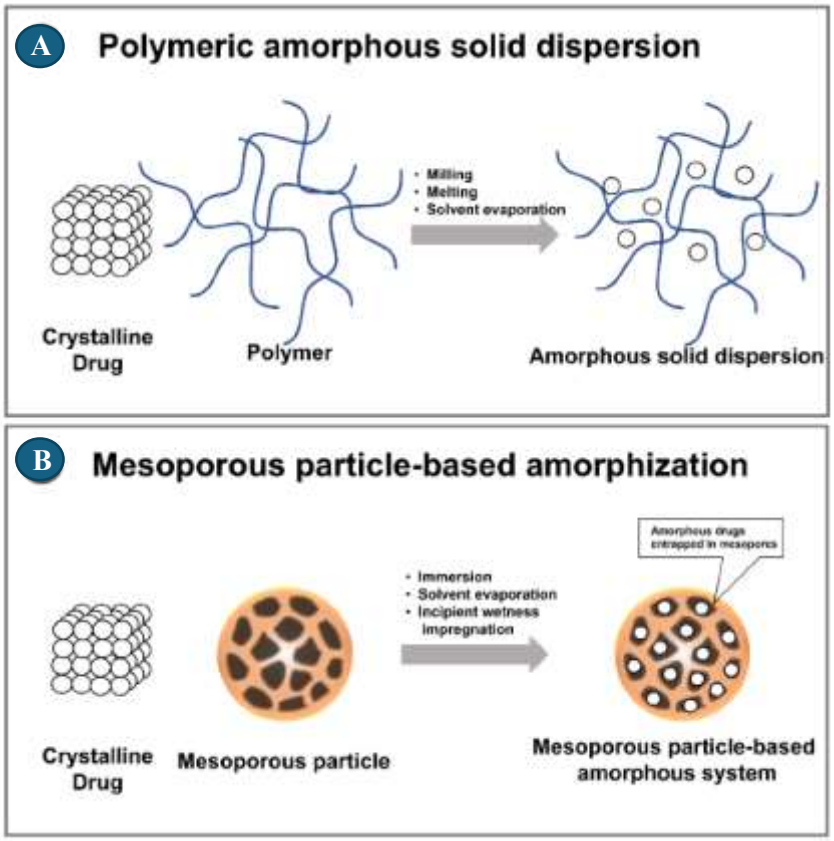

Figure 1.3. *Illustration of two drug amorphisation techniques A) amorphous solid dispersion and B) mesoporous particle with pore confinement of drug (adapted from Kim et al., 2021)*

1.2. Engineering Advanced Mesoporous Particles via Spray Drying

A paradigm shift in the focus of pharmaceutical industry towards novel platforms that enhance the efficacy and safety of challenging drug molecules was noted in the past decade. In fact, by 2028, the value of advanced drug delivery market is expected to rise by 36.7%, at a compound annual growth rate of 6.4% (BCC Publishing, 2024). As inferred from the previous section, conventional delivery strategies, ASDs and lipid-based systems, were employed in PROTAC delivery. However, oral intake remains the preferred route of administration which is difficult to achieve with lipid-based technologies while physical stability and drug recrystallisation remain a concern with ASDs despite the promising solubility enhancement. Creating advanced forms of technologies with established efficacy can help ensure oral delivery to the colon, for example, while overcoming the instability. Refined carriers, namely those based on porous materials, have recently captured the attention of this market for a number of reasons. With advantages like large surface areas with high porosity, easily tuneable pores, and modifiable surface functionalities and chemistries (Zhou et al., 2017), porous materials have found a wide range of applications within the pharmaceutical manufacturing of drug systems (Thananukul et al., 2021). They might, in fact, be superior to conventional strategies like ASDs, particularly in delivering PROTACs to specific areas that enhance the permeation, such as the colon. Several techniques are presented in literature to engineer these delivery systems whether they are ASDs or mesoporous particles, with spray drying dominating as an effective strategy.

1.2.1. Brief Overview of Spray Drying

Spray drying is widely used as a method for the production of porous particles via evaporation of solvents (Thananukul et al., 2021). It works by breaking a liquid feed in the form of a solution or suspension into a fine spray of droplets that eventually dry into solid particles (Wang et al., 2021). The process is composed of four stages: Feed preparation, atomisation of liquid, drying of droplets, and powder collection.

In the first stage, the constituents of the feed such as the type of solvent and polymer used should be determined with care as the properties of the final product are affected by the feed composition. Once the composition of the feed is studied and determined, the atomisation phase begins, whereby the liquid is subjected to an atomiser that disperses it into droplets. Different atomisers have been reported, and a focus on each will be detailed shortly. This stage is crucial because the breakdown into finer droplets increases the surface area and allows for efficient drying. It is, however, important to note that the final particle size and morphology are also influenced by the droplet size generated at this stage.

Next, the droplets are exposed to a stream of drying medium. The drying dynamics, governed by Péclet number, determine the morphology of the particles as well. The final step involves

the collection of the dried powder particles. The product recovery and yield need to be optimised through controlling moisture content and dynamics of the system (Al-Khattawi et al., 2018). Compared to other methods, spray drying is a technique offering several processing advantages. It allows for careful control of final particle properties such as size, shape, and porosity. Moreover, spray drying is a scalable process, operating at a fast pace and low cost of materials and accommodating multiple forms of feed samples. From an industrial perspective, these are considered valuable advantages (Wang et al., 2021).

1.2.2. Atomisation and Different Types of Atomisers

Atomisation is a core component of the spray drying process and is subdivided into several stages (Zafar et al., 2024). It includes the ejection of the liquid stream in the form of droplets that breakup over two phases. At first, the liquid feed experiences a shear force as it flows through the nozzle and the orifice. It then interacts with the surrounding environment, whereby deformations are induced interrupting the integrity of the liquid. However, droplets are not ejected until the induced deformations in the liquid are able to overcome the forces that exist in form of surface tension and viscous stress. It is not until these deformations exceed the capillary stresses and forces that large droplets are ejected. This is referred to as primary atomisation whereas secondary atomisation occurs once large droplets further disintegrate into smaller forms as a result of progressive destabilisation. Finally, the process reaches equilibrium, and droplets dry into solid particles after reaching a stable configuration with solvent evaporation (Zafar et al., 2024).

From an economic perspective, the choice of the nozzle and its operating mechanism affects the particulate production process and the attributes of the final product, specifically the droplet size and particle size distribution (Turan et al., 2016). Therefore, several types of atomisers that vary in their atomising principle and the energy used were reported in literature and include rotary, pressure, pneumatic, and vibrational nozzles as shown in **Figure 1.4** (Naidu et al., 2022).

With rotary atomisers, the liquid feed encounters a rotating surface in the form of a disk or plate and travels down the edges of the nozzle. These surfaces rotate at a high velocity, generating centrifugal forces that disrupt the liquid feed. Once the centrifugal force overcomes the stabilising forces, droplets emerge either directly from the spinning rim or by breaking up from liquid sheets or indirectly from unstable ligaments that are found beyond the rim (Poozesh & Bilgili, 2019). Thus, the driving force for atomisation with rotary nozzles is centrifugal force. On the other hand, pressure nozzles operate by forcing a liquid feed that travels down the nozzle to the orifice under very high pressure. A cone-shaped spray of atomised droplets results when the applied pressure energy is transformed into kinetic energy to break up the liquid into fine droplets. Although pressure nozzles operate with low cost and simple design,

they are often employed to generate relatively large particles with narrow size distribution; however, varying the droplet size at a constant feed flow rate is challenging and can be achieved by changing the nozzle's dimensions or type. The nozzle also struggles with spraying viscous feed solutions as these might cause blockages. In some cases, modified pressure nozzles are used, whereby a swirl is added to create turbulence and achieve better control over the imparted energy and droplet size (Poozesh & Bilgili, 2019; Weng et al., 2024).

Within the drug development sector, pneumatic nozzles, referred to as two-fluid or three-fluid nozzles, are very commonly used with both featuring one gas channel but vary in their liquid channels. The three-fluid nozzle incorporates an extra liquid feed passage that enables two separate solutions to atomise together (Weng et al., 2024). The operational mechanism of these nozzles involves using a compressed gas stream traveling at a very a high velocity, that shatters the slow-flowing liquid feed into fine droplets, as the two get in contact with each other (Poozesh & Bilgili, 2019). Unlike other conventional nozzles (rotary or pressure), it is the atomising gas that travels at high speed rather than the liquid being ejected at high velocity (Poozesh & Bilgili, 2019). Therefore, the droplet size with the two-fluid nozzle is a function of the ratio of the flowing gas to the liquid passing through (Poeiras, 2018). The two-fluid nozzle can, thus, be used in a setting where small, fine particle size is required. Another advantage of the conventional two-fluid nozzle is its ability to handle viscous feeds. However, to disintegrate a viscous liquid, the nozzle must consume large amounts of atomisation energy which is considered a drawback. Hence, pneumatic nozzles are known for high energy consumption and economic cost (Camacho-Lie et al., 2023).

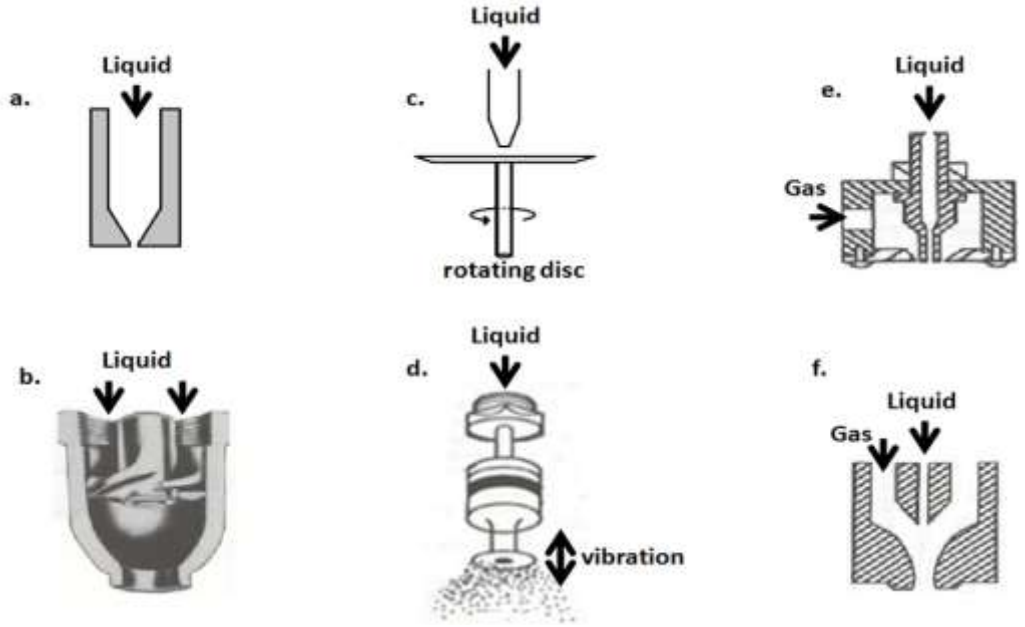

Figure 1.4. *A schematic diagram of atomisers used in spray drying. a) Pressure nozzle b) Pressure-swirl nozzle c) Rotary nozzle d) Ultrasonic nozzle e) Two-fluid nozzle with external mixing f) Two-fluid nozzle with internal mixing (adapted from Shepard, 2011)*

Despite the success achieved by each of the conventional nozzles in the pharmaceutical industry and drug delivery field, they still suffer from limitations. The energy generated by these nozzles whether in the form of pressure, centrifugal, or kinetic energy majorly transforms into kinetic energy imparted to the drying particles, causing droplets to eject with very high speed (Rodriguez et al., 1999; Turan et al., 2015). This can cause defects in the final product. Moreover, conventional nozzles lack precise control over droplet size and, hence, result in a somewhat wide particle size distribution and are susceptible for clogging and orifice blockage (Turan et al., 2015). Also, traditional nozzles consume a large amount of energy (Naidu et al., 2022; Turan et al., 2016). Although spray drying is a cost-effective process, the selection of the nozzle is crucial to avoid further energy consumption and increased costs. An alternative type that addresses these challenges is the ultrasonic nozzle by adopting a different mechanism to disintegrate liquids into droplets.

1.2.3. Ultrasonic Nozzle and the Theories Behind Ultrasound-mediated Atomisation

Vibrational energy is the driving force of atomisation with ultrasonic nozzles (Legako & Dunford, 2010). The nozzle technology is based on the concept of ultrasound, which is characterised by high frequency sound waves beyond the threshold of human hearing (Legako & Dunford, 2010). Typically, the operating frequency range of ultrasound waves is above 20 kHz (Naidu et al., 2022). Because of this high frequency, ultrasound waves are known to propagate with short wavelengths in a narrow and precise direction. However, these wavelengths are not as short as the atomic bonds within the liquid and, thus, cannot induce droplet detachment by simply exciting or interacting with the vibrational energy of the atomic bonds or the internal energy of the liquid molecules (Naidu et al., 2022). Instead, they induce liquid disturbances through mechanical effects that will be discussed shortly (capillary wave and cavitation theories).

Within the nozzle, the piezoelectric transducer converts electrical energy into mechanical energy in the form of ultrasound vibrations. This will be conveyed as a vibrating nozzle tip such that when a thin layer of liquid feed spreads on the vibrating tip, the vibrations will create capillary waves that propagate through the liquid. It is, however, when the vibrations disturb the liquid's surface that atomisation occur, resulting in detachment of droplets from the surface of the liquid that then leave the nozzle in the form of an atomised mist (Khaire & Gogate, 2020). **Figure 1.5** simplifies the mechanism of droplet detachment.

The phenomenon of ultrasonic vibration is not new and dates back to 1831 when Michael Faraday first discovered the onset of capillary waves as a function of vibration with a specific amplitude (Panão, 2022). It was not until 100 years later that a mist or spray was generated by subjecting a liquid to ultrasonic vibrations (Panão, 2022). In the meantime, scientists, such as Lord Rayleigh, introduced the relation between the wavelength of the capillary waves and

frequency (Panão, 2022). Modern research represented by the work of Lang (1962) expanded Rayleigh's theories, set the foundation for the mechanism of droplet generation by ultrasonic atomisation, and quantitatively correlated median diameter of droplets with frequency and wavelength of capillary waves.

Since then, three main hypotheses circulate to explain the mechanism behind droplet formation using ultrasonic atomisation. The first hypothesis is known as capillary wave theory. When a liquid is exposed to ultrasonic vibrations, these vibrations cause disturbances to the surface of the liquid in the form of capillary waves (Khaire & Gogate, 2020). Because of the continuous nature of the applied vibrations, the capillary waves grow in amplitude, causing greater instability (Priyadarshi et al., 2024). The growing capillary waves then exceed the surface tension forces of the liquid (Khaire & Gogate, 2020). Consequently, the surface of the liquid collapses and droplets emerge from crests of the waves, resulting in atomisation (Naidu, 2022).

Cavitation is the second theory proposed to explain the possible mechanism of ultrasonic atomisation. As the term suggests, ultrasonic waves applied to a liquid can result in bubbles or cavities within the liquid spreading on the tip because of some form of instability. These cavities/bubbles undergo a series of expansion and shrinkage until they collapse (Camacho-Lie et al., 2023). Because of this collapse, shockwaves result and trigger the emergence of droplets from the liquid surface (Nii, 2016).

Further research into the area led to the development of a joint theory that combines the two theories. In the conjunction theory, it is hypothesised that droplet disintegration is neither a sole function of capillary waves growing in amplitude nor due to cavitation. It is indeed a matter of co-existence of the two theories such that droplet detachment does occur from crests of the capillary waves; yet, it is intensified by shockwaves that occur in response to the expansion, compression, and collapse of cavitational bubbles (Nii, 2016).

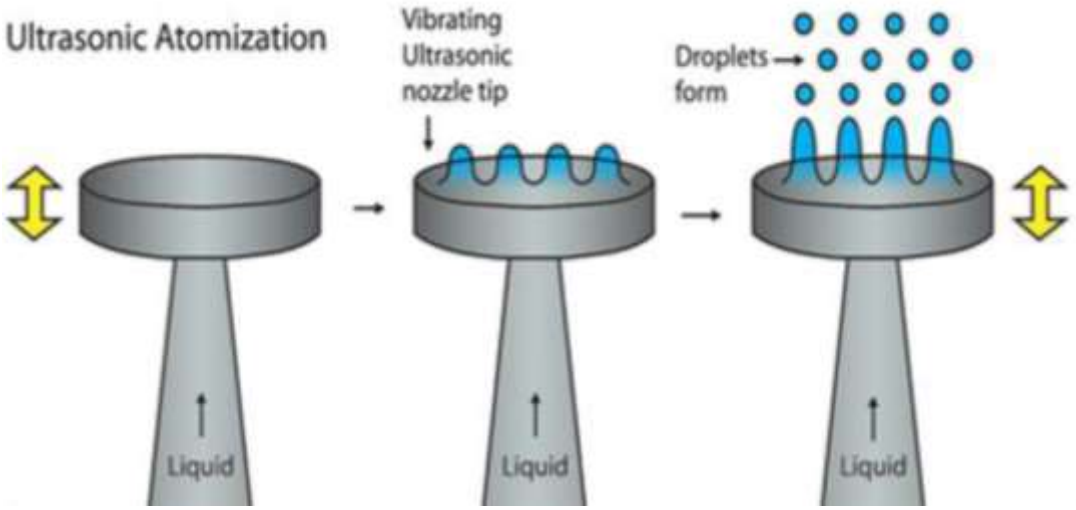

***Figure 1.5**. Mechanism of ultrasonic atomisation (Slegers et al., 2017)*

1.2.4. Advantages and Disadvantages of Ultrasonic Nozzle

Because of the unique mechanism of action of the ultrasonic nozzle, the technology offers several advantages within the pharmaceutical and industrial fields. First, and the well-known hallmark of the technology, is its ability to generate fine droplets with narrow and uniform size distribution (Khaire & Gogate, 2020). Such a uniform distribution is challenging to reach with conventional two-fluid nozzle (Nii, 2016). This advantage is mainly due to the repetitive and consistent oscillations of the waves that are characterised by a defined wavelength over the entire atomisation process. One reason for this organised phenomenon is the precise control of the frequency (Rajan & Pandit, 2001). Unlike conventional nozzles, the process of droplet ejection is not random and is not of chaotic nature (Rajan & Pandit, 2001).

Another key advantage is the low velocity mist that the nozzle generates. According to the operation manual of Buchi's ultrasonic nozzle, the velocity of the spray ranges from 18 to 36 cm/s. This speed is considered gentle when compared to the spray of pressure nozzles which travels at a higher velocity of 10-20 m/s (Ultrasonic Controller Operating Manual, 2014). This milder shear force and soft spray is attributed to the type of energy delivered to the particles. Unlike conventional nozzles, which impart kinetic energy through high-velocity gas or pressure to atomise the liquid feed into droplets, ultrasonic nozzles use mechanical vibrations to atomise. These vibrations form capillary waves on the surface of the liquid, leading to droplet formation with significantly lower momentum and turbulence (Khaire & Gogate, 2020). As a consequence, the lower shear stress of the ultrasonic nozzle and the absence of high-pressure fluids can be beneficial for spray drying biosensitive compounds and maintaining their integrity in addition to reducing the energy consumption and costs (Dalmoro et al., 2013; Khaire & Gogate, 2020; Turan et al., 2016). Besides that, the apparatus size and the dimensions of the chamber can be reduced due to the soft spray (Dalmoro et al., 2013).

While ultrasonic atomisation offers significant advantages, particularly in particle size distribution and velocity of the spray, some drawbacks can still arise. Feed liquids with high viscosities are challenging to spray using ultrasonic atomisation (Gui et al., 2024). Meanwhile, the risk of clogging with viscous solutions also increases, and the lack of an industrial scale apparatus of the ultrasonic nozzle limits the applicability of such process beyond laboratory scale (Khaire & Gogate, 2020).

1.2.5. Ultrasonic Atomisation in Drug Delivery

Conventional nozzles, such as two-fluid atomisers, have been the gold standard of spray drying in the field of drug delivery. A considerable body of literature covers the employment of two-fluid nozzle in microencapsulation, drug loading of amorphous solid dispersions, and mesoporous carrier production. Yet, with all the advantages that ultrasonic nozzles offer, it

emerges as an alternative, dominating not only the food industry but also slowly being integrated in the pharmaceutical sector.

Ultrasonic atomisation has been employed in the production of drug delivery systems to carry both small molecule and large molecule drugs. In one attempt using a model small molecule, Albertini and colleagues (2005) generated chitosan microparticles loaded with theophylline using ultrasonic atomisation. The effect of one of the parameters, viscosity, on the atomisation process was investigated. A viscous solution containing chitosan 3% (w/v) was sprayable, addressing the all-time challenge of ultrasonic nozzles. From a drug delivery point of view, ultrasonic atomisation was able to preserve the polymeric material despite minor depolymerisation reported, which is crucial for an efficient controlled release profile.

Similarly, using the small molecule drug for diabetes, Metformin hydrochloride, M and Gogate (2024) generated metformin-loaded microspheres of sodium alginate using spray drying. Two nozzle types, pressure and ultrasonic, were employed in an attempt to improve the particle size and distribution to enhance the drug's absorption and dissolution profile. Results revealed that small particle size (<10 μm) was obtained with both nozzles, but the ultrasonic nozzle was superior in terms of producing a narrower particle size distribution and better encapsulation. Given this comparison, it seems that ultrasonic atomisation via spray drying was an effective method when fine-sized particles were desired with tight control over size distribution and enhanced encapsulation efficiency compared to conventional nozzles.

The work of Berkland and colleagues (2001) represented another effort yet might be one of the earliest that introduced size control of microspheres via acoustic excitation. This study redefined the generation of microspheres by emphasising the ability of ultrasonic atomisation to provide a good control over particle size. The size of a microsphere plays a crucial role in determining its fate from a pharmacokinetic perspective. Hence, the authors generated biodegradable microspheres via acoustic excitation, whereby more than 95% of the particles showed only 1 to 1.5 μm deviation from the mean size, indicating uniformity.

After providing a proof-of-concept on how ultrasonic-assisted atomisation can provide size control of microspheres, Berkland et al. (2002) succeeded in the year after to translate this concept into an actual application, suggesting how size uniformity can affect the release profile of microspheres. Microspheres of different sizes (small and large) were produced via varying the flow rate and the frequency. Ultrasonic atomisation ensured size uniformity within each batch though. Smaller spheres showed a different release profile compared to the large microspheres, while a mixture of the two sizes achieved the desired zero-order profile. Another take on the same concept of precise control over droplet size was presented by Forde and Friend (2006). In their study, the researchers aimed to control the particle size to achieve enhanced cellular uptake. For this purpose, two atomisation systems were employed, varying in their frequency. It was not the only parameter impacting size that was studied, but the

influence of power, feed flow rate, and solid concentration was also explored. Their work highlighted how frequency can affect the particle size. The lower frequency atomiser (40 kHz) generated microparticles for nasal delivery that were <15 μm. Meanwhile, the second atomising system with a higher operating frequency of 1.645 MHz resulted in nanoparticles with a size of 196 nm, allowing for cellular internalisation. This conclusion added value to the technology when tight control over particle size as a function of frequency was needed (Forde & Friend, 2006).

Two other studies utilised ultrasonic atomisation to produce microspheres for drug delivery to treat hepatocellular carcinoma (Kaushik et al., 2019; Yin et al., 2024); however, Yin et al. (2024) neither provided the methodological rationale and justification behind utilising ultrasonic atomisation over other methods nor did they explain the processing parameters, setting, and optimisation. They only revealed the production of sodium alginate-lanthanum microspheres loaded with doxorubicin for hepatocellular carcinoma via ultrasonic atomisation. On the contrary, Kaushik et al. (2019) justified briefly the reason behind using ultrasonic atomisation and reported uniform particle size within the range of 20-55 μm. However, their work was approached with doubt as it lacked detailed size characterisation techniques (i.e. size distribution curves and analysis) and statistical analysis that would be ideally and routinely performed to claim uniformity of size. Nevertheless, their scientific contribution cannot be overlooked, providing insights into combining ultrasonic atomisation with emulsion method as well as molecular and mathematical modelling to assess the morphology, drug encapsulation, release, and efficacy of the drug delivery system in liver cancer management.

On the other hand, proteins are quite challenging to handle as they are easily susceptible to degradation and destruction. Given that, the employment of ultrasonic nozzles seems quite interesting in this setting. This potential was explored, for example, by the work of Yeo & Park (2004) and Bittner & Kissel (2008). The former produced microcapsules containing a bio-sensitive protein molecule, lysozyme, using a coaxial ultrasonic atomiser. The atomiser allowed a separate flow of the polymer-containing solution and drug-containing solution. When the two met at the tip of the nozzle, ultrasonic vibrations generated droplets of each solution at pre-defined sizes. The droplets then collided to form and arranged into a specific overlapping order based on size, flow rate, and surface tension. The involvement of the ultrasonic atomisation was advantageous to the encapsulation of the protein molecule, offering an overall gentler process to preserve the protein's structure and activity compared to other methods of preparation like emulsification (Yeo & Park, 2004).

The latter research group (Bittner and Kissel, 2008) successfully highlighted the potential of ultrasonic atomisers in generating bovine serum albumin, or BSA, loaded microspheres of PLGA. Because ultrasonic atomisation is known to be of a gentle nature, the integrity of both the drug and the PLGA polymer was restored and was not affected by the process. Tuning

the drug delivery outcomes of the microspheres in terms of loading, release, and morphology was made possible by ultrasonic atomiser by simply adjusting the processing parameters. When compared to microspheres prepared by rotary atomisation, those generated with ultrasonic exhibited a similar glass transition, indicating a similarity between the two. Expanding on the findings of earlier research groups, the research conducted by Ho et al. (2008) advanced the concept of ultrasonic atomisation in drug delivery to new levels. The article highlighted the versatility of ultrasonic atomisation with regards to its applicability from simple large molecule delivery to more sophisticated DNA-based delivery systems.

Ho and co-workers (2008) prepared PLGA microspheres loaded with plasmid DNA under ultrasonic atomiser operating at a frequency of 40 kHz and equipped with a probe. The authors highlighted how careful manipulation of process parameters during ultrasonic atomisation can affect the microsphere properties. For example, several feed flow rates were studied to understand their effect on particle size distribution, which is important for the delivery of the microspheres. Higher flow rates (increased from 18 mL/hr to 90 mL/hr) resulted, unfavourably, in larger microspheres with wider size distribution (Ho et al., 2008). Altogether, the work of the previous groups demonstrated the applicability of ultrasonic atomisation in encapsulating large molecules.

Interestingly, the application of ultrasonic atomisation in drug delivery is not limited to single units but extends to include hybrid or multi-layered systems. Such ability to produce complex delivery systems was demonstrated by the work of Joshi et al. (2023). The authors generated nanoparticles in microspheres by the means of ultrasonic atomisation, allowing for a desirable and consistent control over particle size. The nanoparticles contained anti-cancer drugs, which were piperine and doxorubicin, loaded in PLGA and chitosan nanoparticles, respectively. The nanoparticles were then embedded in alginate-based microspheres. Both phases were conducted by ultrasonic atomisation technology.

Wen et al. (2011) similarly explored the concept of nanoparticles within microparticles, though they developed it in the context of nanocomposite microparticles for injectable cell scaffolds. Nanoparticles made of poly(L-lactide/DL-lactide) and PLGA were prepared and loaded with thrombin receptor activator peptide. Ultrasonic atomisation comes into place by facilitating the encapsulation of the nanoparticles within mPEG-PLGA microparticles. This article further highlighted the applicability of ultrasonic atomisation in complex composite assembly while preserving the integrity of the system (Wen et al., 2011).

It can be inferred from the discussion above that ultrasonic atomisation/nozzle was mainly viewed as a production tool to generate fine particles with uniform size distribution. Unlike this typical application in drug delivery, D'Addio et al. (2012) presented a different utilisation of the technique. The group conceptualised ultrasonic atomisation as a tool to investigate the effect of density on aerodynamic performance of nanoparticles generated by freeze-spray drying for

inhalational delivery. Such an indirect effect arises from the fact that the aerodynamic behaviour is determined by the aerodynamic diameter. The latter is a function of the actual geometric diameter (particle size) and density. To isolate the influence of density (i.e. solute concentration), the geometric size must be constant, which can be easily achieved via uniform droplet formation with ultrasonic atomisation. Hence, ultrasonic assisted spray-freeze drying was used in this context to produce a consistent geometric diameter while varying the density, which can dictate the aerodynamic behaviour of the nanoparticles and their deposition deep in the lungs (D'Addio et al., 2012).

Ultrasonic nozzle has been explored in different settings of spray drying, showcasing unprecedented adaptability. It circulates in application from nano-scale to micro-scale and from conventional spray drying to spray-freeze drying, extending well beyond the encapsulation of proteins to involve engineering of particles and drug delivery systems. This adaptability was well demonstrated by the work presented by Hwang et al. (2023) and Burke et al. (2004).

Hwang and colleagues (2023) proceeded with drying cellulosic nanocrystal into nano-scale particles using ultrasonic nozzle equipped within a nano spray dryer. The authors provided a valuable understanding of how several parameters, namely orifice size, solid concentration, and gas flow rate, can affect particle size and production rate. They also highlighted the fine size in nanometres (300 nm to 5 μm) that an ultrasonic nozzle operating at a frequency of 80-140 kHz can generate if employed within the nano spray dryer.

While still within the context of spray drying using ultrasonic nozzle, Burke and co-workers (2004) provided a comparative analysis between spray drying and spray-freeze drying, both utilising ultrasonic nozzles. Because the methodology between the two varies, operating frequency, power input, and feed flow rate were different for each setting. This created a difference in particle size between the two techniques, with spray drying generating larger particles than spray-freeze drying. Despite that, both systems successfully encapsulated the protein, darbepoetin alfa powder, in PLGA microspheres and achieved a relative control of particle size. It was obvious that the two systems would, nonetheless, produce different particle sizes yet maintain some degree of uniformity within each batch, thanks to the ultrasonic nozzle. This work revealed that ultrasonic atomisation can be a viable technique to encapsulate proteins whilst maintaining their stability.

1.2.6. Implications for Engineering Advanced Carriers via Ultrasonic Atomisation

It can be drawn from the above discussion that the use of ultrasonic atomisation in drug delivery has taken advantage of its ability to provide precise control over droplet and particle size. Thus, particles can be tailored to meet the clinical demands of generating innovative systems that can address the challenges associated with cutting-edge therapeutic agents,

such as PROTACs. The applicability of such systems in the clinical sector needs exploration, with the colon being an ideal site to target molecules with high susceptibility to degradation and efflux.

1.3. Insights into the Potential of Delivery Systems to Achieve Colon Targeting

The clinical application of innovative delivery systems can be investigated via the colonic route. This attempts to bridge the gap between scientific theories behind PROTACs and the delivery of such complex molecules to sites which may help in maximising the therapeutic outcome. Colon-specific targeting is not a new concept but has rather emerged by the end of the 20th century as a drug delivery strategy. Recently, it has regained interest as a promising site, especially with the breakthrough of biologics and targeted therapy. This interest was mainly driven by colonic diseases becoming a global concern with many newly diagnosed cases. Statistics show that colorectal cancer accounts for 9.6% of total cases globally, with 1.9 million new cases in 2022 (Ferlay et al., 2024). This ranks it as the third most commonly diagnosed cancer. Meanwhile, it is ranked second in terms of cancer-related mortalities (Marcellinaro et al., 2023). This indeed reflects a need for effective management and adequate drug delivery, particularly a massive necessity for developing new technologies with a capability of targeting the large intestine whilst minimising undesirable release in the upper gastrointestinal tract (GIT).

Colon-targeted delivery offers various therapeutic advantages that are not only confined to enhancing the treatment of local colonic ailments such as Crohn's disease and ulcerative colitis but also broadened to include delivering proteins and peptides for systemic therapy (Philip & Philip, 2010). In fact, the colon attracted additional attention as a potential site for achieving delayed onset of drugs that treat diseases associated with circadian rhythm (Vemula, 2015).

Ideally, a colon-targeted delivery system should deliver the drug load to the proximal colon while retarding release in upper GIT (Basit, 2005). Because the colon offers a less hostile environment with fewer digestive enzymes compared to the upper GIT and better engagement with absorption enhancers, selective colonic delivery protects proteins, peptides, and drugs from degradation, resulting in fewer systemic side effects, lower dose, and increased bioavailability (Basit, 2005; Nguyen et al., 2019).

A number of physiological features led to an increased interest in exploiting the colon as a delivery site. These include the almost-neutral pH, abundancy of microflora, and long residence time (Basit, 2005). Thus, the physiological properties of the colon were considered during the development of colonic delivery systems, and consequently, several strategies were proposed. Most of the proposed early technologies depended on pH difference across the GIT, variability in gastrointestinal transit time, and enzyme-secreting colonic bacteria (Amidon et al., 2015). In fact, numerous research papers discussed approaches to selectively deliver drugs to the colon. These approaches had their own limitations that include dependency on the individual's physiological factors. These factors are affected by inter- and intra-subject variability. Hence, the required selectivity was not achieved, and premature

release was a concern. The development of novel colonic delivery systems with increased specificity and suppressed premature drug release was therefore deemed necessary.

Despite the ongoing research activity, only few technologies were marketed, most of which were conventional dosage forms utilising traditional colonic delivery approaches or combinations of these. Given that multiparticulates travelled down the GIT and distributed more uniformly with decreased likelihood of dose dumping and incomplete drug release (Basit, 2005), it was evident that the focus of colonic delivery at that time tended to revolve around multiparticulates with combination strategies, the field of nanoparticles, or some novel targeting mechanisms (Amidon et al., 2015; Guo et al., 2018).

1.3.1. Colon-targeted Drug Delivery Approaches

Colon-targeted systems can be categorised roughly into conventional strategies which include pH-dependent systems, time-controlled approaches, and microbially-triggered strategies as well as novel approaches that typically explore other features of the colon or combine several strategies together. These will be discussed in detail in the next few sections.

1.3.1.1. Conventional Strategies

A. pH-dependent Systems

Dosage forms designed with a pH-sensitive coating or material were extensively explored and are still dominant with some modifications (Garcia-Couce et al., 2019). Such dosage forms are based on the varying pH across the GIT, starting with a highly acidic pH of 1-2 in the stomach and increasing gradually to 6.5 and 7.5 in the duodenum and distal small intestine, respectively (Philip and Philip, 2010). However, the large bowel is characterised by a near neutral pH that fluctuates among the different segments of the colon (Amidon et al., 2015). The pH drops from 7.5 at the ileum and the proximal colon to as low as 5.7 in some diseased individuals but rises again to 6.6 in transverse colon and, finally, to 7 in the descending colon (Philip and Philip, 2010).

This difference in pH is exploited for site-specific delivery through coating systems with pH-sensitive polymers. These polymers remain intact in acidic areas but begin to slowly release the drug upon reaching the triggering pH in the colon (Philip and Philip, 2010). Yet, premature drug release was noted with some formulations, indicating the loss of specificity. This was attributed to the effect of food and diseases on pH (Vass et al., 2019). For example, reduced colonic pH is observed in patients with ulcerative colitis, contributing to the failure of the system to release the drug (Vass et al., 2019).

The most common pH-sensitive polymers used are polymethacrylates, commonly known as Eudragit. These polymers come in various grades with different solubilities, such as Eudragit S100 and Eudragit L100 (Nguyen et al., 2019). A commercial example is Claversal®, where

tablets containing mesalamine intended to treat patients with irritable bowel disease (IBD) were coated with Eudragit L-100. In one study, the colonic release of Claversal® was investigated, whereby 70% of the tablets released the drug three hours after administration. The formulation could be further improved by incorporating another polymeric coating that dissolves at a pH >7 or by increasing the thickness of the single coat to delay the disintegration further (Prasanth et al., 2012).

Other single pH-responsive coatings were reported in literature. For example, Naeem and colleagues (2015) investigated the ability of polymeric nanoparticles made with Eudragit FS30D for colon targeting. Results showed that the polymer protected the drug load in acidic environment, but almost the entire dose was released at the ileum (Naeem et al., 2015). Similar findings were reached in two other studies, where formulations coated with Eudragit ES for colonic targeting showed immediate release of metronidazole in the small intestine (Shah et al., 2016) while almost the full dose of indomethacin was released within six hours of administration from nanoparticles coated with Eudragit S100 (Yiming & Allan, 2014).

Based on analysing the aforementioned studies, it could be concluded that a single pH-sensitive coating may not efficiently deliver the drug load to the colon. This could be ascribed to the close similarity in pH values between the small intestine and colon (Cai et al., 2020).

Various solutions have been proposed to overcome the early drug release in upper GIT from single triggered systems. Generally, the contributions presented in literature revolved around integrating several colon targeting approaches (Vemula, 2015). As discussed by Naeem et al. (2015), nanoparticles prepared using a combination of pH and time dependent polymers were superior to single triggered systems, with higher colonic specificity, more efficacious control of colitis, and enhanced localisation of drug in the inflamed colon. A sustained release of the drug was noted, with more than 80% of the drug being released over a period of 24 hours (Naeem et al., 2015).

In a similar manner, the study conducted by Jin et al. (2016) combined pH and enzyme-based techniques in a single formulation. Chitosan-based microparticles were coated with EudragitS100, showing 71% of drug release when exposed to caecal contents in the colon while maintaining drug release to less than 4% in upper GIT (Jin et al., 2016). Combination techniques also included integrating different types of pH-responsive systems in a multilayer fashion; however, these coatings accounted for a high percentage of the tablet weight and were time consuming (Nguyen et al., 2019). Instead, a paper by Nguyen and colleagues (2019) represented another contribution by designing a single-layer pH-sensitive coating of two polymers. In this paper, an attempt was made to formulate a one-layer coat from Zein and Kollicoat®, where the latter dissolved at a pH above 5.5. Together in a ratio of 4:6, Zein and Kollicoat® coating released 70% of the load within 45 minutes of colonic arrival with as low as 10% being released in the upper GIT (Nguyen et al., 2019). The ratio of each component to

the other and the coating thickness were crucial for the success of the formulation (Nguyen et al., 2019). It is important to point out that the applicability of such a coating requires further *in vivo* investigations.

B. Time-dependent Strategies

A time-controlled system is based on the principle of gastrointestinal transit. While the residence time in the stomach varies, the transit time across the small intestine is relatively constant of around three to four hours (Amidon et al., 2015). Guided by this information, formulations were developed to release drugs in the colon after a predetermined lag time of about six hours, taking into consideration the overall transit time.

Investigations were performed by Naeem et al. (2015), where the drug release from nanoparticles was controlled by Eudragit RS100, a time-dependent polymer. Results proved that, irrespective of the pH, this single time-dependent polymer was not suitable for colonic delivery as 70% of the drug was released before reaching the colon (Naeem et al., 2015).

Yet, in a different study, another time-dependent polymer, hydroxypropylmethylcelluose or HPMC, was proven to successfully deliver the loaded tablets to the colon (Vemula & Veerareddy, 2012). Applied as a coating by compression, HPMC allowed for a lag time of around four hours, during which a small amount (<7%) of the drug was released (Vemula & Veerareddy, 2012). Noticeably, the degree of HPMC viscosity affected drug release, where polymers with low viscosity grades failed to prevent premature release since 80% of the dose was found in upper GIT (Vemula & Veerareddy, 2012).

The latter finding is in accordance with a study conducted by Vemula (2015). Compared to the previous study, a more viscous HPMC was used to formulate mini tablets with an additional pH-sensitive coat compressed on top. Due to the increased viscosity of the time-dependent polymer and the extra pH-responsive coat, drug release in this study was superior as the premature release was minimised to less than 4% over a period of five hours (Vemula, 2015). Both studies agreed that as the viscosity of HPMC increases, the drug release decreases (Vemula, 2015; Vemula & Veerareddy, 2012).

From the discussion above, it could be concluded that the efficacy and colonic selectivity of single time-dependent formulations is controversial as they release the drug once the predetermined time is reached regardless of the site. Additionally, the transit time of a dosage form, particularly the time at which it reaches the colon, cannot be precisely determined due to variations in gastric emptying and gastrointestinal transit. They are influenced by formulation properties such as size and shape, fasted/fed state, and health status (Basit, 2005). It was noted that patients with IBD or diarrhoea experience a faster colonic transit, affecting drug release (Philip and Philip, 2010). Moreover, a delayed transit occurs often during night time in comparison with daytime (Basit, 2005).

Pulsincap is an experimental technology that adapts this strategy. It is composed of a capsule with a soluble cap and an insoluble body that harbours the drug and a hydrogel plug. Upon exposure to the intestinal fluids, the cap dissolves followed by swelling of the plug. The plug is engineered to swell for a predetermined time before ejection and subsequent drug release. A study involving 23 patients was conducted to assess the performance of Pulsincap systems engineered to release at pre-set time of 5 hours. Gamma scintigraphy revealed premature release in the stomach and small intestine in seven patients whereas successful colonic release either in the proximal or distal colon was achieved with the rest (Basit, 2005).

Another marketed time-dependent technology is OralogiK™ (BDD, 2020). It is composed of a barrier layer that is programmed to erode gradually in accordance with a pre-determined lag time, which can be adjusted to suit colon-targeted purposes.

C. Microbially-triggered Systems

Unlike the stomach and small bowel, the largest microbial community inhabits the colon as it houses more than 400 species of bacteria (Prasanth et al., 2012). This microbial density is dominated by anaerobic bacteria (e.g. Bacteroides) that function to produce energy by secreting enzymes, such as azoreductases and glycosidases, to ferment undigested polysaccharides. These undigested polysaccharides resist upper GIT degradation but are susceptible for colonic microbial digestion by being employed in polymers, coatings, or drug conjugates. Once such a formulation reaches the colon, the polymer is subjected to degradation by the residing microorganisms (Prasanth et al., 2012). The presence of these enzymes only in the colon imparts selectivity to drug carriers, exploiting colonic microbes as release triggers (Amidon et al., 2015).

Prodrugs were studied for colonic delivery, and many were marketed. To achieve site-specificity, the drug is conjugated with a moiety and is then cleaved only by enzymatic activity in the colon. However, this approach is highly dependent on chemical modification and the presence of certain functional groups, hindering its practical utility (Barea, 2012). Moreover, prodrugs are recognised as new chemical entities and hence require further costly clinical evaluation compared to the parent compound (Amidon et al., 2015).

Another way to utilise microbial triggers is to entrap or coat drugs using biodegradable polymers, such as azo-containing polymers. They are degraded by azoreductases, but toxicity concerns were raised against such synthetic polymers. Thus, natural polysaccharides (e.g. pectin and dextran) are safer alternatives that can be used to fulfil this function (Philip & Philip, 2010).

Polysaccharide-based systems were developed with several advantages, namely biodegradability and availability (Amidon et al., 2015). Despite that, they are not ideal carriers due to their hydrophilic nature and swelling capability, and physical or chemical modification

is necessary (Wang et al., 2020). To illustrate the need for polysaccharide modification, Zhu et al. (2019) prepared beads with porous starch, pectin, and chitosan. *In vitro* release investigations revealed 67% drug release before reaching the colon from single pectin beads, indicating the lack of selectivity attributable to swelling of pectin. Meanwhile, addition of porous starch to pectin-based beads significantly hindered premature release to as low as 17% which was further decreased to 13% by the addition of chitosan. Although the system was successful in minimising premature release, testing in simulated colonic fluid with the presence of enzymes would provide a more precise simulation.

In contrast, Oliveira et al. (2010) demonstrated the need for additional release controllers to prevent early drug release from pectin/chitosan-based system and aid microbial activation in colon. Without enteric polymers, the system released almost 60% of the drug load within five hours (Oliveira et al., 2010). This suggested that future research remains indeed open for further optimisation of microbially-based systems.

1.3.1.2. Other Approaches

Given the limitations of conventional approaches used in colon-targeted delivery, selective targeting is still an area for research and innovation to develop optimal colonic formulations with enhanced therapeutic efficacy, maximum specificity, and minimal side effects. For example, pressure stimulated delivery systems have been developed, given the higher luminal pressure within the colon compared to the small intestine as a result of peristaltic activity (Amidon et al., 2015).

On the other hand, osmotically-driven devices were recently employed for colonic delivery. Alza corporation invested in OROS®-CT as a technology that utilises osmotic pressure to deliver agents to the colon. In these systems, drug release is triggered when water diffuses into the push compartment through the semipermeable membrane, causing it to swell. The swelling forces the drug to be released through an orifice. To achieve colonic specificity, the swelling is manipulated to allow drug release after a period of four hours following gastric emptying (Amidon et al., 2015).

Another feature of the colon being exploited in literature is its thick mucus layer formed by negatively charged mucins (Duan et al., 2016). Mucoadhesion facilitates the contact between the delivery system and colonic mucosa and increases the retention time (Lu et al., 2016). Based on this concept, Jelvehgari et al. (2014) and Bigucci et al. (2010) designed microspheres composed of polysaccharides. In general, the combination of different polysaccharides showed increased adhesion to mucosal membranes in simulated intestinal fluids as compared to gastric media. This could be attributed to the ionisation of carboxyl moieties of the polymer at higher pH values and gel formation (Bigucci et al., 2010; Jelvehgari et al., 2014). The latter facilitated the adhesion of the system to the colonic mucosa. The point

made by these studies regarding mucoadhesion was valuable as it can be combined with any other colon targeting approach for further enhancement of selective drug release (Bigucci et al., 2010; Jelvehgari et al., 2014).

Lipid-based formulations have been of interest for colon-targeted delivery, but the role of bile salts and pancreatin in digesting the lipid bilayer and causing noticeable premature leakage could not be overlooked. For example, liposomes coated with Eudragit S100 as a single pH-responsive polymer were not selectively releasing the drug in the colon due to the degradation of lipid bilayer by the bile acids. Thus, an attempt was made to improve the liposomal formulation by coating it with chitosan followed by encapsulation in Eudragit-coated microspheres (Barea, 2012). Dissolution studies showed that liposomes in microspheres remained intact and resisted degradation in upper GIT with negligible drug release unlike chitosan-coated liposomes, in which 60% of the drug was prematurely released (Barea, 2012). Likewise, a liposomal carrier coated with aminoclay and Eudragit S100 protected the system from acidity with as low as 10% released at pH 1.2 while higher drug release was noted at pH 7.4 (Kim et al., 2020).

Moreover, another distinctive feature of the colon is its low redox potential, indicating that the large bowel is a reducing environment (Lim et al., 2013; Ng et al, 2020). Given that, stimuli-responsive polymers were designed to release their drug load at colonic sites after responding to redox changes. Azo- and disulphide-based polymers are two examples (Lim et al., 2013; Ng et al., 2020). For example, Ng and co-workers (2020) measured thiol concentrations in simulated fluids and noticed a ten-fold increase in thiol concentration in the colonic fluid in the presence of bacteria compared to upper GIT (Ng et al., 2020). This indicated the likelihood of colon-selective reduction process, leading to a possible application in drug delivery.

Recent advancements in colon-specific delivery involved the use of mesoporous nanomaterials. They have been widely adopted as carriers for their large surface area and tuneable pore properties that increase dug loading capacity in addition to their biocompatibility, stability, and ease of tailoring in terms of size and surface functionalisation (González-Alvarez et al., 2017; Kumar et al., 2017; Tian et al., 2017). Drugs are incorporated within the pores of mesoporous nanoparticles and are capped or gated by different materials that allow drug release upon exposure to certain stimuli (Kumar et al., 2017).

Mesoporous silica nanoparticles (MSN) capped with guar gum for colon-specific delivery of 5-florouracil were investigated by Kumar et al. (2017). Without the presence of enzymes, a favourable profile of no release was achieved in simulating media whereas drug release was triggered upon the incubation of the system with colonic enzymes (Kumar et al., 2017). Although the idea presented by Kumar and colleagues (2017) is quite promising for future application of MSN in colonic diseases, a closer examination showed that further *in vivo* assessment would generate more reliable results.

The views presented by González-Alvarez et al. (2017) were more accurate since *in vivo* studies were conducted on a proposed capsule formulation. The group prepared three safranin O-loaded MSNs that are either capped with a lipid bilayer (F1) or coated with disulphide-containing polymer (F2) or starch derivative (F3). In line with the previous study, almost zero drug release was observed with F2 and F3 in the absence of the appropriate stimulus (González-Alvarez et al., 2017). Upon exposure to stimuli, F1 and F2 released 80% of their drug load immediately within 20 minutes whereas the same amount was released over a longer period for F3. Compared to free drug, MSN increased the drug levels intracellularly, with F3 achieving the optimal performance. Further encapsulation of F3 in a pH sensitive polymer, Eudragit FS 30D, showed a higher distribution to the colon (65%) compared to other organs, indicating colonic targeting capability (González-Alvarez et al., 2017).

A similar approach was adopted by Tian et al. (2017), whereby MSNs were capped with a pH-sensitive polymer called polyacrylic acid (PAA) for colonic delivery. The authors are to be acknowledged for using PAA as a gate keeper for the following reason. Contrary to the general agreement that drug loading capacity depends on surface area and pore volume (González-Alvarez et al., 2017; Kumar et al., 2017), Tian and colleagues (2017) made a new contribution to the field by adopting the concept of increasing the drug loading capacity through electrostatic interactions between the MSN and the drug load. Because PAA is negatively charged, and doxorubicin is positively charged in a neutral medium, the resulting electrostatic interaction lead to an increase in drug loading (Tian et al., 2017).

Several attempts were made to combine all of the aforementioned techniques to enhance specificity and overcome the limitations. Accordingly, the collaborative effort of a group of researchers in London resulted in a new technology that combines pH-dependent and microbially-stimulated approaches. The technology is named Phloral®, whereby Eudragit S and resistant starch were integrated into a single coating that surrounds the drug core. This technology is characterised by a dual trigger mechanism that ensures the precise delivery of the drug load to the colon irrespective of the feeding status. It adopts the “fail-safe” concept such that if the pH required to trigger drug release is altered, the enzyme-dependent mechanism compensates and works to achieve the target. Results from gamma scintigraphy proved the colonic specificity of this system. Thus, Phloral® shows superiority by surpassing the limitations of conventional delivery systems (Varum et al., 2020).

Furthermore, a company called Intract Pharma was able to expand the application of Phloral® technology into a system called Soteria®. This modified version has a permeability enhancer included within the formulation, where the drug or peptide and the enhancer are present together in the core while coated on the exterior with Phloral®. The enhancer incorporated within the core has a unique dual action as it does not only enhance the permeation of the product into the colonic tissues but also functions to protect the molecule from degradation as

it travels down the alimentary tract, allowing safe oral delivery of biologics. Phloral® coating then ensures delivery to the colon through the mechanism described earlier (Intract Pharma, 2020).

One of the early technologies utilising combination strategy is CODES™ (Katsuma et al., 2002). It is composed of a core containing the drug and lactulose. The latter is degraded by bacterial enzymes present specifically in the colon. The formulation is double coated with Eudragit E (acid soluble) and Eudragit L (acid insoluble) as the inner and outer coats, respectively. After administration, the tablet is protected from acidic environment of the stomach. However, the enteric coating disappears as the formulation enters the small intestine. Once in the colon, microflora begin to ferment lactulose into lactic acid. This acidic product lowers the pH of the colonic medium and facilitates the dissolution of Eudragit E. Drug release finally follows (Katsuma et al., 2002).

Evonik, a leading pharmaceutical company, announced the development of Eudratec™ COL that is designed with aim of providing sustained drug release during colonic transit. It is composed of two separate coatings that function differently. pH-dependent enteric coating protects the formulation throughout its gastric residence period but allows drug release to start upon reaching the ileum at a pH of 7. Eudragit FS 30D is incorporated for this purpose. Meanwhile, the inner coating layer is composed of Eudragit RL/RS and is only able to release the active pharmaceutical agent in a sustained manner when reaching the colon through diffusion (Evonik, 2020).

1.4. Research Aims and Objectives

[redacted from open access thesis]

The objectives of this research are presented for each chapter as follows:

Chapter 2: *[redacted]*

Chapter 3:

- To demonstrate MESOPAC's ability in acting as dissolution enhancing technology for novel medium-sized molecules like MZ1

- To characterise MZ1 and evaluate its loading efficiency into MESOPAC

Chapter 4:

- To identify different polysaccharides with potential for colonic delivery

- To translate the CAB mesoporous carrier into a colon-specific delivery system using guar gum as a capping agent and assess its release in different dissolution media simulating the GIT

- To explore and optimise different techniques for preparing a colonic technology using mesoporous particles combined with polysaccharides

- To adjust the parameters and establish a correlation in release profile between small-volume dissolution vessels and large-volume setup involved in assessment of enzyme-triggered systems for colon delivery

- To implement the optimal formulation design in the delivery of a model PROTAC to the colon

[Chapter Two (redacted from open access thesis]

Chapter 3

Loading Novel Mesoporous Carrier with PROTACs: A Study to Enhance the Dissolution of MZ1 for the Potential Treatment of Colorectal Cancer

Publications related to chapter 3

Alshatti, S., Al-Khattawi, A. & Al-Rifaie. (2023). Are we ready to formulate the next generation of small targeted therapeutics? *International Biopharmaceutical industry*, **6**(2): 24-25.

3.1. Introduction

Interest in proteolysis-targeting chimeras (PROTACs) is growing over their potential to mediate degradation of undruggable oncogenic protein targets through engaging with the body's ubiquitin proteasome system. The bromodomain and extra-terminal (BET) family of proteins are identified as new therapeutic targets in oncology that regulate gene transcription and consist of the following members: BRD2, BRD3, and BRD4 (Zengerle et al., 2015). Aberrant expression of BRD4, in particular, mediates the development of cancers that include acute myeloid leukaemia, neuroblastoma, breast cancer, and colorectal cancer (Cimas et al., 2020; Otto et al., 2019; Zhang et al., 2022b).

The expression of BRD4 in colorectal cancer is of importance to this study, given that the technology developed herein is intended later for colon-targeted delivery. Previous studies have demonstrated an increased expression of BRD4 in cancerous colon cell lines versus healthy colon cells (Hu et al., 2015). Being a transcriptional regulatory protein, BRD4 controls the transcription of MYC oncogenes, whose over expression is commonly associated with colorectal cancer (Otto et al., 2019). Hence, degradation of BRD4 by the PROTAC molecule MZ1 down regulates this oncogene, affecting cell proliferation and viability of colorectal tumour cells. This degradation effect was demonstrated by the work of a group of researchers who investigated the effect of BRD4 inhibitor, JQ1, and BRD4 degrader, MZ1, on the expression of MYC oncogene mediated by BRD4 in several colorectal cell lines (Otto et al., 2019). In seven of the tested colorectal cell lines, concentration dependent depletion of BRD4 by MZ1 was observed, and subsequent down regulation of MYC was reported (Otto et al., 2019). In light of this, research has proved that BRD4 plays a crucial role in the pathogenesis of colorectal cancer. Therefore, the development of BET-targeting PROTACs, for example MZ1, have received increased attention from researchers and, particularly, from our research group due to the fact that MZ1 can be recognised as a future PROTAC to target to the colon.

MZ1 is considered the first-in-class molecule that utilises the VHL E3 ligase to knockdown BET proteins (Tang et al., 2023). It links JQ1 inhibitor and E3 ubiquitin ligase VHL and was chosen as the model VHL-based molecule that targets the degradation of BRD4 (Zengerle et al., 2015). Similar to other PROTACs, MZ1, with a molecular weight of 1002.640 Da, is considered a molecule that violates Lipinski's rule of five (see **Figure 3.1**) and, subsequently, resides beyond the rule of five chemical space (Madan et al., 2022). Because of the properties imposed by this chemical space, MZ1 comes with its own set of formulation challenges. This includes low solubility and permeability, all of which hinder its effective translation into a therapeutic molecule in the market. Of importance, MZ1 is considered a poorly soluble molecule since its calculated log S (mol/L) is -4.42 (Jiménez et al., 2022), and only 19 µg/mL

of MZ1 is soluble at physiological pH (Opnme, 2025). Therefore, solubility enhancement technologies can improve the dissolution of MZ1 and increase its oral bioavailability.

It is estimated that 90% of drug molecules compromising the pharmaceutical pipeline are poorly soluble (Le et al., 2019). This is not only limited to small molecules but also includes mid-sized molecules such as MZ1. Although formulation technologies to facilitate the delivery of MZ1 are clearly deemed necessary, their integration into research has been poorly addressed, with only few attempts being published to date.

Cimas and colleagues (2020) worked to improve the pharmacokinetic profile and site-specific delivery of MZ1, with a focus on assessing the cytotoxic effect of the molecule on breast cancer cells. The group reported encapsulating MZ1 in polymeric nanoparticles that were further conjugated with trastuzumab to treat positive human epidermal growth factor receptor 2 breast cancer. Compared to neat MZ1, the conjugated nanoparticles containing the PROTAC revealed stronger cytotoxic effect against MZ1 resistant cell lines. This could be attributed to improved internalisation and uptake by the cells that resulted in releasing most of drug molecules at the affected site upon conjugating the drug-loaded nanoparticles with trastuzumab (Cimas et al., 2020).

With no articles addressing the use of polymeric mesoporous particles to enhance solubility of molecules, MESOPAC emerges, herein, as a pioneer technology in the field of PROTAC delivery, particularly oral delivery. To date, this chapter is the first to discuss the oral delivery and solubility enhancement of MZ1, specifically through the use of mesoporous particles for this purpose.

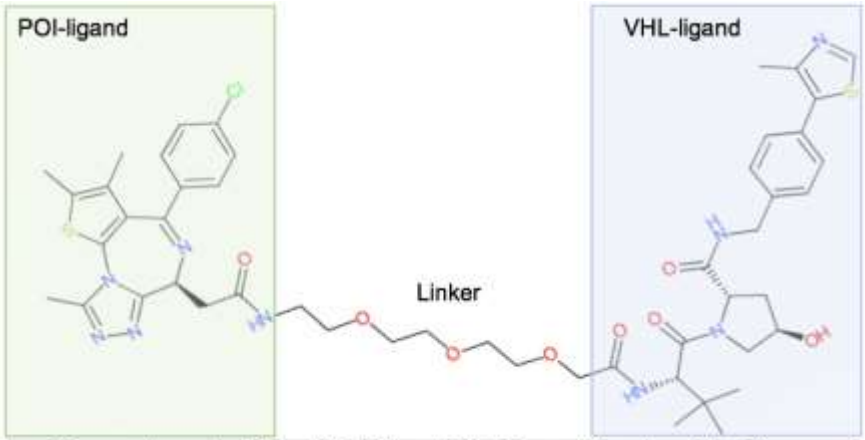

Parameter	Lipinski's Rule of Five	MZ1 Properties	Violations
Molecular weight	<500 Da	10002.64 Da	Yes
Number of hydrogen bonds	<5	4	No
Number of hydrogen bond acceptors	<10	>10	Yes
Log P	<5	5.23	Yes

Figure 3.1. *2D chemical structure of MZ1. The table shows how MZ1, as a model PROTAC, violates Lipinski's rule of five (Redrawn based on IUPHAR/BPS Guide to PHARMACOLOGY (n.d.))*

The objectives of this chapter were as follows:

- To develop a proof-of-concept of whether the novel porous particles can address the delivery challenges associated with poorly soluble PROTACs intended for oral delivery

- To provide a better understanding of the carrier's practical applications with regards to loading a variety of therapeutic molecules and acting as a solubility enhancing technology

- To improve the solubility and oral delivery of a model PROTAC, MZ1, that targets colorectal cancer cells

3.2. Materials and Methods

3.2.1. Materials

Mesoporous particles were engineered in-house using spray drying. MZ1 was purchased from Broad Pharm based in California, United States. Ethanol 99.8% (HPLC grade) and acetonitrile were bought from Fisher Scientific located in Loughborough, UK. Sodium dodecyl sulfate, sodium phosphate monobasic monohydrate, and phosphoric acid were all purchased from Sigma-Aldrich in Dorset, UK. Sodium phosphate dibasic heptahydrate was obtained from Acros Organics via Fisher Scientific in UK. Ammonium acetate was bought from Fluka Analytical via VWR (Leicestershire, UK). When needed, purified water was supplied by Elga Purelab Prima system (High Wycombe, UK).

3.2.2. HPLC Method Development of MZ1

HPLC method development of MZ1 was conducted using WATERS e2695 device (Massachusetts, USA). The method was based on the procedure reported by Jiménez and colleagues (2022) with some modifications. The device was run at an injection volume of 40 µL with a flow rate of 1.2 mL/min. The mobile phase consisted of ammonium acetate buffer and acetonitrile mixed in a ratio of 40:60, respectively. A C18 column with dimensions of 15 cm x 4.6 mm and particle diameter of five µm was used (Restek, UK) with the ultraviolet detector being set at 261 nm.

The analytical method validation was performed following the ICH guideline, whereby the following parameters were assessed: Specificity, linearity, range, precision, accuracy, limit of detection, and limit of quantitation (ICH, 1997).

The specificity of the method was determined by running a known concentration of MZ1 (100 µg/mL) against a blank and comparing the two chromatograms to ensure no interference with analytical peak.

The linearity of the method was studied by performing serial dilutions of a stock solution containing MZ1 in mobile phase solution to achieve concentrations of 100, 50, 25, 12.5, 6.25, 3.125, 1.6, and 0.8 µg/mL. The dilutions were conducted in triplicate. Linear regression analysis was done to obtain a correlation coefficient above 0.999, and the range with which the samples were linear was determined.

Precision of the HPLC method was evaluated as intra-day repeatability. One concentration of 12.5 µg/mL, with six replicates, was chosen to determine the precision of the analytical procedure. Mean peak areas, standard deviation, and relative standard deviation were determined. The relative standard deviation was calculated as (SD/mean) x100.

Similarly, the accuracy of the method was investigated using three replicates of three concentration levels within the range (25, 50, and 100 µg/mL). The mean percentage recovery and RSD value of MZ1 were calculated and reported. Lastly, the parameters LOD and LOQ

were determined. From the calibration curve, the calculations for these parameters were derived from the slope of the graph as well as the standard deviation of the y-intercepts of regression line following the equations below (Albadarin et al., 2017):

LOD= 3.3*(σ/S)
LOQ= 10*(σ/S)
Where σ = the standard deviation of the intercept and S = the slope of the calibration curve

3.2.3. Loading MESOPAC with MZ1 by Spray Drying

Spray drying was chosen as the technique to load MZ1 into mesoporous carrier and evaporate the solvent following the method reported by Le at al. (2019) with some modifications. Initially, feed suspensions were prepared at two drug loads, 5.5% and 15.6% (w/w). At a drug load of 5.5% (w/w), MZ1 was dissolved in ethanol to create a solution at a concentration of 4 mg/mL. It was then followed by the addition of the mesoporous carrier. Similarly, for a drug load of 15.6% (w/w), a suspension of MZ1 with ethanol and MESOPAC was created. The resulting suspensions at both drug loads were subjected to constant stirring for 24 hours to impregnate the pores with the drug molecules. The samples were then subjected to spray drying using Buchi B-290 mini spray dryer apparatus fitted with a two-fluid nozzle from Flawil (Switzerland). The flow rate at which the feed samples were pumped was set at 1 mL/min. Operating in a closed mode was necessary. The samples were exposed to drying at an inlet temperature of 60°C. The outlet temperature, on the other hand, fluctuated between 45°C and 48°C. The atomising gas was flowing at 600 L/hr while the aspiration rate was maintained at 35 m^3/hr (equivalent to 90%). MZ1-loaded mesoporous particles were then collected, weighed, and subjected to analysis.

3.2.4. Loading Efficiency and Drug Load Quantification

The amount of MZ1 embedded within the mesoporous particles was quantified using WATERS e2695 HPLC apparatus (Massachusetts, USA) following the method described earlier. Initially, samples containing MZ1 were weighed and followed by the addition of 10 mL of acetonitrile. They were, then, left on the stirrer for 15 minutes to ensure full dissolution. Full dissolution was ensured because both the carrier and MZ1 are soluble in acetonitrile, and visual inspection confirmed the absence of undissolved particles. The resulting solutions were filtered and placed into HPLC vials for analysis (ThermoFisher Scientific, Langerwehe, Germany). MZ1 molecules that were successfully entrapped within the pores were quantified by calculating the amount from the obtained peak area. The analysis was carried out in triplicate. According to the equations listed below (Goelo et al., 2020; Le at al., 2019), the loading efficiency and product yield were determined:

Loading efficiency (%) = $\frac{Actual\ drug\ load}{Theoritical\ drug\ load}$ x 100

Product yield (%) = $\frac{Mass\ of\ dry\ powder\ obtained\ in\ spray-dryer}{Total\ mass\ of\ raw\ materials\ used\ in\ the\ feed\ solution}$ x 100

3.2.5. Morphology Assessment Using Scanning Electron Microscopy

The morphological characterisation of MZ1-loaded MESOPAC and raw MZ1 was conducted using SEM. Crude MZ1 was studied at magnifications of 300x and 1000x while micrographs of MZ1-loaded particles were captured at 1000x, 6000x, and 15000x. The scanning electron microscope (ZEISS, Germany) functioned at a voltage of 3.00 kV for raw MZ1 and 5.00 kV for drug-loaded mesoporous particles. Before imaging began, the samples (approximately 1 mg) were mounted on an adhesive slip and coated with a very thin layer of gold coating. Micrographs of each specimen were then obtained.

3.2.6. Morphological Assessment Using Raman Spectroscopy

The distribution of the PROTAC molecule within the carrier's porous network was visualised by the aid of Raman spectroscopy. Confocal Raman spectra of the empty mesoporous carrier, raw MZ1, and the drug-loaded MESOPAC at both drug loads were obtained via Renishaw InVia Qontor confocal Raman microscope coupled to a high-performance spectrometer (Gloucestershire, UK). The laser beam was excited at a wavelength of 830 nm with a power of 100%. An objective lens with 50x magnification was used. The resulting spectra were recorded over a range of 400-3200 cm^{-1} and overlaid to identify the peaks of interest. These peaks were then integrated using a calibration curve, from which the drug load in each sample was quantified. A strong correlation (0.994) was achieved between the intensity signals and MZ1's drug load. Renishaw WiRE software (version 5.4) was used to conduct the analysis.

To obtain the color-coded images that highlight the distribution of the drug within the carrier particles, stimulated Raman scattering (SRS) was employed. The imaging was conducted using Leica SP8 microscope (Milton Keynes, UK) that was fitted with PicoEmerald-S laser system. The laser system consisted of two laser beams, the Stokes and the tuneable pump beam. The former was set to operate at a wavelength of 1031 nm. The laser power was kept at 20-30%. The system was also composed of the objective lens at 40x with a numerical aperture of 1.1 (Lieca, UK) and an oil condenser lens with a numerical aperture of 0.9 (Lieca, UK). The signals generated were detected by transmission mode using an ultra-high frequency lock in amplifier by Zurich Instruments (Zurich, Switzerland), and the images acquired were analysed via Leica LAS-X software. Mapping of the images was performed to generate color-coded regions that resemble either the carrier particles or the drug.

3.2.7. Thermal Behaviour Characterisation Using Differential Scanning Calorimetry

The thermal behaviour of MZ1 prior to and after loading into mesoporous particles in comparison to unloaded carrier was investigated using differential scanning calorimeter TA Q200 (New Castle, USA). Any endothermic or exothermic events, either before or after

loading, were identified from the thermograms obtained. The analysis was completed with the aid of TA universal analysis 2000 software (version 4.5). A tzero low mass aluminium pan (TA Instruments, UK) was filled with approximately 2 mg of each sample. The samples were then subjected to heating using the conventional heating cycle alongside a reference pan within a temperature range of 50 to 250°C. The heating rate was set at 10°C/min while the nitrogen air was flowing at a rate of 50 mL/min. Heat-cool-heat cycles were conducted as well under the exact same conditions but within a temperature range of 50 to 200°C to further understand the thermal behaviour. Each sample was analysed thrice.

3.2.8. Solid State Characterisation Using X-ray Powder Diffraction

Following the method reported by Pöstges et al. (2023), powder X-ray diffraction (XRD) patterns were obtained via Rigaku 6 Miniflex diffractometer (Tokyo, Japan) using Cu Kα radiation source. Prior to analysis, powder was placed into a small volume sample holder having the following dimensions: 5 mm x 0.1 mm (diameter x depth). The samples were then analysed over an angular range from 5–45° (2θ) at a scanning step size of 0.017°. Meanwhile, the device was set to operate at a voltage and current of 45 kV and 40 mA, respectively.

3.2.9. Porosity Assessment of MZ1-loaded MESOPAC

To assess the changes in porosity before and after loading, gas adsorption porosimetry was performed on loaded samples and MESOPAC via Quantachrome Nova2000 Touch LX2 surface area and pore size analyser (Florida, USA). Nitrogen adsorption-desorption isotherms were generated within a pressure range of 0-0.99 P/P0 at a temperature of 77 K. Data were analysed to estimate the pore size, pore volume, and specific surface area of the samples. Prior to analysis, 200 mg of each sample was degassed at 100°C. The degassing was meant to be carried out under vacuum for as long as 24 hours. BET and BJH methods were selected to determine the specific surface area and pore size distribution of the samples, respectively (Brunauer et al., 1938; Barrett et al.,1951). The specific surface area was obtained at a relative pressure of 0-0.3 P/P0. On the other hand, the total pore volume was measured from a single point of nitrogen adsorption at a relative pressure of 0.99 P/P0.

3.2.10. *In Vitro* Release of MZ1 and MZ1-loaded MESOPAC

To explore the release behaviour of the raw MZ1 and MZ1-loaded porous carrier for oral delivery, *in vitro* release studies were performed in environments that simulate the small intestine. Careful selection of the pH values was made to closely resemble the biological environment (Pöstges et al., 2023). A 0.05M phosphate buffer of pH 6.8 was chosen as the dissolution medium in attempt to mimic the conditions of the small intestine (Pöstges et al., 2023). However, 0.3% (w/v) of sodium lauryl sulfate was added to the medium to achieve sink conditions.

The tests were performed using Copley Scientific DIS 6000 dissolution apparatus (Nottingham, UK). MZ1 is an experimental drug undergoing investigational trials and lacks a standardised monograph to guide in designing studies. In addition, the product supply was very scarce, hindering the use of conventional dissolution vessels and paddles. Instead, small volume dissolution conversion kit was adapted to precisely analyse low amounts and small volume samples. Using a heater system, the temperature was set at 37.4 ± 0.5°C throughout the duration of the study. Meanwhile, as reported by Pöstges and colleagues (2023), the rotation speed was set to 75 rpm. Since no data is yet available regarding MZ1's therapeutic dose for treating colorectal cancer, a theoretical dose of 2.5 mg was used which would achieve adequate analytical sensitivity but still preserve the amount of drug in hand. For that, one hard gelatine capsule was filled with an equivalent of 2.5 mg of MZ1 and placed into a metal wired sinker. Then the capsule was added to a vessel containing 35 mL of release medium. The release behaviour of raw MZ1 and both drug-loaded MESOPAC was assessed for two hours in 0.05M phosphate buffer of pH 6.8 (Pöstges et al., 2023) with 0.3% SLS to mimic the small intestinal environment. At specified time intervals of 0, 15, 30, 45, 60, 90, and 120 minutes, 0.3 mL aliquots were withdrawn, filtered using 0.45 µm syringe filters, and filled into 0.3 mL glass screw top microvials (SureStart^{TM} ,Fisher Scientific, Loughborough, UK). Fresh medium was always added to replace the withdrawn samples. The samples were then assayed using the HPLC method reported in **section 3.2.2.** Cumulative drug release plots as a function of time were obtained.

3.2.11. Statistical Analysis

Data repeated in triplicate were represented as mean and standard deviation, which were then statistically analysed using Graphpad Prism 10.0 software (California, USA). T-test was used to statistically analyse the loading efficiency data while two-way ANOVA test was used to assess the release data of MZ1. The tests were chosen based on the nature of the data. A p-value less than 0.05 was set for statistical significance.

3.3. Results and Discussion

3.3.1. HPLC Method Development of MZ1

3.3.1.1. Specificity

Specificity is defined as the ability of the developed method to sperate the molecule of interest without interference from other components present within the formulation. The chromatograms of a blank sample and MZ1 at a concentration of 100 µg/mL were obtained. MZ1 was eluted at 2.1 minutes with a clear peak and no interfering signal. On the other hand, no peaks were detected around the retention time of MZ1 with the blank sample, indicating that the peak eluting at 2.1 minutes pertains to MZ1 (**Figure 3.2**).

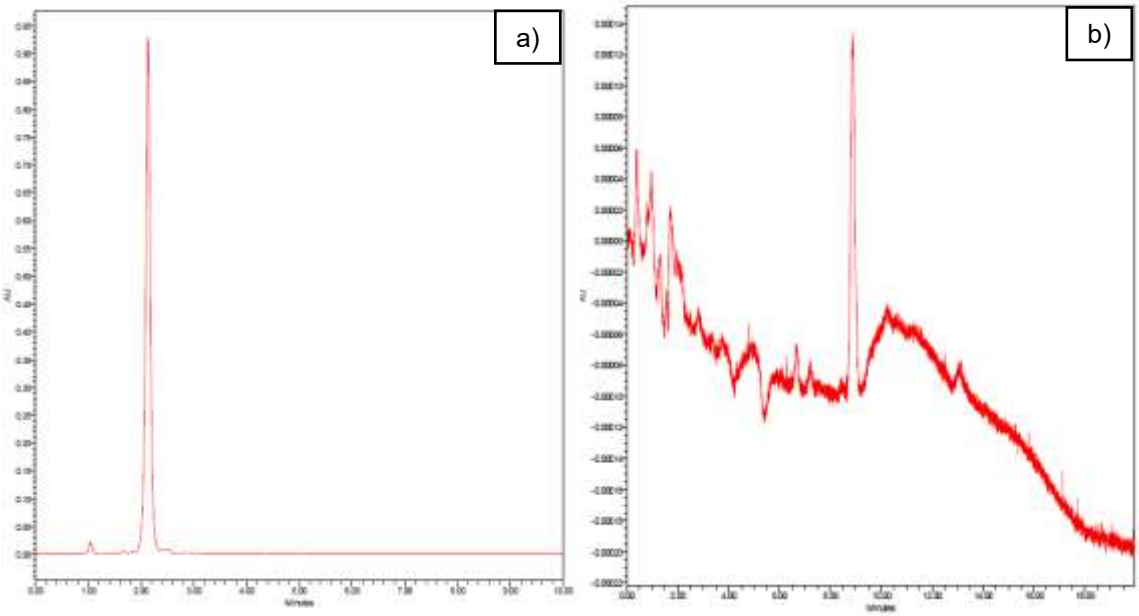

Figure 3.2. *Chromatograms of a) MZ1 (100 µg/mL) and b) blank sample to test for the specificity of the method*

3.3.1.2. Linearity and Range

To assess the linearity of the HPLC method, different stock solutions were prepared to obtain sets of diluted samples. The concentrations that were generated created a range, whereby the expected levels of MZ1 in case of low or full release can fit. Peak areas were plotted against the concentrations to obtain the mean calibration curve presented in **Figure 3.3**. The graph was linear over the concentration range 0.7 – 100 µg/mL with an R^2 of 0.9998. This demonstrated good linearity, suggesting the ability of the method to determine the concentration of interest in proportionality to the peak area.

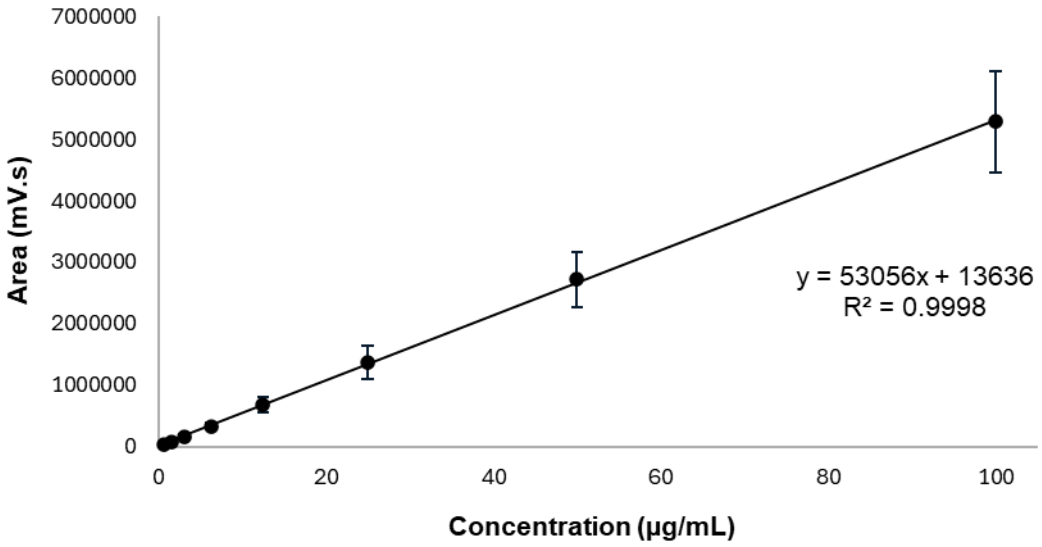

Figure 3.3. *Calibration curve of MZ1 [Data are represented as mean ± SD (n=3); C18 column 15 cm x 4.6 mm x 5 µm; UV detection at 261 nm, injection volume= 40 µL, flow rate= 1.2 mL/min, mobile phase 40:60 ammonium acetate buffer: acetonitrile]*

3.3.1.3. Precision

The precision of the HPLC method in terms of instrument repeatability was assessed by analysing six replicate injections of a standard solution at a concentration of 12.5 µg/mL. Each sample was injected consecutively under identical conditions. **Table 3.1** represents the peak areas for six replicate injections, mean, standard deviation, and relative standard deviation. The relative standard deviation was found to be 0.61%, which was well below the cut-off value of 2%. The method was thus rendered precise and repeatable.

Table 3.1. Peaks areas and relative standard deviation percentages for precision analysis (concentration: 12.5 µg/mL, n=6)

Sample	Peak Area (mV.s)
1	732515
2	739748
3	738291
4	734568
5	727445
6	732295
Mean (mV.s)	**734143.7**
Standard Deviation (mV.s)	**4466.1**
RSD (%)	**0.61**

3.3.1.4. Accuracy

The accuracy of the method was determined, and the mean values are reported in **Table 3.2**. The percentage recovery should fall between 98% and 102%. The values obtained fell within this range, meeting the requirements.

Table 3.2. Accuracy analysis represented as percentage recovery

Level	Theoretical concentration (µg/mL)	Mean Measured Concentration (µg/mL)	Mean Accuracy (%)
Low	25	25.5	102
Medium	50	50.93	102
High	100	99.42	99

3.3.1.5 Limit of Detection and Limit of Quantification

The limit of detection was found to be 2.24 µg/mL. This value represented the minimum concentration that can be detected but not necessarily quantified reliably. On the other hand, the limit of quantification represented the value at which MZ1 can be both detected and quantified confidently. In this validation process, the LOQ value was determined to be at 6.80 µg/mL.

3.3.2. Optimisation of Spray Drying Parameters to Prepare MZ1-loaded Mesoporous Particles

3.3.2.1. Varying Process Parameters

Spray Drying is a well-known technique to generate drug-loaded particles via solvent evaporation. The efficiency of the spray drying process is governed by multiple process conditions that include but are not limited to inlet temperature, feed flow rate, aspiration rate, and feed's solid content (Singh & Van Den Mooter, 2015). These parameters affect the properties and characteristics of the final product as well as the process yield. The quest to optimise the latter has been ongoing, as low powder yield is sometimes encountered with spray drying (Maury et al., 2005).

In this section, the effect of multiple process parameters on the yield of MZ1-loaded mesoporous particles was investigated. However, given that MZ1 is an investigational drug with limited supply and high cost, the process of optimisation was initiated without the addition of MZ1 for the very first trials. Once the ideal process conditions were identified, MZ1 was added to the feed and spray dried under the selected parameters. Such an approach to preserve expensive molecules was mentioned by LeClair and colleagues (2016). In previous work utilising the novel mesoporous carrier, the optimal drug loading parameters were determined at an inlet temperature of 60°C, feed rate of 5 mL/min, aspiration rate of 90%, and nitrogen flow rate of 10L/min (Le, 2021).

Starting with the aspiration rate, the range was varied to include four different values at 60, 70, 80, and 90%. It seemed that setting rate at 90% achieved the highest percentage yield of 29.8% so far, which was in line with previous studies that have stated that high aspiration rates enhance air throughput resulting in higher circulating air velocity and volume. This created

greater turbulence, eventually minimised wall deposition, and led to a higher process yield (Gallo et al. (2011); Laier et al. (2019)).

Another variable to consider whilst optimising the spray drying process is the inlet temperature. As previous experiments were conducted at an inlet of 60°C, it was necessary to explore the impact of various temperatures on product yield. Keeping the aspiration rate constant at 90%, temperature ranges from 40°C to 80°C were studied. From **Table 3.3**, it can be noted that the powder yield was negligible at 40°C but increased to 29.8% upon increasing the temperature to 60°C. This finding aligned with previous literature, such that increasing the inlet temperature was associated with improved powder recovery (Tontul & Topuz, 2017). Researchers like Tay and co-workers (2021) explained the reason behind this increase. They revealed that higher temperatures were associated with enhanced rates of solvent evaporation, resulting in lower solvent content. This decrease in solvent content minimised powder loss due to sticky deposits on the spray drying apparatus, particularly the heating chamber and the glass elbow. Consequently, an improvement in both yield and overall drying efficiency was observed.

Moreover, Permal and co-workers (2020) noticed an increased yield of avocado wastewater with increasing inlet temperature, reaching a maximum yield of 49% at the highest inlet used. However, excessive heat can negatively affect the yield, as the glass transition temperature is exceeded. This finding was demonstrated when the temperature in this study was set at 80°C, and a decline in yield was observed. It is well known that the glass transition temperature of a pharmaceutical ingredient is the one that allows the transformation of the drug from the glassy state to the rubbery form (Solomos et al., 2023). If an amorphous material is spray dried above its glass transition, then the rubbery form enables it to become sticky and exhibit the tendency to adhere to surfaces (Solomos et al., 2023). This ultimately leads to an increased rate of deposition on the walls of the spray dryer, accounting for the decreased yield. MZ1 was shown to be amorphous in nature, exhibiting a glass transition at 63.46 ± 3.30°C as discussed below (**sections 3.3.6 and 3.3.7**). Therefore, spray drying at 80°C exceeded the glass transition of the PROTAC, resulting in MZ1 gaining increased flexibility and motion at the molecular level and softening even further. This transition into the rubbery state could be presumed for increased stickiness and subsequent reduction in yield. Due to limited amounts of MZ1 initially available, DSC analysis to determine its glass transition temperature could not be performed before spray drying. Thus, 80°C was chosen based on standard practice. Later analysis showed this temperature exceeded the Tg of MZ1, leading to increased molecular mobility and softening. Despite that, a number of factors were found to have contributed to the decreased yield observed at higher temperatures in this investigation. The observed trends can be attributed to the fact that the optimisation process cannot be represented by a single process condition, particularly due to its complexity and the interplay of multiple parameters. Obviously, the challenge lied in optimising the interplay of feed

parameters and experimental conditions to achieve the optimal yield. Herein, the highest yield, however, was recorded with an inlet temperature of 60°C.

Table 3.3. Spray-drying yields (%) of CAB mesoporous particles at varying inlet temperatures (40, 60, and 80°C), performed with a constant feed flow rate of 1 mL/min, aspiration rate of 90%, and drying gas flow of 10 L/min. All samples were sprayed using two-fluid nozzle and ethanol as a solvent

Varying Inlet Temperature				
Inlet Temperature (°C)	**Feed Flow Rate (mL/min)**	**Aspirator (%)**	**Drying Gas Flow (L/min)**	**Yield (%)**
40	1	90	10	Negligible
60	1	90	10	29.8
80	1	90	10	11.03

The third factor that was studied was the feed flow rate. It is important to note that a feed flow rate of 5 mL/min was not feasible, and the highest achievable flow rate was 3.5 mL/min. According to **Table 3.4**, increasing the flow rate resulted in lower yields. This finding was in agreement with that concluded by Telang & Thorat (2010) and Behboudi-Jobbehdar et al. (2013), whereby the latter reported a maximised yield of microencapsulated probiotic strain of lactobacilli with reduced feed flow rate. In general, a linear relationship between product yield and flow rate was previously described by Behboudi-Jobbehdar et al. (2013). As the flow rate increased, the throughput became higher, so did the demand for higher evaporation energy. This left the final particles with a wet and sticky nature due to insufficient drying, which ultimately affected the powder yield (Buchi UK Ltd, 2025). Therefore, the optimal flow rate was chosen to be the lowest at 1 mL/min.

Table 3.4. Spray-drying yields (%) of CAB mesoporous particles at different feed flow rates (1–3.5 mL/min), using a constant aspiration rate of 90% and drying air flow of 10 L/min. Experiments were performed with a two-fluid nozzle

Varying Feed Flow Rate			
Feed Flow Rate (mL/min)	**Aspirator (%)**	**Drying Air Flow (L/min)**	**Yield (%)**
1	90	10	29.8
2	90	10	16.9
3	90	10	11
3.5	90	10	6.8

From the discussion above, it can be observed that the highest yield (29.8%) was achieved with the following parameters: inlet temperature of 60°C, feed flow rate of 1 mL/min, and aspiration rate of 90%. However, spray drying on a laboratory scale is considered satisfactory only if the product yield is greater than 50% (Maury et al., 2005; Tontul & Topuz, 2017). Given that, adjusting spray drying process parameters to reach an acceptable yield was not

successful as the yield was not even close to 50%. It was thus fundamental to additionally explore the effect of feed characteristics, namely solid content, in an attempt to reach a higher yield.

3.3.2.2. Varying Feed Characteristics

The impact of increasing the solid content in the feed on the product yield is highlighted in **Table 3.5**. A positive trend can be noticed, whereby increasing solid concentration increased the yield up to 52.8% if the feed and aspiration rates were kept constant as selected above. Such a percentage slightly exceeded the cut off value for acceptable yields. This finding corroborated previous work that suggested low solid content in the feed negatively affected the yield due to the higher solvent ratio and moisture content, which created sticky powder and minimised the final amount collected (Zhang and Youan, 2010). Similarly, it was previously reported that feed solutions with low solid content tended to be of high moisture content and low viscosity, both of which caused the wet droplets to hit the surface of the apparatus at a very high speed, resulting in the droplets depositing on the walls and reducing the dry powder yield (Tontul and Topuz, 2017).

A yield of 52.8% was found to be acceptable for laboratory-based spray drying, and the process parameters (inlet temperature 60, feed flow rate 1 mL/min, aspiration rate 90%, and solid content of 4.4% (w/v)) were considered as optimal for loading MZ1 into the novel carrier. Thus, MZ1-loaded mesoporous particles were generated at two theoretical drug loads; 10% (w/w) and 20% (w/w). Powder yields of 55.08 ± 7.03% and 63.4 ± 0.04% were obtained for the 10% (w/w) and 20% (w/w) MESOPAC formulations, respectively, indicating successful drug loading to some extent. A similar powder yield (>65%) was obtained with another research group who attempted to spray dry the PROTAC, MS4078, with Soluplus to produce amorphous solid dispersions (Hofmann et al., 2024). This finding provided some important insights into loading of PROTACs via spray drying, as literature was not highly populated with articles discussing this.

Table 3.5. Spray-drying yields (%) of CAB mesoporous particles prepared at varying solid contents (0.4–4.4% w/v), using an inlet temperature of 60°C, feed flow rate of 1 mL/min, and aspiration rate of 90%. Drying was performed with a two-fluid nozzle

Varying Solid Content				
Inlet Temperature (°C)	**Feed Flow Rate (mL/min)**	**Aspirator (%)**	**Solid Content (% w/v)**	**Yield (%)**
60	1	90	0.4	<30
60	1	90	2.2	36.7
60	1	90	3.3	42
60	1	90	4.4	52.8

3.3.3. Loading Efficiency and Quantification

For MZ1-loaded mesoporous particles, the mean loading efficiencies were calculated to be 55.57 ± 4.96% and 78.00 ± 6.88% for 10% and 20% (w/w) drug loads, respectively, as presented in **Table 3.6**. The results suggested that some powder was lost during the process but indicate successful loading to some extent, especially with the higher drug load. This aligned with observations in the literature, which showed that the encapsulation efficiency of MZ1 in polymeric nanoparticles reached 55.7% (Cimas et al., 2020).

Interestingly, a significantly higher loading efficiency was achieved with the higher drug load (p-value < 0.05). One possible explanation is related to the theory of establishing a concentration gradient for drug molecules to diffuse into the pores; it is well known that drugs occupy the porous network of carrier particles through adsorption into the walls, which results in a concentration gradient between the inner and the outer surroundings of the carrier particles as they are immersed in the solvent (Farzan et al., 2023). More drug molecules then occupy the internal porous network via diffusion. Therefore, as the drug concentration in the loading solvent increases, the concentration gradient becomes steeper, favouring the diffusion of drugs particles towards the internal pores of the carrier (Farzan et al., 2023). Hence, the number of drug molecules occupying the pores increases, resulting in higher drug loading efficiency, as seen when MZ1 was loaded into MESOPAC at a higher drug load (20% (w/w)). Quantification essays revealed actual drug loads of 5.56 ± 0.50% and 15.6 ± 1.38% (w/w) compared to theoretical drug loads of 10 and 20% (w/w), respectively. The discrepancy between the two can be ascribed to the losses during atomisation or incomplete diffusion of the drug molecules into the pores of the carrier particles for example. The actual drug loads will be used to refer to the different formulations throughout the study.

Table 3.6. Drug loads and loading efficiencies of MZ1-loaded mesoporous particles prepared at inlet temperature of 60°C, feed flow rate of 1 mL/min, aspiration rate of 90%, and nitrogen flow rate of 10 L/min

Formulation	Theoretical Drug Load (%, w/w)	Actual Drug Load (%, w/w)	Loading Efficiency (%)
MZ1-loaded Mesoporous Particles (Low drug load)	10	5.56 ± 0.50	55.57 ± 4.96
MZ1-loaded Mesoporous Particles (High drug load)	20	15.6 ± 1.38	78.00 ± 6.88

3.3.4. Morphology Assessment of MZ1-loaded Mesoporous Particles

The morphological characteristics of the PROTAC-loaded particles were captured in an attempt to gain an insight into MZ1's loading into the pores. **Figure 3.4, Figure 3.5,** and **Figure 3.6** illustrate the SEM micrographs of raw MZ1 and unloaded carrier versus those obtained after loading MZ1 into mesoporous particles at both drug loads.

The micrographs revealed the distinctive spherical structure of the carrier particles, obviously indicating the porous nature of the carrier (**Figure 3.4 (a)**). The porous structure was clearly visible externally on the surface as well as internally. **Figure 3.4 (b)** depicts unprocessed MZ1. It was quite a surprise to find that, after the incorporation of the PROTAC, MESOPAC particles maintained their porous structure but lost their sphericity. It could be seen that, regardless of the drug load, the majority of the particles were flattened after loading as shown in **Figure Figure 3.5 (a)** and **Figure 3.6 (a)**.

A possible explanation might be that drug particles need to distribute evenly within the porous network to preserve the spherical structure. Because MZ1 has a relatively large molecular weight, its ability to diffuse to the core of the carrier was limited, leaving the centre of the particle unoccupied (as proved later with Raman spectroscopy in **section 3.3.5**).

Previous studies raised the issue of uneven drug distribution in relation to Péclet number and its effect on particle morphology (Alhajj et al., 2021). As discussed earlier in chapter 2, surface recession occurs during drying in response to solvent evaporation. This causes a diffusional flux of solute particles towards the centre of a droplet. However, in certain cases, the rate at which the solvent evaporates exceeds the rate of diffusion, resulting in the build-up of solute particles around the surface. This is referred to as an uneven distribution of solute particles that is a consequence of limited diffusion, resulting in a hollow particle.

It is not only the rate of evaporation that governs the morphology of the dried particle, but also the molecular diffusion of the solute. The two are related by Péclet number. A high *Pe* suggests that evaporation is occurring faster than the rate at which diffusion can redistribute the solute particles, resulting in surface accumulation of solute and a hollow core (Al-Khattawi et al., 2018; Alhajj et al., 2021; Vehring et al., 2007). From this discussion, it can be inferred that in the case of MZ1, its high molecular weight limited its diffusion capability through the porous carrier as concluded from Raman spectroscopy in **section 3.3.5**. As MZ1 struggled to diffuse to the centre of MESOPAC, the rate of evaporation began to dominate over diffusion, resulting in a high *Pe*. An uneven distribution of the PROTAC molecule consequently occurred, as the core then became primarily composed of carrier material while the surface became dense with MZ1 molecules. This uneven distribution left the core vulnerable to collapse when high shear forces were exerted with spray drying. That provided, a droplet with an empty core could not withstand that high force. It lost its structural integrity and flattened in alignment with the theory of *Pe.*

Interestingly, **Figure 3.5 (c)** and **Figure 3.6 (c)** provide a closer look into the loaded mesoporous particles and point to some drug particles present on the surface as denoted by the red circles. These spherically shaped nanometric entities were most likely spray-dried MZ1 particles. Compared to unprocessed MZ1 (**Figure 3.4 (b)**), they acquired the spherical shape which is a hallmark of spray drying (Hofmann et al., 2024). They were, however, residing on the surface rather than the pores due to incomplete loading and diffusion. This phenomenon can be seen to greater extent with 5.5% (w/w) drug load, most likely because of a lower diffusive force to drive the molecules towards the pores compared to the highly concentrated 15.6% (w/w) MESOPAC. This finding correlated well with the loading efficiencies reported earlier (**section 3.3.3**), whereby the 5.5% (w/w) MESOPAC did not show a high drug recovery percentage only to indicate that some drug molecules were not fully embedded within the pores. Unlike the lower drug load, the phenomenon of MZ1 particles being spray dried on the outer surface was less evident with the 15.6% (w/w) MESOPAC. This reflected the efficient loading process and explained the higher loading efficiency obtained earlier (78%). Altogether, SEM images showed successful loading of MZ1 into the carrier; however, additional imaging techniques were required to provide further certainty.

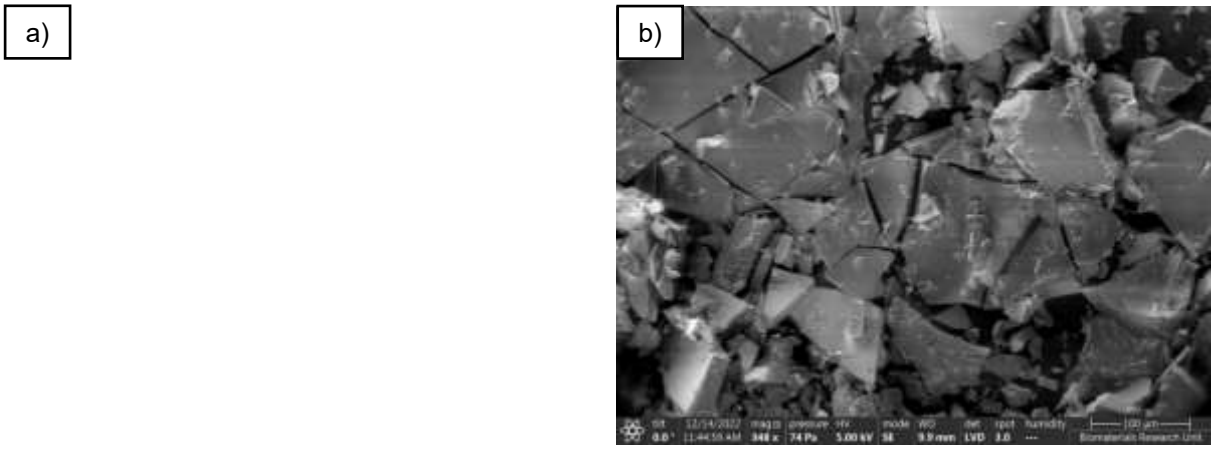

Figure 3.4. *SEM images of (a) [* ***Redacted*** *], (b) raw MZ1[Magnification 348x]*

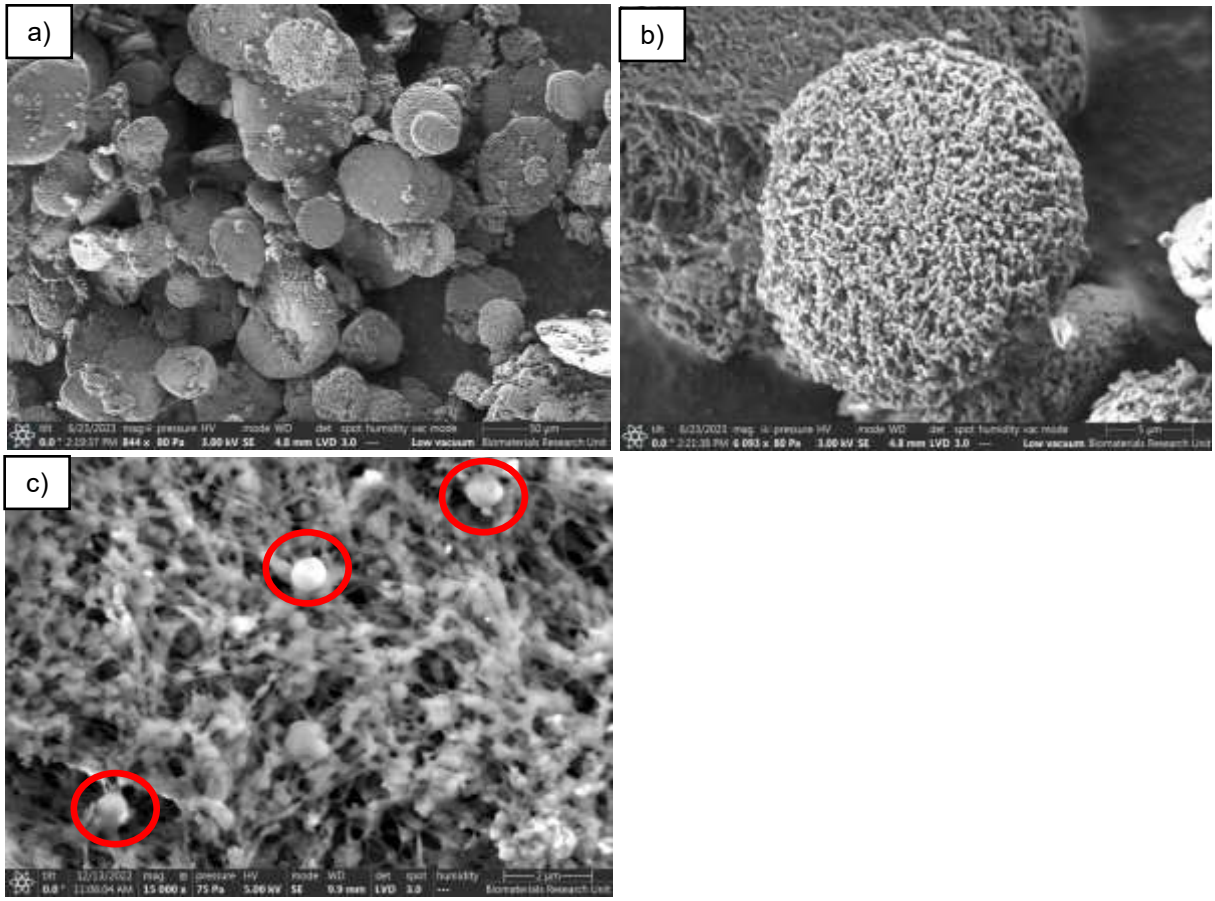

Figure 3.5. *SEM images of 5.5% (w/w) MZ1-loaded MESOPAC: (a) Flattened particles [Magnification 844x], (b) Spherical, porous loaded particles [Magnification 6093x], (c) Spray-dried MZ1 particles on the surface of MESOPAC denoted by red circles [Magnification 15000x]*

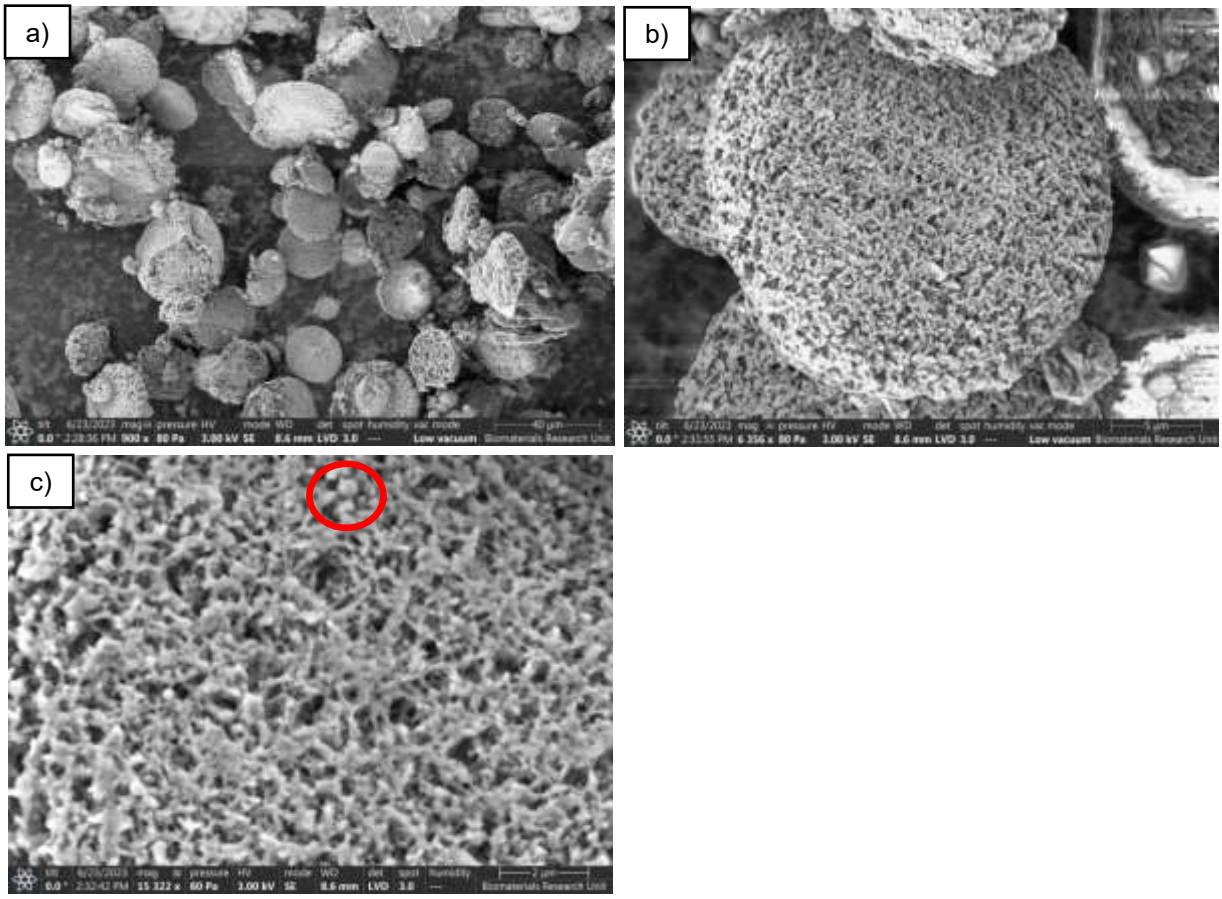

Figure 3.6. *SEM images of 15.6% (w/w) MZ1-loaded MESOPAC: (a) Flattened particles [Magnification: 900x], (b) Spherical, porous loaded particles [Magnification: 6356x], (c) Spray-dried MZ1 particles on the surface of MESOPAC denoted by red circle [Magnification: 15322x]*

3.3.5. Drug Distribution Analysis of MZ1 within MESOPAC

Raman imaging was employed to evaluate the extent of localisation of MZ1 within the carrier particles (**Figure 3.7**). A homogenous distribution of the API within the porous network was assumed to preserve the sphericity of carrier particles, as discussed earlier. Successful drug loading should show uniform distribution of MZ1 between the outer edges and the porous core of the carrier particles. The constituents of the samples are observable in the Raman images of the loaded carrier particles containing MZ1, with MZ1 being represented in red and mesoporous particles in blue (**Figure 3.7**). The maps of both drug loads clearly confirmed the presence of the PROTAC within the carrier, indicating successful loading. It was, however, the distribution of MZ1 that differed between the two; neither image showed a homogenous diffusion of the drug molecules towards the core, as the core of MESOPAC remained unoccupied by lacking any red zones. With 5.5% (w/w) loading, MZ1 was depicted as small clusters scattered within the first few micrometres of the porous network and was clearly not evident in the core. A different pattern was noticed with 15.6% (w/w) loaded MESOPAC, whereby the PROTAC seemed to border the carrier particle and distribute evenly around the edges only, leaving the core of the particle unoccupied. This pattern of distribution was

hypothesised to be due to the PROTAC's large molecular size [1002.64 Da] that prevented its diffusion deep towards the centre of the carrier and disturbed the creation of a homogenous distribution as discussed earlier in **section 3.3.4**. Such a finding was in close agreement with SEM imaging and loading efficiency data, as it proved the lack of homogeneity within the carrier and explained the resulting flattening of the particles after loading. It was hypothesised that this distribution pattern around the edges only could be accounting for the flattening of mesoporous particles. The rigidity of the carrier particles could not withstand the shear force of spray drying, as no MZ1 molecules could be seen within the core to strengthen the porous network. As a result, the particles lost their three-dimensional sphericity and were flattened, supported by the theory of *Pe*.

Moreover, particle deformation is a phenomenon seen with spray drying that is a direct effect of several parameters (Eijkelboom et al., 2023). High spray velocity or shear force could be one of the underlying causes for particle collapse although not explicitly stated in literature. In fact, it could be argued that different nozzles spray feed solutions at different velocities. The gentler ultrasonic nozzle, for example, generates spherical particles since its spray velocity is reported to be milder (18 to 36 cm/s) than that of the two-fluid nozzle (10 m/s to 30 m/s) (Hsieh et al., 2024; Ultrasonic Controller Operating Manual, 2014). This difference in spray velocity identifies the shear forces imparted by the two-fluid nozzle as an additional factor behind particle flattening with spray drying.

From another point of view, Hofmann and colleagues (2024) generated amorphous solid dispersions of a model Cereblon-based PROTAC via spray drying. Unlike the results reported herein, Raman imaging demonstrated homogenous distribution of the PROTAC within the polymeric matrix of their ASDs. Although the technique of loading was quite similar, with spray drying used for solvent evaporation, the type of the carrier used herein could account for such a difference in drug distribution; it is known that the properties of the delivery vehicle such as the chemical composition, pore size, pore volume, and surface area affect the drug loading capacity (Bavnhøj et al., 2019). In fact, the stabilisation of the amorphous drug is achieved differently with mesoporous materials than with ASDs. This difference perhaps accounted for the homogeneity of the drug within the polymeric matrix. With mesoporous particles, pore filling is achieved via adsorption to stabilise the amorphous system (Bavnhøj et al., 2024). This pore filling and adsorption is size-dependent, meaning that molecules that are larger in size than the pore's diameter will struggle in achieving pore filling or covering the pore with a monolayer (Bavnhøj et al., 2019). Hence, the molecules will not distribute evenly, and this explained why the PROTAC molecule in this study did not show a homogenous distribution across the porous network. Meanwhile, with ASDs, the amorphous stabilisation is simply independent of the API's size and depends on the drug-polymer interaction, mainly the solubility of the drug within the polymer (Pöstges et al., 2023). Altogether, Raman imaging

showed the presence of MZ1 within the porous network, indicating an effective loading process. Yet, the distribution pattern of the PROTAC within the carrier particles needed further optimisation.

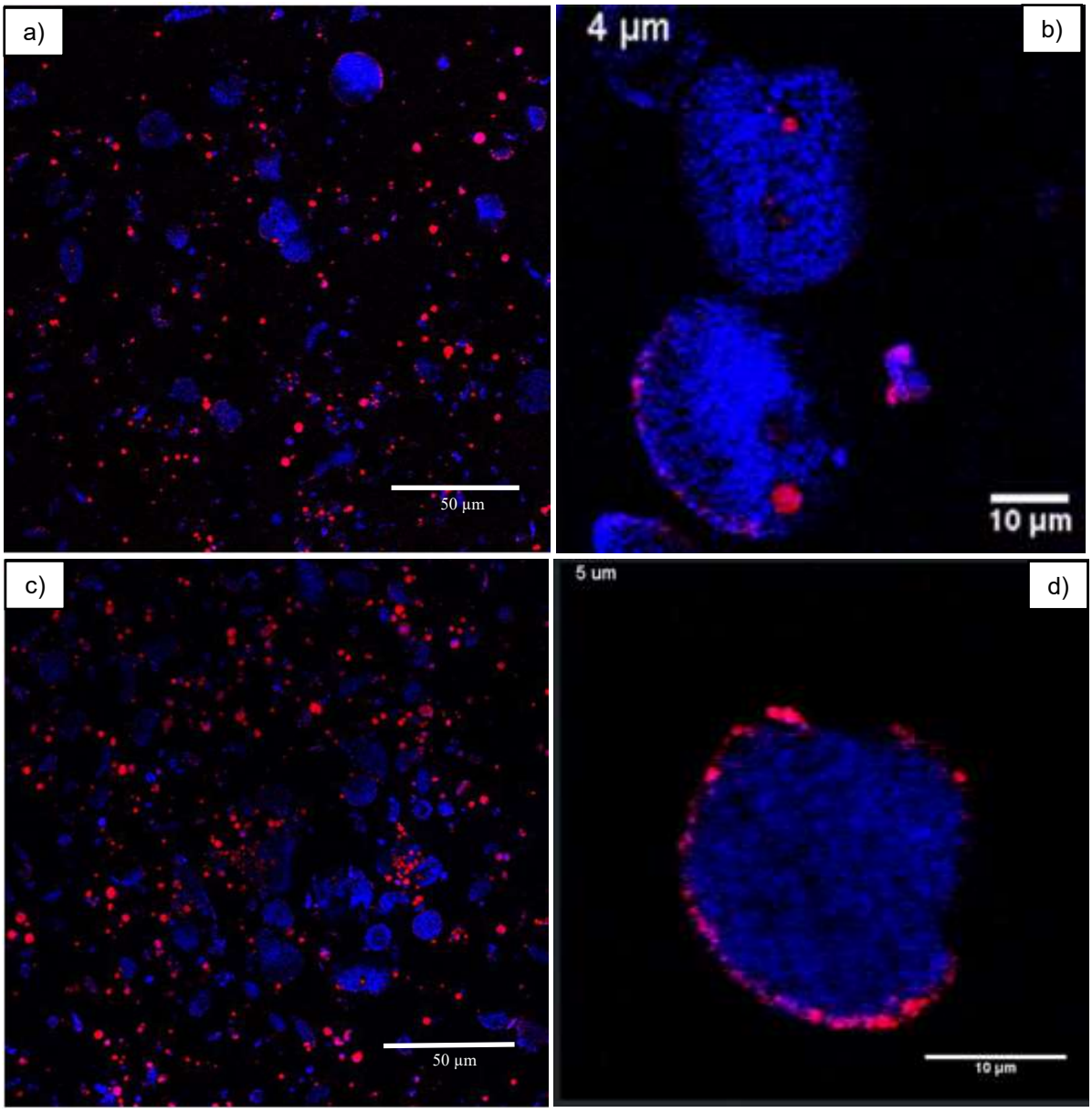

***Figure 3.7**. Raman imaging of MZ1-loaded MESOPAC formulations: a) & b) 5.5% (w/w) MZ1-loaded samples and c) & d) 15.6% (w/w) MZ1-loaded sample. Blue zones represent carrier regions while red zones represent MZ1-populated regions [Magnification: 40x (1.1 NA)]*

3.3.6. Analysis of the Thermal Properties of MZ1 and Loaded Mesoporous Carrier

DSC was employed to investigate the thermal behaviour of raw PROTAC prior to and after loading into the proposed carrier formulation. **Figure 3.8** reveals the thermograms of the pristine MZ1, spray-dried mesoporous particles, and MZ1-loaded particles. ***[two sentences redacted from open access thesis].*** This indicated the thermal stability of the proposed carrier before and after spray drying.

The figure also shows the thermograms of the drug-loaded MESOPAC, with both drug loads characterised by the absence of any endothermic or exothermic events; only the glass transition of the carrier particles was detected within the expected range, suggesting that the PROTAC remained amorphous after loading into MESOPAC.

The controversy, however, lied within the thermogram belonging to raw MZ1, whereby a broad and very shallow endothermic event was noted at an average of 64.07 ± 2.89°C. However, it was not clear or sharp enough to be interpreted as the PROTAC's melting point. Unfortunately, no previous papers examined the thermal behaviour of MZ1, causing this peak to be very ambiguous. Thus, it was viewed as a debatable area, whereby current and future research is meant to explore its underlying significance. Hence, it could be hypothesised that this event may correspond to either a broad melting event or glass transition of the drug.

To further confirm that, a heat-cool-heat cycle was conducted for raw MZ1. The rationale behind this run was that if the shallow event starting at nearly 64.07 ± 2.89°C was actually the drug's melting point, then a crystallisation peak should be observed upon cooling and a sharp melting point is expected in the second heating curve as a result. Yet, by looking at **Figure 3.9** which illustrates the heat-cool-heat cycle of raw MZ1, no sharp endothermic or exothermic events were detected, neither upon cooling nor upon second heating cycle. One interesting finding though was the step change occurring with second heating cycle as denoted by the purple arrow in **Figure 3.9**. This finding implied that the original broad shallow event at nearly 63.46°C might be actually MZ1's glass transition temperature, but shifted with the second heating cycle, acquiring a clearer and steeper step transition. It was apparent from this DSC cycle that MZ1 displayed an amorphous solid state. Pöstges and co-workers (2023) reported a similar finding, whereby thermograms of raw ARCC-4, a VHL-based PROTAC, revealed that the PROTAC existed naturally in its amorphous form with a glass transition temperature detected at 100 ± 0.3°C. One possible explanation for why PROTACs tend to be amorphous in nature is the large size they possess along with their structural-based flexibility (Yang et al., 2024). This structural flexibility stems from their flexible linkers and rotatable bonds (Cecchini et al., 2021). These flexible linkers that PROTACs are known for could possibly hinder the formation of an ordered crystalline structure. Likewise, Hofmann and colleagues (2024) found

that the PROTAC intended for solubility enhancement in their research was amorphous in nature as well. The enhanced dissolution performance of the PROTAC was thus attributed to a homogenous distribution of the API within the polymeric matrix and not to a change in the solid state of the PROTAC. Nonetheless, both research groups saw benefits with regards to solubility enhancement of PROTACs when using ASD approach. Indeed, poorly soluble PROTAC molecules that exhibit a naturally amorphous state can still be candidates for solubility enhancing technologies. This conclusion was promising and may be reflected in this present study, given that the poorly soluble MZ1 molecule possessed an amorphous state and was loaded into solubility enhancing mesoporous carrier particles.

In sum, neither MZ1 nor the loaded mesoporous particles showed any melting or crystallisation peaks in the thermograms, indicating the overall amorphous state of the PROTAC before and after incorporation into the carrier particles. However, further analysis using other solid-state profiling and spectroscopic techniques was required for a comprehensive confirmation.

Figure 3.8. *[redacted]*

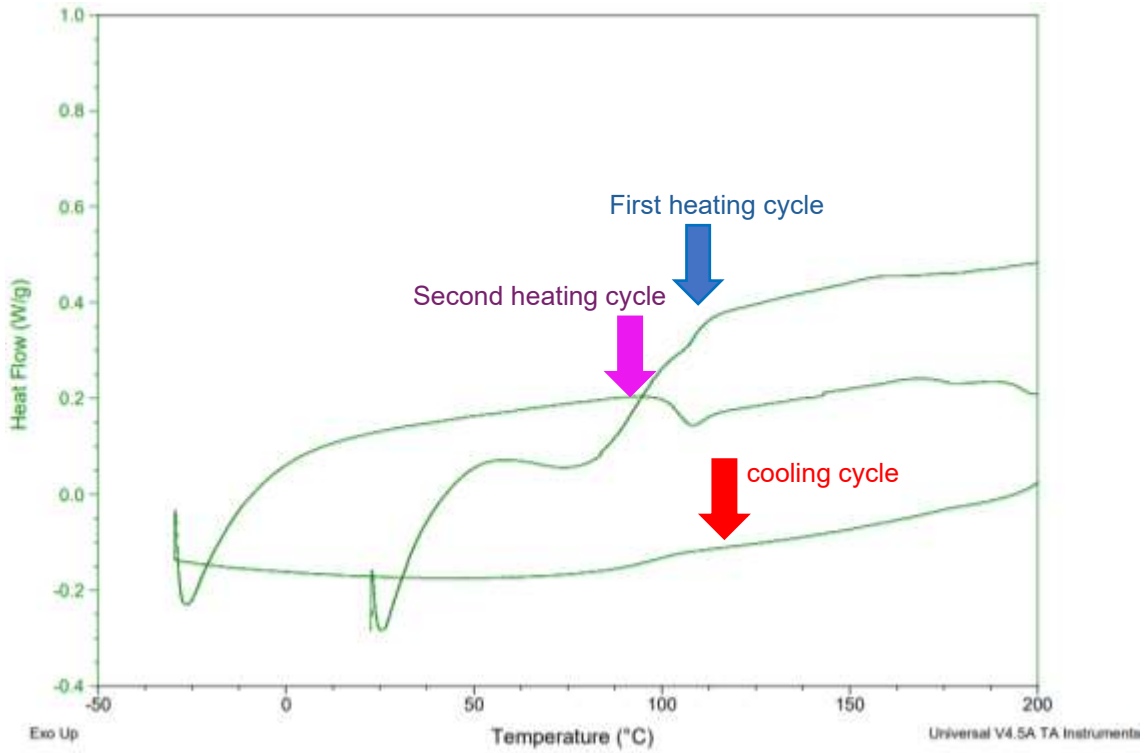

Figure 3.9. *DSC heat-cool-heat cycle of raw MZ1*

3.3.7. Solid-state Analysis Using XRD

Whether the observed broad, shallow peak was an actual melting peak cannot be solely determined based on DSC thermograms. The cause of such an event was difficult to determine from a conventional heating cycle on DSC, and further tests were required as suggested by Dedroog et al. (2020). It is not preferred to use DSC nor XRD as stand-alone techniques, and a combination of the two is recommended to strengthen any conclusions drawn from these analytical techniques (Dedroog et al., 2020). Hence, X-ray powder diffraction analysis was necessary to characterise the structure of the molecule. Diffraction X-ray patterns of neat MZ1 and PROTAC-loaded mesoporous particles are shown in **Figure 3.10**. Since a broad hump and no sharp diffraction peaks were detected with both samples, it could be confirmed that MZ1 exhibited an amorphous character as demonstrated by previous research with other PROTACs (Hofmann et al., 2024; Posteges et al., 2023). Collectively, the findings of DSC and XRD analyses corroborated and confirmed the amorphous nature of the PROTAC. Consistent with our finding, the research conducted by Mareczek and colleagues (2024) proved that some PROTACs do exist in an amorphous solid state. The PROTAC investigated in their study retained its amorphous nature following spray drying and embedding into an ASD, as indicated by the amorphous halo observed via XRD diffractograms (Mareczek et al., 2024). Although amorphisation via delivery technologies is an approach normally employed for crystalline drugs to enhance their solubility, the technique can be beneficial for poorly

soluble drugs that are already amorphous in nature, like MZ1 (Posteges et al., 2023). This is perhaps due to increased thermodynamic stabilisation within the pores that preserves the amorphous form of the drug.

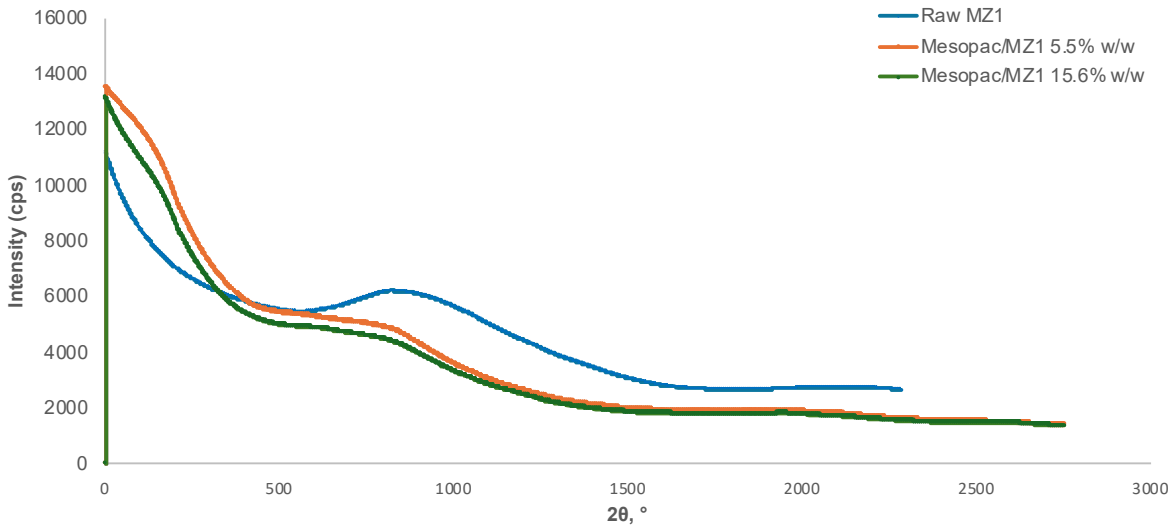

Figure 3.10. *XRD analysis of raw PROTAC and MZ1-loaded mesoporous particles at two drug loads: 5.5% (w/w) and 15.6% (w/w)*

3.3.8. Effect of Drug Loading on Porosity

Nitrogen porosimetry is a characterisation technique employed in assessing the extent of pore filling by drug molecules via measuring the changes that happen with surface area and pore volume. The analytical technique consumes a considerable amount of powder with each run. With this taken into consideration, triplicate analysis was not feasible at that stage because of the limited amount of MZ1 that was available.

The porosity properties of MESOPAC were examined prior to and after loading with MZ1. **Table 3.7** shows the pore properties (specific surface area, pore volume, and pore size) of unloaded carrier versus MZ1-loaded mesoporous particles at 5.5 and 15.6% (w/w) drug loads. ***[three sentences redacted].*** Although the percentage decrease in pore volume was quite similar between the two drug loads, investigating higher drug loads would have generated a more pronounced decrease in pore volume as the difference between 5.5% and 15% (w/w) was very marginal when it comes to efficient drug loading. Yet, collectively, the decrease in surface area and pore volume of MESOPAC after loading probably indicated some occupation of the

pores by the PROTAC molecules. However, it is important to note that the decrease was not massive as relatively large regions of the carrier, particularly the core, remained unoccupied. This finding complemented the data provided by Raman imaging, such that if MZ1 was able to diffuse to the centre of MESOPAC particles, a steeper decrease in surface area and pore volume would have been noted. Christoforidou et al. (2021) reported similar findings when loading two similar mesoporous particles that differ in pore network connectivity with an API. The group noticed a decrease in surface area and pore volume of the generated mesoporous particles after loading, indicating the successful entrapment of the API within the porous network.

The overall difference in pore properties between the empty mesoporous carrier and the PROTAC-loaded particles, regardless of the drug load, was discussed above. The transition towards comparing the impact of different drug loads of the relatively large PROTAC on the pore properties of the carrier becomes necessary to allow for a comparative analysis of the two.

A general observation can be noted, whereby increasing the drug load resulted in a more pronounced decrease in surface area and increased pore size while the pore volume remained relatively unchanged. Two possible theories can explain the decrease in surface area with increasing drug load. Firstly, a higher drug load meant more of the active ingredient being added to the formulation per amount of the carrier. This increased amount of active ingredient was translated as higher loading efficiency, especially around the edges of the mesoporous particles as depicted by Raman spectroscopy. As more of the drug molecules occupied the pores when the drug load increased, the surface area available for nitrogen to adsorb became less, ultimately leading to a decreased surface area.

The second theory revolved around pore blocking rather pore filling. In case of a relatively large PROTAC like MZ1, its amorphous state as confirmed by DSC and the associated structural flexibility made the molecule likely prone to aggregation. This structural flexibility of PROTACs that enables them to adapt to different environments was reported by Jiménez et al. (2024). When MZ1 molecules aggregate, they might block the surface of the pore, hindering the nitrogen gas from adsorbing to the inner walls of the pore and resulting in decreased surface area. Although the structural flexibility might be hampered by spatial confinement, the uneven drug distribution within MESOPAC might disrupt optimal pore entry and filling, causing more molecules to aggregate at outer pores. This phenomenon of pore blocking by large molecules, especially peptides, was reported by Carrozza and colleagues (2023). Although not specifically directed towards PROTACs, the concept of pore blocking can still be generalised to involve any large-sized molecule other than peptides (Carrozza et al., 2023).

With regards to the pore volume, it seemed that it remained unchanged despite higher drug loading. Before exploring the reason behind such a phenomenon, one should understand that

the pore volume measurement refers to the overall volume of available voids within the whole carrier particle, collectively. When the pore volume remains constant, the drug molecules could be filling a small fraction of the pores that is not large enough to induce a detectable change in the overall pore volume between the two drug loads. This speculation could be somewhat true, given that MZ1 settled into the outer edges of the particles only, leaving the majority of the core unoccupied with both drug loads and accounting for a close decrease in pore volumes between the two.

Table 3.7. Pore properties (Specific surface area, pore volume, and pore size) of empty MESOPAC and PROTAC-loaded samples

Formulation	Specific Surface Area (m^2/g)	Pore Volume (cm^3/g)	Average Pore Size (nm)
[redacted]	[*redacted*]	[*redacted*	[*redacted*]
MESOPAC loaded at 5.5% (w/w)	17.14	0.0886	20.68
MESOPAC loaded at 15.6% (w/w)	13.04	0.0897	27.53

3.3.9. Dissolution Performance of MZ1 and MZ1-loaded Mesoporous Particles

Keeping in view the solubility enhancement effect of the porous carrier and the advantages that porous delivery systems confer to poorly soluble drugs, it became crucial for this study to establish a relationship between MZ1 and MESOPAC. Therefore, dissolution studies of MZ1 in phosphate buffer pH 6.8 were carried out in an attempt to simply verify the ability of the delivery system to enhance the dissolution of MZ1 at a pH resembling the small intestine. SLS at a concentration of 0.3% (w/v) was added to all media to achieve sink conditions.

The release profiles of neat MZ1 compared to loaded MESOPAC formulations are depicted in **Figure 3.11**. At 30 minutes into dissolution, only 15.22 ± 3.36% of crude MZ1 was dissolved. In contrast, 48.39 ± 5.31% of MZ1 was released when loaded at 5.5% (w/w), and 68.82 ± 6.49% of MZ1 was detected in 30 minutes when the PROTAC was loaded at a drug load of 15.6% (w/w). An appreciable difference in release behaviour could be noted between the samples, with the dissolution rate of MZ1-loaded mesoporous carrier being increased by 4-folds compared to that of neat MZ1 at 30 minutes (p-value <0.05). The two profiles were different, and MESOPAC showed faster initial dissolution rate. This finding may be explained by the fact that the spatial confinement of the molecule within the porous network provided additional stability of the PROTAC by restraining any molecular mobility that could affect its dissolution profile. Similar reports of enhanced amorphous stability of small molecules and proteins in porous cavities due to spatial confinement were found (Mäkilä et al., 2014; Radhakrishna et al., 2013; Ukmar et al., 2011). Ukmar and colleagues (2011) revealed restricted mobility of small molecules when confined within pores that was measured by NMR. It can be also seen from **Figure 3.11** that the release was higher when the drug load increased

despite having lower surface area of MESOPAC for release. One possible explanation might be related to the distribution pattern of MZ1 with different drug loads as described in **section 3.3.5**. With the higher drug load, MZ1 molecules were packed densely around the outermost edge of the surface, creating a well-defined boundary or a ring-like pattern around the particle. Unlike the higher drug load, scattered clusters that were located slightly deeper but still around the surface were observed with the lower drug load. This distribution pattern between the two might have facilitated the accessibility of dissolution medium to the PROTAC molecules in the ring-like structure as they are more exposed, accounting for higher release.

Moreover, although the drug was already amorphous in nature, the difference in dissolution could also be ascribed to the increased surface area of the PROTAC molecules. Solid MZ1 particles, which existed micrometric range as shown in SEM images (see **Figure 3.4**), were forced to confine within the nano-sized pores during solvent evaporation. This decrease in size from the micrometric range to form the nano-solidified drug particles increased the surface area compared to the raw, unloaded drug and probably resulted in enhanced dissolution. This explanation was inspired by Hofmann and colleagues (2024), who discussed the effect of surface area on the dissolution kinetics of a PROTAC molecule embedded within ASDs of different polymers. Upon storage, one of the polymers used resulted in the fusion of particles and thus an increase in size. This increase in size led to a decrease in surface area and impaired dissolution kinetics.

Literature reports on utilising delivery systems to enhance the solubility of PROTACS were very scarce; yet a paper reported that the encapsulation of PROTACs within the cavities of a delivery vehicle, such as mesoporous silica nanoparticles, is a potential technique to amend the release behaviour of these molecules (Chen et al., 2022).

Moreover, a similar finding was reached in two studies, whereby amorphous solid dispersions (ASD) potentially improved the dissolution of two PROTAC molecules (Hofmann et al., 2024; Pöstges et al., 2023). The former group of researchers observed nearly 31-fold increase in dissolution between crude PROTAC and ASDs. Meanwhile, the latter group aimed to stabilise the amorphous PROTAC within the polymeric matrix by generating an aqueous supersaturated solution of the drug resulting in enhanced bioavailability. In their study, Raw ARCC-4 showed very little dissolution in phosphate buffer (<0.4 ug/ml) while polymeric ASD enhanced the dissolution of the poorly soluble PROTAC up to 31.8 ± 0.6 µg/mL (Pöstges et al., 2023). The dissolution profile of another PROTAC molecule, SelDeg51, after embedding in a solid dispersion with polyvinyl alcohol was investigated by Mareczek and co-workers (2024). Although the drug exhibited an amorphous solid state naturally, its dissolution performance was significantly improved by the use of ASDs compared to the non-dispersed, raw form. The enhanced dissolution effect was attributed to the increased stability of the PROTAC molecule within the ASD that restricted its tendency to flex (Mareczek et al., 2024).

These findings suggest that drug delivery vehicles in general, such as mesoporous carriers, can be developed to optimise and circumvent the challenges associated with the oral delivery of PROTACs. As reported herein, MZ1's dissolution was improved significantly with the use of the solubility enhancement technology, MESOPAC. However, it is important to note that the incomplete release observed with MZ1-loaded MESOPAC can be attributed to the differences in hydrodynamics between small-volume and large-volume dissolution setups. To obtain a release profile that accurately represents the formulation's true potential, adjustments to key conditions, particularly paddle rotational speed, were necessary. Unfortunately, due to the limited supply of the PROTAC molecule, full optimisation of the hydrodynamic conditions in the mini dissolution vessels to match the performance of the compendial setup and achieve complete drug release was not feasible. A more comprehensive discussion of how hydrodynamics influence drug dissolution can be found in the next chapter (**section 4.3.3.4**). To our knowledge, this is the first report of studies into the release of MZ1 from mesoporous delivery systems.

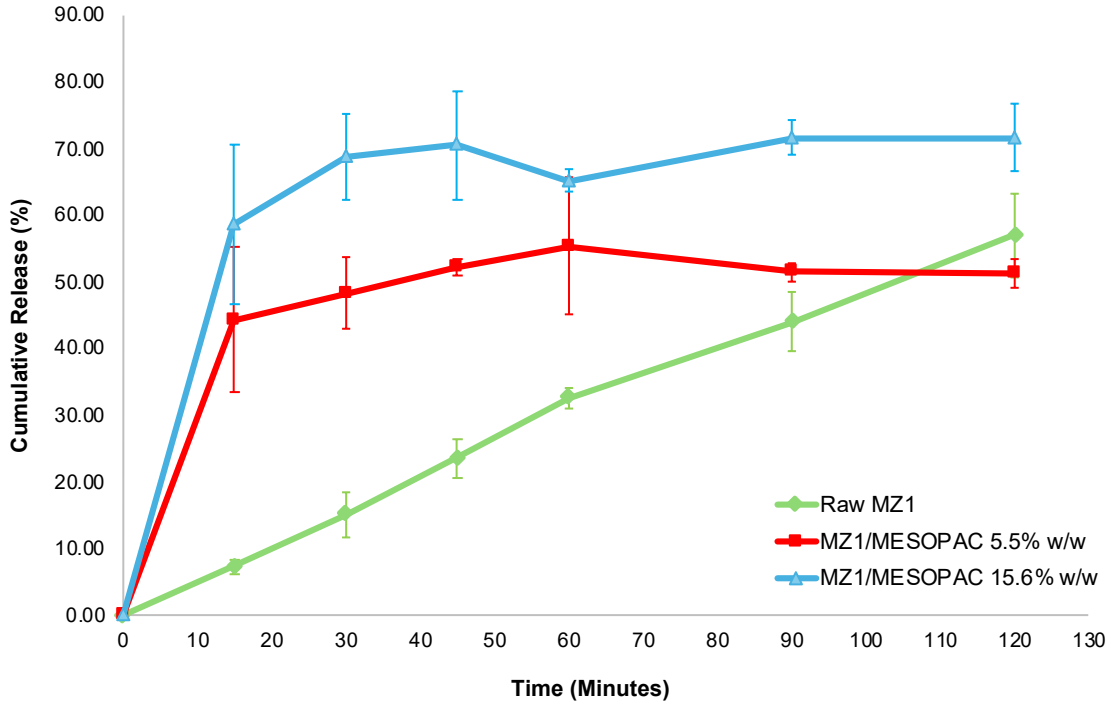

Figure 3.11. *Dissolution analysis of raw PROTAC and MZ1-loaded mesoporous particles in buffer pH 6.8 with 0.3% (w/v) of SLS (n=3 for each timepoint)*

3.4. Conclusion

Drugging the previously thought undruggable protein targets, PROTACs represent a revolutionary therapeutic modality in the pharmaceutical industry. Given their increased specificity and safety profile, in addition to their ability to utilise the cell's own degradation machinery, PROTACs can degrade proteins driving multiple diseases including cancer. However, their inherent low solubility and permeability delay their clinical translation from bench to bedside and impede their oral delivery. Hence, mesoporous particles could be employed to tackle the solubility challenges associated with PROTACs. MZ1, a model PROTAC molecule for colorectal cancer with low solubility, was loaded into novel cellulosic mesoporous carrier. Spray drying process parameters were studied with regards to their effect on the powder yield. Acceptable yields and loading efficiencies were achieved with the following parameters for both drug loads: inlet temperature of 60° C, feed flow rate of 1 mL/min, and aspiration rate of 90%. SEM images revealed flattening of mesoporous particles despite successful loading due to limited diffusion of MZ1 into the bulk of the particles because of their large molecular size. Raman imaging further confirmed the restricted internal distribution of MZ1, showing that MZ1 distributed around the outer edges of the mesoporous particles and left the core unoccupied. Meanwhile, thermal analysis confirmed the amorphous nature of MZ1 prior to and after loading into mesoporous carrier, which conferred additional stabilisation of MZ1 in the pores against any conformational changes. The change experienced in pore properties of MESOPAC after introducing MZ1 indicated a successful degree of loading, as reflected by the decrease in surface area and pore volume when compared to the unloaded form of the carrier. The ability of mesoporous particles to enhance the solubility of MZ1 was also investigated. It was proved that MZ1-loaded MESOPAC were superior in terms of dissolution as opposed to raw MZ1, with a 4-fold increase in dissolution at 30 minutes. This finding demonstrated that the novel mesoporous carrier proposed herein is a promising technology for solubility enhancement of not only small molecules, but also for those that lie outside the rule-of-five chemical space. From these findings, one can conclude that oral delivery of PROTACs is challenging but could be improved utilising mesoporous carriers. The permeability aspect, however, should be considered in future studies to fully exploit their potential as oral therapeutics.

Chapter 4

Colon-targeted Delivery of Small Molecules and PROTACs Using Mesoporous Particles: An Enzyme-triggered Approach

4.1. Introduction

In the previous chapters, an innovative PROTAC, representing a complex class of molecules with challenging physiochemical properties, was examined using a novel mesoporous carrier technology. The targeting application of the system is, however, yet to be explored, particularly with regards to colon-specific delivery. The process of generating the mesoporous particle proved to be reproducible, and its capability of encompassing complex molecules was demonstrated. Yet, its true potential as a modern technology resides in making the most of the advantages that the colonic environment offers for drug delivery but acknowledging its challenges too.

The interest in the colon stems from being a microenvironment with unique features. These features can be summarised into a varying pH gradient within its segments that is quite elevated compared to the other regions of the GIT, a long transit time of more than 18 hours, and harbouring the largest microbial community that secrete enzymes capable of fermenting indigestible polysaccharides (Awad et al., 2022). These have been widely explored for site-specific targeting of drugs locally and systemically (Details in chapter 1).

Nevertheless, one particular aspect was not brought into focus in existing literature. The colon displays lower proteolytic activity compared to the small intestine, which acts as a promising delivery opportunity for vulnerable drugs (Rubinstein et al., 1997). In fact, research has shown that the colon exhibits low levels of drug uptake and reduced expression of efflux transporters and metabolising enzymes like cytochrome P450 (McCoubrey et al., 2023). Altogether, this might be advantageous for drugs that are affected by these processes, particularly those that experience extensive efflux or are metabolised in the small intestine and possess low bioavailability as a result (Awad et al., 2022; McCoubrey et al., 2023). Thus, the gentler environment that the colon offers might enhance the bioavailability of these drug molecules, offering prospects for colonic delivery.

Of importance is the low concentration of p-glycoprotein (P-gp) efflux transporter in the colon compared to the small intestine (McCoubrey et al., 2023), which might be beneficial for the delivery and permeability of PROTAC molecules in particular. It has been reported that MZ1 is susceptible to significant P-gp efflux, affecting its oral bioavailability (Opnme, 2025). Therefore, delivering MZ1 to the colon as a site with reduced P-gp expression is hypothesised to enhance its bioavailability and effectiveness. This served as the framework for the work conducted in this chapter, aiming at delivering PROTAC-loaded MESOPAC to the colon and exploring the advantages that this site provides.

Given these advantages, it is no doubt that there is an increased demand on designing colon-targeted drug delivery systems, particularly for complex molecules. Several technologies have been proposed in literature to promote colonic delivery of drugs. These vary between pH-dependent strategies, time-based technologies, and enzymatic-triggered formulations

(Nguyen et al., 2019). The latter is noteworthy, given that some polysaccharides are resistant to digestion in upper GIT but are completely fermented by colonic microflora, releasing the drug load specifically within the designated region upon the action of enzymes (Gong et al., 2024b). They are known to possess good biodegradability, biocompatibility, and safety profile (Gong et al., 2024b). Natural polysaccharides, like gaur gum and pectin, exhibit properties that could be imparted to MESOPAC to facilitate its colonic-targeting. Both are selectively degraded in the colon and are, thus, possible candidates for colonic delivery. However, pectin might require modification due to high solubility in the small intestine (Akhgari et al., 2010). Guar gum, on the other hand, displays a key characteristic, which is its ability to swell in upper GIT, forming a viscous gel network that delays drug release and prevents the ingress of dissolution medium (Krishnaiah et al., 2002). The integration of these polysaccharides with drug delivery technologies allows controlled release of drugs to maximise the efficiency of treatment.

Guar gum and pectin have been long studied for colon targeting purposes. In early work, the emphasis was primarily on utilising guar gum in simple drug delivery systems such as matrices, compression coats, and hydrogels (Gliko-Kabir et al., 2000; Krishnaiah et al., 1998; Prasad et al., 1998; Vemula & Bontha, 2013; Shyale et al., 2006; Yellela et al., 2009). Altogether, the findings of early research suggested that drug release can be minimised in upper GIT but was triggered in the colon when guar gum was used, depending on the concentration within the formulation and the thickness of the swellable network formed. Yet, recent advances found that guar gum can be effectively combined with other polymers, like Eudragit, HPMC, xanthan gum, or pectin; it can also be combined with other formulation strategies, such as nanotechnology, microspheres, mesoporous silica particles, or liposomes, in addition to being chemically modified to have a dual- control over drug release and optimise the efficacy of the proposed strategies (Chandel et al., 2020; Hanmantrao et al., 2022; Kuar et al., 2017; Kumar et al., 2017; Moutaharrik et al., 2023; Seeli, & Prabaharan, 2016). Collectively, these efforts emphasised the versatility of guar gum with regards to colonic applications, spanning through various delivery platforms and originating from its ability to delay drug release until acted on by enzymes in the colon.

Likewise, pectin emerged as a polysaccharide with colonic targeting potential that stems from its backbone chains being specifically broken down by pectinases found in the large intestine (Gong et al., 2024b). The interest in pectin started in the early 1990's, where the employment of pectin for colon delivery was centred around simple strategies and focused on unveiling its degradability and versatility. For example, Ashford and colleagues (1993) applied high-methoxy pectin as a compression coat on tablets designed for colon-targeted delivery. Soon after, researchers identified the challenges associated with native pectin, whereby premature release occurred due to high solubility. The native polysaccharide was modified to generate

more water-resistant forms that overcome this issue (Gong et al., 2024b). The emphasis transitioned to modified pectin derivatives, such as calcium pectinate that is formed through ionic interactions to reduce water solubility. For instance, Rubinstein et al. (1993) prepared compressed tablets containing the active ingredient and calcium pectinate for colon-specific delivery. Notable enhancement in drug release was noticed upon exposure to colonic enzymes. Moreover, gel beads of calcium pectinate were generated by Sriamornsak & Nunthanid (1998) for controlled release of drugs that exhibit poor solubility. Mixed polymer systems that are based on combining pectin with other materials like Eudragit, chitosan, HPMC, or ethylcellulose were also reported (Akhgari et al., 2010; Chang & Lin, 2000; Turkoglu & Ugurlu, 2002; Wakerly et al., 1996). Years of research followed, and the significance of pectin still persists. It is the shift, however, to more sophisticated and complex strategies that marks the ongoing evolution of pectin in colonic delivery. Nowadays, research proved the adaptability of pectin within a range of colonic applications as in multi-layered and hybrid systems, smart-gated delivery technologies, stimuli-responsive strategies, and nanotechnology (Awad et al., 2022; Ribeiro et al., 2014; Wu et al., 2025).

Achieving controlled release within the colon is certainly advantageous for many drug classes, especially for novel molecules like PROTACs to ensure optimal therapeutic efficacy. The choice of polymers becomes crucial to meet this objective. Introducing new polymers to the market is complicated and lengthy, while using polymers that are already approved facilitates the industrial translation if needed. Hence, the selection of pectin and guar gum was based on the fact that they are generally regarded as safe (GRAS), with established profiles and extensive documentation in drug delivery applications. While PROTACs might be ideal candidates for colon delivery, there remains a need for an innovative drug delivery technology that could host these molecules. Incorporating colon-specific polysaccharides into the novel mesoporous carrier proposed herein opens new avenues in colon-targeted delivery, such that guar gum and pectin were exploited differently and innovatively compared to past work. To date, this chapter is the first to report the delivery of a model PROTAC molecule to the colon. It is also the first to combine CAB-based mesoporous particles with guar gum for colonic release of drugs.

The objectives of this chapter were as follows:

- To design an enzyme-triggered drug delivery system for colon-specific delivery using MESOPAC
- To identify and analyse appropriate polysaccharides that could retard drug release in upper GIT but facilitate the release specifically in the colon
- To assess the *in vitro* drug release in simulated media representing different GIT segments

- To establish a correlation and achieve a comparable release profile between the small-volume dissolution vessels and the compendial setup by adjusting the dissolution parameters
- To implement the optimal formulation design in the delivery of a model PROTAC to the colon

4.2. Materials and Methods

4.2.1. Materials

Pectin citrus USP and guar gum NF were purchased from Spectrum Chemicals (New Jersey, USA) and VWR (Leicestershire, UK), respectively. Hydrochloric acid and methanol were supplied by Fisher Scientific (Loughborough, UK). Endo-1,4 β-Mannanase (*Aspergillus niger*) and α-galactosidase (*Aspergillus niger*) powder were bought from Megazyme (Bray, Ireland). All other materials are listed in **sections 2.2.1 and 3.2.1**.

4.2.2. Preparing MESOPAC, Loading with Felodipine and MZ1, Calculating Loading Efficiency and Drug Load Quantification, and Performing Statistical Analysis

MESOPAC was generated via spray drying using ultrasonic nozzle following the method in **section 2.2.2**. Loading MESOPAC with felodipine and MZ1 was conducted at a theoretical load of 20% (w/w) according to the methods stated in **sections 2.2.3 and 3.2.3**, respectively. The samples generated were quantified via HPLC as reported in **sections 2.2.4 and 3.2.2**. Statistical analysis was performed in accordance with **section 2.2.12**.

4.2.3. Designing Pectin and Guar Gum-based MESOPAC Formulations via Spray Drying

Spray drying was investigated as a pore capping technique using Buchi B-290 mini spray dryer with a two-fluid nozzle from Flawil (Switzerland). A dispersion of pectin at a concentration of 0.8% (w/v) in water was created and homogenised, to which felodipine-loaded MESOPAC was added at polymer-to-formulation ratios of 5:1 and 10:1. The dispersion was kept on the stirrer throughout the run (VWR, Leicestershire, UK). The process proceeded at the following parameters: inlet temperature of 165°C, outlet temperature 120°C, aspirator rate of 90% (or 35 m^3/hr), feed flow rate at 2.5 mL/min, and nitrogen flow rate at 10 L/min.

On the other hand, guar gum was similarly dispersed in cold water at concentrations of 0.5% and 0.8% (w/v) and homogenised. Spray drying parameters were varied throughout, testing a range of variables. The investigations were carried out at an aspirator rate of 90% (35 m^3/hr), nitrogen gas flow of 10L/min, inlet temperatures of 165 and 180°C, feed flow rates at 2.5 and 5 mL/min, solid contents of 1 and 1.6% (w/v), and guar gum concentrations of 0.5% and 0.8% (w/v).

4.2.4. Designing Physical Mixtures of Pectin and Guar Gum-based MESOPAC Formulations with Felodipine-loaded MESOPAC for Colon-targeted Delivery

Physical mixtures of pectin were prepared at polymer-to-MESOPAC ratio of 10:1. Accurate amounts of guar gum and felodipine-loaded MESOPAC were weighed and transferred into a glass vial. To ensure uniformity, the powders were blended using flask shaker (Stuart Scientific Surrey, UK) at 700 oscillations per minute for 30 minutes. Following that, the samples were

mixed manually for five minutes to ensure additional homogeneity. The samples were then stored in glass vials at room temperature.

Physical blends of guar gum with felodipine-loaded MESOPAC were prepared similarly but at three guar gum-to-MESOPAC ratios, namely 3:1, 5:1, and 10:1.

4.2.5. *In Vitro* Dissolution of Pectin-based MESOPAC Whether Prepared via Spray Drying or as Physical Blends with Felodipine-loaded MESOPAC

The release behaviour of felodipine-loaded MESOPAC with pectin was studied across the upper GIT segments in small-volume dissolution apparatus by Copley (Nottingham, UK). Formulations, either spray dried at 5:1 or 10:1 of polymer-to-MESOPAC ratio or physically blended at 10:1, were studied in 30 mL of 0.1N HCL with 1% (w/v) SLS to simulate the acidic environment of the stomach followed by phosphate buffer pH 6.5 with 1% (w/v) SLS to mimic the small intestine (Wong et al., 1997). The dissolution media were maintained at 37 ± 0.5°C with a stirring speed of 50 rpm according to USP monograph. Samples containing 2.5 mg of felodipine were weighed, filled into hard-shell gelatine capsules size 00, and wrapped in sinkers. The same capsule was transferred between the vessels, with samples withdrawn every 30 minutes for two hours in the gastric stage. Then, the capsule was examined for four hours in media simulating the small intestine, during which samples were also collected every 30 minutes. Aliquots of 0.3 mL were withdrawn at predefined time points and replaced with fresh media. The withdrawn samples were filtered with 0.45 µm syringe filters (Fisher Scientific, Loughborough, UK) and transferred into small-volume HPLC vials (Thames Restek, Buckinghamshire, UK). After that, the withdrawn samples were analysed using the HPLC method reported in **section 2.2.4**. Cumulative drug release plots as a function of time were obtained.

4.2.6. *In Vitro* Release of Raw Felodipine and Felodipine-loaded MESOPAC in Compendial Dissolution Apparatus and in Small-volume Dissolution Apparatus

Because colon-targeted delivery assessments involve the use of enzymes to mimic the microbial community responsible for digesting polysaccharide-based coats, the use of a compendial dissolution setup was not feasible as it requires large quantities of the enzymes to be added. It was necessary to establish a correlation in drug release between the compendial setup and the adapted miniaturised apparatus. To evaluate the effectiveness of small-volume vessels in achieving a similar performance to that of compendial large vessels, *in vitro* dissolution tests were initiated. Raw drug along with drug-loaded carrier particles were investigated in phosphate buffer with a pH of 6.5 and 1% (w/v) SLS for two hours following USP 36 monograph with slight modification. USP apparatus 2 (rotating paddle, 50 rpm) was used as the model compendial large-volume setup, whereby dissolution tests were conducted in an Erweka DT 126 dissolution apparatus (Heusenstamm, Germany). Hard-shell gelatine

capsules were filled with samples equivalent to 41.6 mg of felodipine and added to 500 mL vessels containing dissolution medium at 37 ± 0.5°C. The amount was selected to achieve the same theoretical concentration of 83 µg/mL as the small-volume setup. It was necessary to use the same theoretical drug concentration for meaningful comparison between the two, as concluded by Hellberg et al. (2021) and Klein & Shah (2008). Sinkers were used to restrict floating of capsules. A volume of 5 mL was withdrawn every 30 minutes over a period of 120 minutes, filtered using 0.45 µm filters (Fisher Scientific, Loughborough, UK), and injected into HPLC vials supplied by Thames Restek (Buckinghamshire, UK). Experiments were repeated in triplicate for the raw form and the drug-loaded MESOPAC. The samples were finally analysed by HPLC according to the method reported in **section 2.2.4.**

For the small-volume vessels, the release behaviours of raw felodipine and felodipine-loaded MESOPAC were examined under identical conditions as compendial setup but with adjusting some parameters to accommodate the differences that exist between the two. These parameters mainly involved the speed of the rotating paddle, the volume of the dissolution medium and the sample withdrawn, and the fill powder amount. Samples equivalent to 2.5 mg were filled into capsules and introduced to 30 mL of dissolution media. This amount ensured the same theoretical concentration as that with large-volume vessel was met. Paddle speed was varied to investigate three different speeds: 50, 150, and 200 rpm. At designated time intervals, aliquots of 0.3 mL were collected and replaced with fresh phosphate buffer. All other settings were the same as the compendial setup.

4.2.7. *In Vitro* Release of Felodipine-loaded MESOPAC and MZ1-loaded MESOPAC Using Guar Gum for Colon-specific Delivery in Small-volume Dissolution Apparatus

Dissolution experiments to test the colonic specificity of the drug-loaded MESOPAC with and without guar gum were performed in small-volume vessels to preserve the API as well as the enzymes using Copley Scientific dissolution tester (Nottingham, UK). The miniaturised vessels with mini paddle can fit directly onto the existing dissolution bath. Tests were performed in 30 mL at 37 ± 0.5°C, with hard-gelatine capsules containing samples equivalent to 2.5 mg of felodipine. Different guar gum-to-drug-loaded MESOPAC ratios were investigated, namely 3:1, 5:1, and 10:1. The mini paddle speed was set at 150 rpm. To assess whether the formulations remain intact in upper GIT, they were studied in environments mimicking the mouth-to-colon transit. Initially, the capsules with sinkers were placed in 0.1 N HCL with 1% (w/v) SLS for two hours to mimic the stomach and then were transferred to phosphate buffer of pH 6.5 with 1% (w/v) SLS for four hours to represent the conditions of the small intestine (Naeem et al., 2018; Wong et al., 1997). Drug dissolution in the colon was evaluated by continuing the release for additional 18 hours in the presence and absence of enzymes. The simulated colonic fluids consisted of phosphate buffer pH 7.4 with 1% (w/v) SLS (Naeem et

al., 2018; Narala et al., 2023). Tests conducted in colonic environment without enzymes served as control. Meanwhile, to assess the effect of colonic microflora on drug release, the media were spiked with one or both enzymes, endo-1,4 β-mannanase at 0.166 U/mL and α-galactosidase at 0.033 U/mL (Burke et al., 2005; Gliko-Kabir et al., 2000). Aliquots of 0.3 mL were withdrawn every 30 minutes in gastric and small intestinal conditions. In colonic environment, sampling was done at the following time intervals: 1, 2, 3, 4, 5, 9, and 18 hours. Fresh medium was introduced each time a sample was withdrawn. The aliquots were injected into Eppendorf tubes, to which 0.3 mL of methanol was added. The samples were then centrifuged at 3000 rpm for 20 minutes before being filtered and injected into low-volume HPLC vials (SureStart™ ,Fisher Scientific, Loughborough, UK). HPLC analysis was performed as reported in **section 2.2.4**, but using a different HPLC device. Agilent 1220 Infinity II was used to analyse the samples at the pre-established parameters (Cheshire, UK). All tests were run in triplicate, and release data obtained from peak areas were reported as mean ± standard deviation.

For PROTAC delivery to the colon using guar gum as release modifier and MESOPAC, dissolution tests were performed under the same conditions as those with felodipine but with slight modifications. Only the optimal guar gum-to-drug-loaded MESOPAC ratio (5:1) was investigated upon adding two enzymes to the test. The SLS concentration was reduced to 0.3% (w/v) to avoid interference with the HPLC peaks. The chromatographic analysis was, however, conducted according to the method reported in **section 3.2.2** using Agilent 1220 Infinity II HPLC (Cheshire, UK). All other test parameters were kept the same.

In this chapter, two categories of control samples were tested. One, detailed earlier, was employed to assess the effect of enzyme addition in drug release, whereby media without enzymes were involved. The other included samples of drug-loaded MESOPAC (drug load 20% (w/w)) without guar gum to correlate the effect of site-specific release to the presence of the polysaccharide. Felodipine or MZ1-loaded MESOPAC without guar gum were simply studied at a sequential pH gradient that represents the different segments of the GIT. Capsules, containing approximately 2.5 mg of API, were placed for 120 minutes in 0.1N HCL with 1% (w/v) SLS to represent the stomach. A new capsule was added each time to phosphate buffer pH 6.5 and 7.4 with 1% (w/v) SLS to mimic the small intestine and the colon, respectively. Ideally, one capsule should be added and studied under each phase of the GIT for the entire duration of the study by transferring it between the vessels. Because guar gum was not present, this approach was not possible as a transferrable plug of powder particles was not formed. Moreover, gradual pH adjustment using buffering agents to shift the medium from acidic to basic to represent the transit from the stomach to colon was also not feasible since small-volume vessels are used, where analytical sensitivity and sink conditions would be disrupted in that case. Therefore, individual capsules were introduced to each phase, such

that a separate assessment was carried out. Every 30 minutes, 0.3 mL samples were withdrawn from the vessels representing the gastric and small intestinal region and replaced with fresh media. In those mimicking the colon, samples were withdrawn hourly for five hours and then at the ninth and eighteenth hour to represent the colonic transit. The tests were conducted at 150 rpm using Copley's mini vessels with 30 mL of dissolution media equilibrated at 37 ± 0.5°C. For each withdrawn sample in Eppendorf tubes, 0.3 mL of methanol was added to match the experimental conditions of guar gum-based samples. The samples were then centrifuged (Hettich Mikro 20, Tuttlingen, Germany), filtered, and injected into small-volume HPLC vials (SureStart™ ,Fisher Scientific, Loughborough, UK) for analysis. The runs were performed in triplicate. HPLC analyses were done as reported earlier, depending on the API.

4.2.8. Statistical Analysis

Data repeated in triplicate were represented as mean and standard deviation, which were then statistically analysed using Graphpad Prism 10.0 software (California, USA). Appropriate statistical methods (either one-way ANOVA or two-way ANOVA) were chosen based on the nature of the data. A p-value less than 0.05 was set for statistical significance.

4.3. Results and Discussion

4.3.1. Investigating Pectin as a Potential Polymer for Colon-targeted Delivery

Pectin is widely recognised for its colon-specific microbial degradation and gelling property that facilitate its application as a drug delivery vehicle (Das, 2021). But being a polysaccharide in nature, pectin is classified as a hydrophilic or water-soluble material, which is quite undesired for colonic targeting (Das, 2021). Despite being inherently water soluble due to the abundant presence of carboxylic groups that can form hydrogen bonds with water (Zhang et al., 2024), the practicality with which it is dispersed or solubilised is somewhat challenging. It is well known that the solubility and gel-forming properties of pectin are dictated by several factors, such as its degree of esterification and molecular weight, in addition to other conditions present within the setting such as ions, pH, and temperature (Arias et al., 2021). Of importance is the degree of esterification, whereby pectin's hydrophilicity can be reduced when esterified. Therefore, high methoxy pectins (HMPs) show reduced hydrophilicity. They exhibit a slightly hydrophobic nature due to the high esterification that minimises the interaction with water molecules (Zhang et al., 2024). This leads to incomplete dissolution of HMPs when added to water, due to this hindered hydration.

Given that pectin is insoluble in organic solvents (Würfel & Heinze, 2025), water becomes the default solvent to create a solution or suspension of pectin for spray drying. In water, pectin exhibits the tendency to gel under specific conditions only (Abboud et al., 2020), which if not present, pectin molecules tend to clump (Said et al., 2023). To start the spray drying process, a dispersion of pectin in water was created at a concentration of 0.8% (w/v). A homogeniser was required to disperse the lumps. It is also noteworthy to mention that dispersions of higher concentrations were not feasible as the viscosity highly increases. This increase in viscosity impeded the spray drying process, particularly atomisation. A similar finding was reported by Nguyen and colleagues (2024). In their investigation, pectin formed lumps and was not dispersed at a concentration of 20% (w/w). At lower concentrations of 10% and 9% (w/w), the solutions were highly viscous, lacking flowability and dispersibility.

During the preliminary studies, spray drying of blank pectin particles was attempted to understand the effect of the process on pectin itself and to optimise the spray drying parameters prior to the addition of drug-loaded MESOPAC. This aligns with earlier investigations to preserve the materials during spray drying in the early stages of pharmaceutical product development (Li et al., 2022). The effect of four parameters, namely inlet temperature, feed flow rate, solid content, and aspirator rate, on the yield were initially studied (**Table 4.1**). It can be inferred from the data that increasing the inlet temperature increased the yield until it reached a point beyond which the increase in temperature adversely affected the yield. A similar behaviour was reported by Li et al. (2022) such that the powder

yield was maximised as inlet temperature kept on increasing until lower powder recovery was noticed when excessive high temperatures were reached. The increase in yield observed with increasing inlet temperature was discussed in **section 3.3.2.1.** However, the decline towards higher temperatures with pectin in this chapter can be attributed to approaching pectin's degradation temperature. Research showed that pectin molecules vary in their structure and degree of modification, and this variability, subsequently, influences their thermal behaviour (Einhorn-Stoll et al., 2007). For example, pectin extracted from different sources, such as apple and citrus peel, degrade at different temperatures (Dranca & Oroian, 2019). However, a general agreement was reached by several authors suggesting that pectin from citrus peel, similar to the one used herein, undergoes degradation between 220 and 240°C (Dranca & Oroian, 2019; Einhorn-Stoll et al., 2007; Rentería-Ortega et al., 2023; Wang et al., 2014). Although eventually some powder was obtained when spray drying at 180°C, the yield was declining because the temperature was operating near the degradation threshold of pectin. In fact, Ruano et al., (2020) reported that deacetylation of pectin molecules begins at 183.27°C, explaining the suboptimal spraying performance captured as lower yield at 180°C.

Similarly, the effect of feed flow rate on yield followed a comparable pattern. An initial increase in flow rate led to improved yield, but beyond a certain value, further increases resulted in a decline. Li and colleagues (2022) described such a pattern and attributed it to large droplets being generated at high flow rates. These larger droplets require a higher temperature input to sufficiently dry and flow without sticking to the walls of the spray dryer. Most likely, this could explain the decrease in yield herein when the feed flow rate was set at 5 mL/min, requiring higher inlet temperatures that were not feasible as pectin's degradation threshold was approached.

On the other hand, the aspiration rate showed a continuous increase in yield, which was explained in **section 3.3.2.1.** Additionally, upon optimising spray drying of pectin microparticles, Li and co-workers (2022) revealed that higher aspiration rate minimised the moisture within the system, accounting for lower tendency of wall deposits and thus enhanced yield.

On the contrary, an inverse relationship existed between solid content and powder recovery. It was shown that the lowest solid content of 0.8% (w/v) achieved the highest yield when spray drying pectin. This contrary finding to that discussed in **section 3.3.2.1** of the effect of solid content on powder yield could be explained by pectin's viscous nature. When the concentration of pectin increased within a solution, the system became non-flowing and non-sprayable as observed by Siles-Sánchez et al. (2024). In their study, Siles-Sánchez and colleagues (2024) operated with the solution of the lowest pectin concentration (10 mg/mL) among several concentrations tried because their spray drying process was limited by the increased viscosity of the solution as pectin's concentration increased. Similarly, Sarabandi et

al. (2018) reported a decline in the powder yield when pectin concentration exceeded 2% (w/w).

Following the preliminary optimisation trials, the parameters resulting in maximised yield were determined as: inlet temperature of 165°C, feed flow rate of 2.5 mL/min, aspiration rate of 90%, solid content of 0.8% (w/v), nitrogen flow rate of 10 mL/min, and water as solvent. Two polymer-to-loaded MESOPAC ratios, 5:1 and 10:1, of pectin to felodipine-loaded MESOPAC were selected to proceed with at the optimised parameters. Spray drying was conducted, with powder yields ranging between 40 and 53%. Felodipine-loaded MESOPAC powder that is capped with pectin was obtained and subjected to colonic drug release studies to study the ability of the pectin as a colon-degradable polysaccharide in protecting the drug load throughout the upper GIT.

Table 4.1. The effect of varying spray drying parameters on the yield of pectin powder

Inlet temperature (°C)	**Yield (%)**
135	42.4
165	46.7
180	40.7
Feed flow rate (mL/min)	**Yield (%)**
1	25.5
2.5	46.7
5	27.4
Solid content (%)	**Yield (%)**
0.8	46.7
1.5	38.6
3	33.6
Aspirator rate (%)	**Yield (%)**
70	24.4
80	31.3
90	46.7

In addition to spray drying, physical blending of pectin with drug-loaded MESOPAC was attempted for comparative purposes. Physical mixtures present with versatile applications as the cost of fabricating new polymers to meet the desired formulation outcomes is extensively high. Hence, the drug release characteristics can be easily tuned by varying the blend ratio, with each blend contributing to a distinct overall performance (Silva et al, 2009). For example, dissolution enhancement was seen with a physical mixture over raw drug that was dependent on the polymer's choice and the polymer-to-drug blend ratio (Chokshi et al., 2007). This suggested that a physical mixture can still be valid as an alternative to other strategies to design a targeted delivery system through precise polymer selection. The concept of blending different polymers was also extended for site-specific delivery. Silva and colleagues (2009) produced tablets composed of physical blends of two starch-grafted copolymers at several ratios for colon-specific delivery. In light of this, physical mixtures of MESOPAC and pectin were created for colon-targeted delivery.

4.3.2. *In Vitro* Drug Release of Pectin-based MESOPAC for Colon-targeted Delivery

In developing a colon-specific drug formulation, dissolution studies under conditions that mimic the gastrointestinal environment are very crucial. These studies help ensure minimal drug release in the upper gastrointestinal tract while maximising release in the colon. They also assess the formulation's ability to withstand the different pH conditions along the gastrointestinal tract. For that reason, experimental studies proceeded with subjecting the two formulations of varying pectin-to-drug-loaded MESOPAC ratio to dissolution studies in two media. One was the acidic environment with a pH of 1.2 to mimic the gastric region and the other was that with a pH of 6.5 to represent the small intestinal environment. **Figure 4.1** depicts the dissolution profiles of the spray-dried 5:1 and 10:1 formulations in addition to the physical mixture of pectin and drug-loaded MESOPAC at a ratio of 10:1 over a period of six hours, representing the expected time for a formulation to travel down the upper GIT.

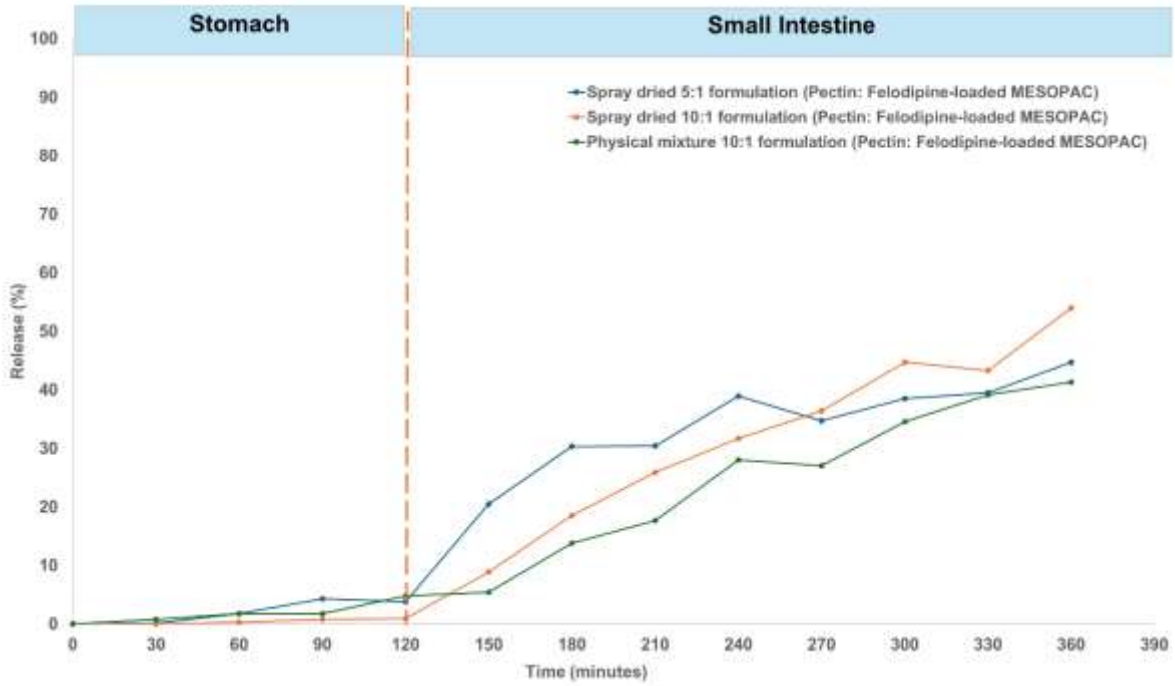

Figure 4.1. *Release profiles of felodipine from spray-dried and physically blended pectin and loaded MESOPAC formulations in media simulating the upper GIT. [Testing conditions: 0.1 N HCL with 1% SLS for gastric medium; phosphate buffer pH 6.5 + 1% SLS for small intestinal region, 30 mL with mini vessel, mini paddle, 50 rpm]. A single capsule was used for the test and transferred between media*.

It appears that the drug release in acid was very minimal with all drug-loaded MESOPAC with pectin formulations, suggesting the successful retardation of premature release in the acidic environment of the stomach. Contrary to expectations, the release of felodipine exceeded 41.32%, regardless of the preparation technique, when subjected to intestinal environment. With spray-dried formulations, the release was measured as 44.72% and 54.0% with 5:1 and 10:1 ratios, respectively, by the end of the sixth hour at a pH of 6.5. Unfortunately, these percentages indicated that a substantial amount of the dose was released in the small intestine

prior to reaching the colon, which rendered the drug-loaded MESOPAC capped with pectin unsuitable for colon-specific targeting. Both physically mixing the carrier with pectin or spray drying them together, proved inadequate for colon-specific delivery at the specified ratios.

One possible reason for the stability of the pectin-coated MESOPAC in the gastric environment is the characteristic gelation of HMPs at low pH values. This gelling capacity forms a barrier against drug release. According to Khotimchenko (2020), pectin gels tend to be stable in acidic environments. However, as the pH shifts towards more neutral pH values as that of the small intestine, the gel loses its stability and viscosity (Khotimchenko, 2020). **Figure 4.2** illustrates the gelling behaviour of pectin-capped MESOPAC and demonstrates the loss of this characteristic as the pH shifts to that of the small intestine over time. It can be seen that pectin swelled over a period of two hours in medium simulating the stomach. Nevertheless, the swellable plug decreased in size in the small intestinal conditions, suggesting the dissolution of pectin and accounting for the observed turbidity of the system. This visual observation correlated with the high drug release percentages reported earlier in regions prior to the colon.

Altogether, these results suggested that pectin-coated MESOPAC cannot withstand the journey to the colon without exposing their drug load. Thus, the results indicated that further modification was needed to minimise upper GIT release. The findings discussed above align with those of Ribeiro et al. (2014), who investigated the colonic delivery of 5-aminosalicylic acid (5-ASA) using pectin-coated chitosan beads. Part of their research investigated pectin beads encapsulating either the pure drug or intercalated form with layered double hydroxide. The release of 5-ASA from pectin-based beads, regardless of how the drug was incorporated, did not exceed 10% when exposed to the acidic medium simulating the stomach. Conversely, when the formulations were exposed to higher pH values, both demonstrated increased drug release; however, the release from pectin beads containing the pure form of the drug was much higher than that from inorganic matrix, since diffusion from the matrix hindered the drug release and required additional time. Their work supported our findings, as it reinforced the protective role of pectin in acidic media but raised concerns about premature drug release due to pectin's solubility in conditions that represent the small intestine (Ribeiro et al., 2014). Similar findings were reported by Vaidya et al. (2009), who studied the potential of pectin microspheres harbouring metronidazole for colonic delivery. The system showed promising results with regards to minimising early drug release if coated with acid-resistant material such as Eudragit. But, it would otherwise release almost the entire dose before reaching the colon. In addition, Turkoglu & Ugurlu (2002) found that applying pectin alone as a compression coating around 5-ASA tablets was not sufficient to hamper drug release in the upper GIT. They also found that HPMC was needed to manipulate the solubility of pectin. Together, these

results further emphasised the need to modify pectin when it is intended for colon-specific applications.

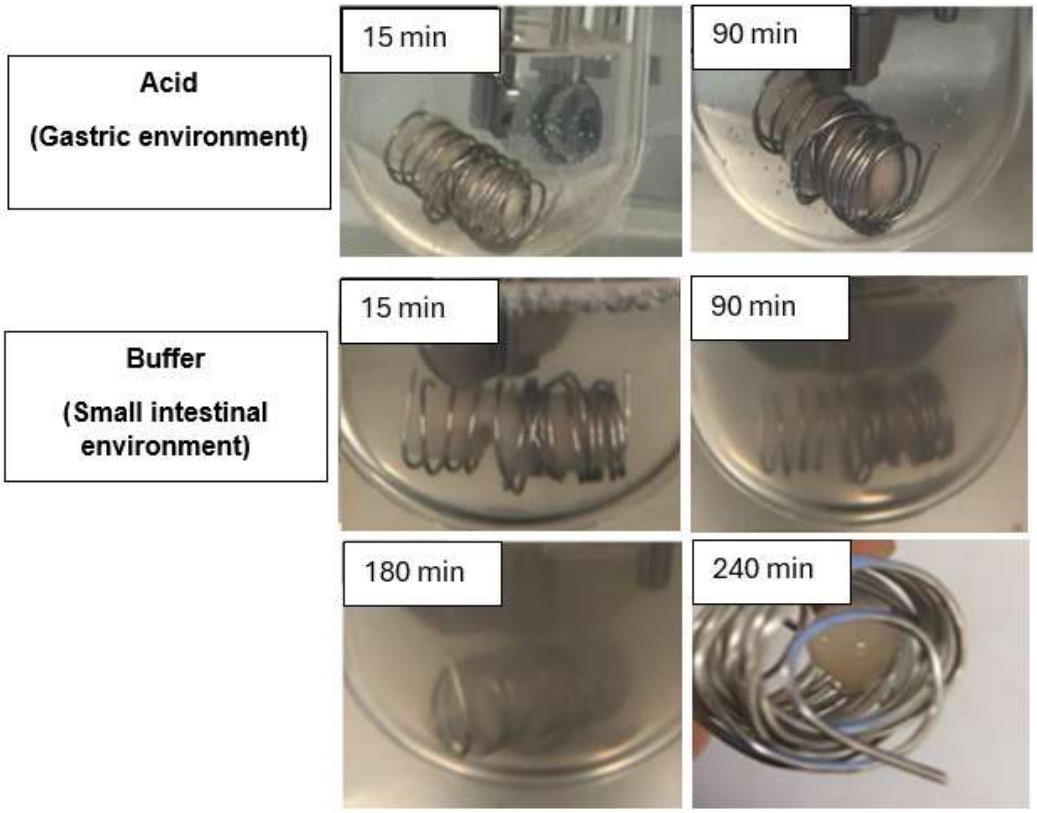

Figure 4.2. *The stages of spray-dried, pectin-based formulation of MESOPAC (ratio: 10:1) as it swells and forms a plug in acidic medium but dissolves and loses stability in the conditions representing the small intestine, causing premature drug release before reaching the colon*

Doubts then surrounded our choice of pectin and questioned its use with MESOPAC if previous work in literature had revealed premature drug release with pectin for colon-targeted delivery. However, one can argue that pectin's resistance to degradation by enzymes present in upper GIT and ability to reach the colon intact, where it becomes susceptible to selective microbial degradation, is a pivotal characteristic that overlooks any inherent, modifiable flaws (Khotimchenko, 2020).

Moreover, of the different pectin types, HMP was selected over low-methoxy pectin because it showed reduced water solubility. Hence, it might be beneficial in minimising upper GIT release (Jacob et al., 2020). From this perspective, it was a common act in literature to combine pectin with other polymers as matrix agents or coat-forming materials in an attempt to reduce its water solubility and generate a long-lasting barrier to drug release (Moutaharrik et al., 2024). In fact, the incorporation of insoluble polymers, such as ethyl cellulose, was frequently employed with pectin-based formulations and showed delayed drug release onset in upper GIT but promoted release specifically in the colon upon exposure to microbes (Bose et al., 2014; Wakerly et al., 1996; Wakerly et al., 1997; Wei et al., 2007). It was found that

when combining pectin with insoluble polymers, the ratio of one polymer to another manipulated the percentage of drug released. Therefore, combining pectin with MESOPAC, a form of cellulose, was hypothesised to minimise premature drug release. Moreover, the rate at which pectin hydrates in aqueous fluids was of importance as it affected the degree of swelling, which in turn impacted drug release (Wakerly et al., 1997). HPMC, chitosan, and Kollicoat are other examples of polymers integrated into pectic formulations to achieve colon-specific targeting (Moutaharrik et al., 2024; Turkoglu & Ugurlu, 2002; Wei et al., 2007; Zhu et al., 2019). Together, these data highlighted pectin's potential for colonic delivery through careful combination with other additives or through technical processing. Otherwise, early drug release would be an issue; thus, alternative polysaccharides, such as guar gum, were explored.

4.3.3. Investigating Guar Gum as a Potential Polymer for Colon-targeted Delivery

The quest to find a polymer that retards upper GIT release but is susceptible to colonic microbial degradation kept ongoing despite the early premature release observed with pectin during the preliminary analysis. Guar gum is another polysaccharide that has been widely explored for colon-targeted delivery in compression-coated tablets, nano- and microcarriers, matrices, and hydrogels (Gong et al., 2024b). Its ability to swell and subsequently gel when in contact with an aqueous environment, in addition to its degradation by colonic enzymes, make it an appealing choice for colon-specific applications.

Like pectin, however, guar gum hydrates in water to form a viscous dispersion with gel-like consistency (Prabaharan, 2011). This feature is assumed to help minimise premature drug release. However, uncontrolled rate of hydration or extensive swelling might impair its performance and lead to rapid drug release outside the targeted region (Manna et al., 2024; Gong et al., 2024b). Careful design of the colon-specific formulation helps in overcoming this limitation by selecting the appropriate proportion of guar gum, adjusting its viscosity, or combining and modifying it with other materials (Krishnaiah et al., 2001; Manna et al., 2024). It is because of guar gum's swelling and hydration that solubilising it in water as a solvent is challenging. Like pectin, guar gum is not soluble in many organic solvents such as alcohols and esters; hence, water was selected among all (Sharma et al., 2018).

4.3.3.1. Spray Drying of Guar Gum

Guar gum dispersions in cold water at four different concentrations (0.4, 0.8, 1 and 2% (w/v)) were trialled. As the concentration of guar gum increased, the dispersion became very viscous. Highly concentrated dispersions (1% and 2% (w/v)) exhibited a gel-like consistency that was either not pumpable or not sprayable through the spray dryer even after full hydration of the gum. Similarly, Ravichandran et al. (2012) attempted to encapsulate Betalains with guar

gum via spray drying, but the dispersion was highly viscous and consequently not sprayable. In the present study, the concentration was reduced to 0.8% (w/v) or lower, whereby the system was dispersed with minimal lumps using a homogeniser as reported by Tripathi et al. (2019). Low concentration dispersions were of visually accepted consistency and were, therefore, subjected to spray drying. This step aimed to study the behaviour of blank guar gum upon spray drying before initiating the capping trials of MESOPAC with guar gum for colon-specific delivery. As high guar gum concentrations were ruled out, it became evident that any concentration of 0.8% (w/v) or below could be sprayed and pumped. This justifies the choice to proceed with dispersions containing 0.8% (w/v) of guar gum or less.

The trials discussed above were part of very early investigations to determine the sprayability and pumpability of guar gum dispersions rather than to analyse the efficiency of the process. It was essential at this point to progress to more solid investigations by spray drying guar gum dispersions with drug-loaded MESOPAC to assess the potential of designing a colon-targeted system via spray drying. A dispersion of guar gum in cold water was created at 0.4% (w/v) using a homogeniser, to which drug-loaded MESOPAC was added. The guar gum-to-MESOPAC ratio was set at 5:1, resulting in a solid content of 0.48% (w/v). Initially, spray drying was conducted at an inlet temperature of 120°C to ensure effective droplet drying which happens above the boiling point of the solvent. The choice of this temperature range for the drying gas was supported by the work of Cheow and colleagues (2010). In their paper, it can be implicitly elucidated that a temperature range of 120-140°C was selected to ensure sufficient water evaporation (Cheow et al., 2010). However, in this chapter, visual inspection revealed two important observations regarding the efficiency of the process. First was the detection of residual droplets on the chamber, indicating suboptimal drying at the specified drying temperature. Second was the absence of powder yield. These findings could be explained by the need of higher drying temperature to achieve complete moisture removal and water evaporation. This would ultimately increase the powder yield. In addition, the findings implied that the solid content might be too low to achieve adequate powder yield. According to Ousset et al. (2018), the solute concentration in a spray drying feed should ideally be set at 2% (w/v) or more to obtain satisfactory powder yield. However, this concentration was not feasible due to restrictions imparted by the viscosity of the dispersions.

To maximise the yield, several spray drying parameters required further optimisation, since changing the type of solvent or increasing the inlet temperature, solid concentration, and drying gas flow can affect the yield positively (Buchi UK Ltd, 2025). The influence of feed flow rate on the powder yield, on the other hand, may vary. It is important to note that replacing water with an organic solvent was not possible because guar gum would precipitate. Moreover, the drying gas flow was already set at maximum. Inlet temperature, feed flow rate, and solid concentration were therefore identified as variables to be modified in the pursuit of

enhanced powder recovery. Inlet temperatures higher than 120°C, namely 165 and 180°C, were selected in addition to increasing the solid concentration in the feed dispersion to 1 and 1.6% (w/v). The feed flow rate was varied between 2.5 and 5 mL/min. The ratio of guar gum-to-MESOPAC was also adjusted to 1:1. It is noteworthy to mention that the concentration of guar gum upon dispersion in cold water was still maintained within the sprayable range that was identified earlier (0.8% (w/v) or less). **Table 4.2** summarises the results of these preliminary investigations of spray drying guar gum with drug-loaded MESOPAC for colon delivery.

Table 4.2. Percentage of powder recovery obtained when spray drying parameters were altered as a function of inlet temperature, solid concentration, feed flow rate, and guar gum concentration

a. Feed flow rate= 5 mL/min

Inlet temperature (°C)	Guar gum concentration in cold water dispersion (%w/v)	Solid concentration of guar gum and drug-loaded MESOPAC in the feed (%w/v)	Powder recovery (%)
165	0.5	1	5
165	0.8	1.6	1.04
180	0.5	1	5.3
180	0.8	1.6	0

b. Feed flow rate= 2.5 mL/min

Inlet temperature (°C)	Guar gum concentration in cold water dispersion (%w/v)	Solid concentration of guar gum and drug-loaded MESOPAC in the feed (%w/v)	Powder recovery (%)
165	0.5	1	9
165	0.8	1.6	3.2
180	0.5	1	7.2
180	0.8	1.6	2.3

Although triplicate analyses were not conducted for these preliminary investigations due to limited material availability, some trends can still be drawn. Comparing the two flow rates, it seemed that the lower feed flow rate of 2.5 mL/min resulted in slightly higher powder recovery in general. This could be attributed to the viscosity of the dispersion being sprayed. When spray drying viscous feed samples, such as those containing guar gum, higher flow rates tended to produce larger droplets. This compromised heat and mass transfer during the process and negatively impacted powder recovery, as similarly reported with viscous solutions of date fruit extracts embedded in Arabic gum and maltodextrin (Arumugham et al., 2023).

A common expectation is to observe an increased powder recovery with an increase in solid concentration (Tontul and Topuz, 2017). The findings inferred from **Table 4.2** revealed the contrary to what is expected. As both, the guar gum concentration and general solid content within the feed dispersion, increased, a drop in the yield was noticed, regardless of the drying temperature or the feed flow rate. Viscosity, again, plays a major role in explaining the reason

behind this decrease in yield. Guar gum dispersions were highly viscous, and their viscosity increased with higher solid concentrations, as demonstrated visually. Viscous dispersions tended to generate large droplets that required more energy and time to dry. These droplets were more likely to deposit on the chamber walls due to insufficient drying and could not be efficiently separated by the cyclone, resulting in minimal powder recovery (Ribeiro et al., 2024; Klein et al., 2015).

The third trend to be elucidated from **Table 4.2** is related to the effect of inlet temperature on the yield whilst keeping the solid concentrations and feed flow rates constant. The effect of the drying temperature was very marginal; yet, it can be seen that higher drying temperatures (i.e. 180°C) were associated with a reduction in powder recovery. Exceeding the glass transition temperature of MESOPAC and the melting temperature of felodipine were possible reasons behind the decline in the yield. [*redacted*] ... felodipine undergoes melting at 146.0°C (Le et al., 2019). Spray drying above these temperatures resulted in sticky droplets that caused a decline in the yield.

In a broad sense, **Table 4.2** implies that spray drying is not a viable technique to generate guar gum-capped MESOPAC for colon-specific delivery, since the powder recovery does not meet the required standards. The efficiency of performance was compromised by the viscosity of the dispersion, leading to the loss of the polysaccharide throughout the process, as previously reported elsewhere (Ravichnadran et al., 2014; Tripathi 2022). It was then deemed necessary to adopt another method to design the guar gum-based colonic system.

4.3.3.2. Oven Drying of Guar Gum

Oven drying was attempted as an alternative technique to dry the guar gum dispersion. Guar gum was dispersed in cold water using a homogeniser at two concentrations, 0.4 and 0.8% (w/v). Drying under vacuum was attempted at a pressure of 600 mbar for two hours. The drying temperature was set at 50, 100, and 120°C. Results showed that no evaporation of the solvent was detected at the lowest drying temperature. Nevertheless, minor solvent drying of about 15 and 20 mL was noted at 100 and 120°C, respectively. It was less likely that the dispersion would dry and be of acceptable texture under these conditions given the very slow evaporation rate. In fact, it likely exhibited the morphological features of dehydrated guar gum gel after solvent removal via external heat and stirring as depicted in **Figure 4.3**.

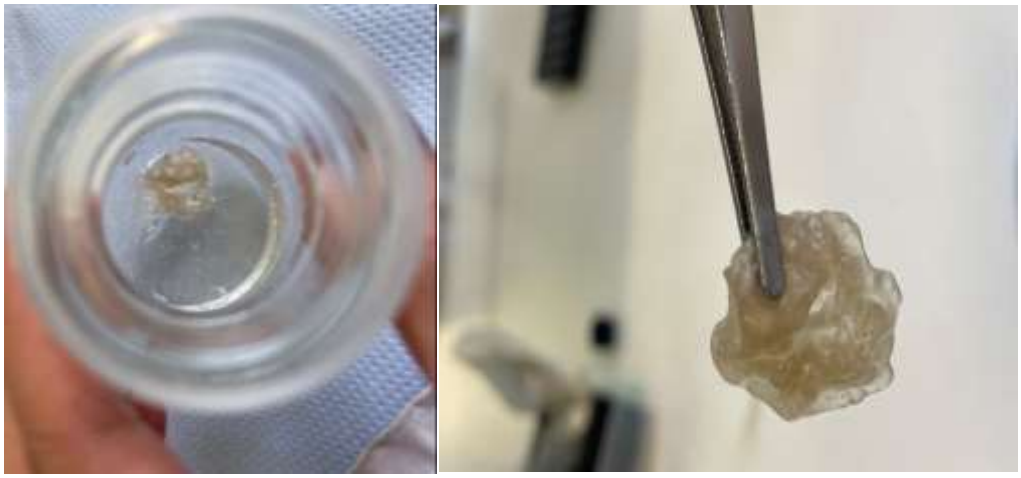

Figure 4.3. *Dried guar gum gel after solvent removal whilst being heated and stirred*

4.3.3.3. Physical Mixture of Guar Gum and Felodipine-loaded MESOPAC

After evaluating different processes, the transition to another method of preparation that ensures adequate gelling of guar gum within the specified environments was required. As with pectin, the simplest method was a physical blend of guar gum with drug-loaded MESOPAC, which provided a simple yet an effective approach that was worth exploring. It was hypothesised that the gel plug formed upon the hydration of guar gum in aqueous environments would hinder and delay drug release. It should also create a lag period prior to reaching the colon, with the thickness of the plug controlling the rate of hydration and drug release (Krishnaiah et al., 1998; Krishnaiah et al., 2002).

Initially, three blend ratios of guar gum-to-MESOPAC formulation, at 3:1, 5:1, and 10:1 respectively, were prepared as stated in **section 4.2.4**. These ratios represented varying compositions to evaluate the effect of different guar gum mass on the release properties. The different formulations were subjected to dissolution studies in media simulating the stomach, small intestine, and colon. The latter was conducted under the presence and absence of enzymes that breakdown guar gum to trigger drug release specifically within the colonic region. **Figure 4.4** summarises the data of the preliminary colonic release studies.

From a broad perspective, the prevailing trend observed with all ratios aligned with the core concept of colonic delivery, whereby the drug release was kept to low levels in physiological environment of the stomach and small intestine but rose specifically in the colon under the presence of enzymes. In upper GIT, the suppression of release seemed to depend on the proportion of guar gum within the formulation, with 3:1 composition showing the highest release in upper GIT release overall at an average of 11.53 ± 5.10%, versus 6.38 ± 0.57% and 3.23 ± 0.13% for 5:1 and 10:1 guar gum-coated MESOPAC, respectively. Such a finding was reliable because the higher the guar gum content in the formulation, the thicker the plug becomes. This thickness prolongs the hydration time needed, restricting drug release in upper

GIT, as seen with 10:1 MESOPAC formulation. Once the formulations reach the colon, the plugs become susceptible to enzymatic degradation, accounting for the higher release percentages in the colon compared to the stomach and small intestine. It is, again, that the proportion of guar gum was a key determinant of release behaviour even in the presence of enzymes. According to Krishnaiah et al. (1998), varying guar gum coating thickness impacted the release of the drug, with 200 mg coat thickness achieving only around 7.87% release after 26 hours. It was shown that when coat thickness was reduced to 125 mg, the release was suppressed in the stomach and small intestine but allowed 92.49% of the drug to be released upon complete degradation of the guar gum coat by colonic enzymes. The diagram below conveys a similar idea, such that the highest release in the colon was achieved with 3:1 MESOPAC formulations when compared to other ratios because it was easily accessible by enzymes due to little guar gum present.

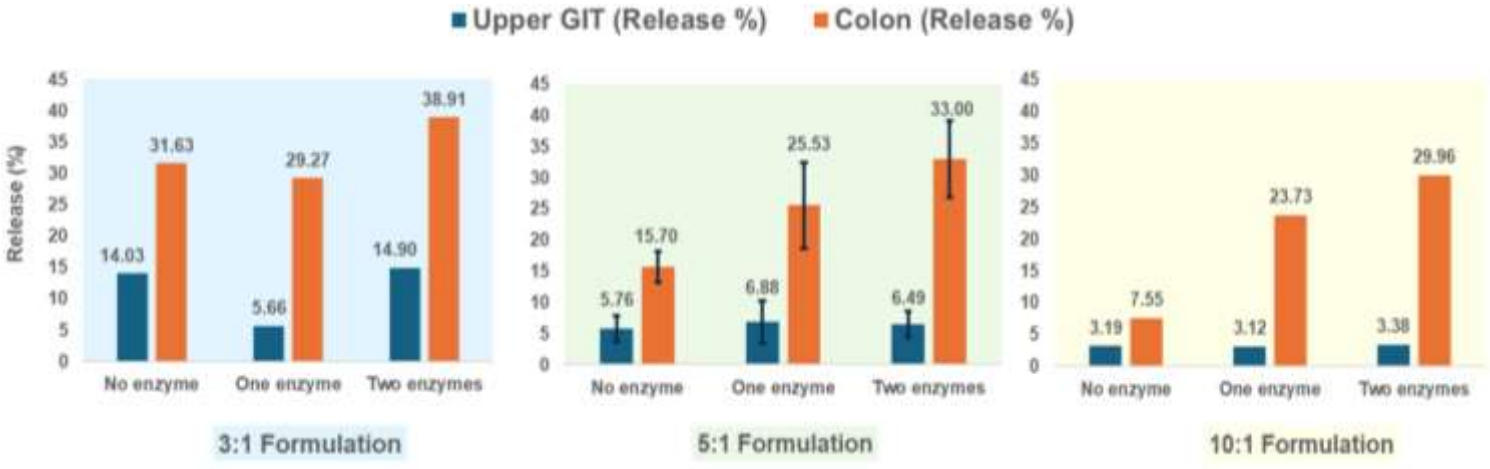

Figure 4.4. *Drug release profiles of physical mixture of guar gum with felodipine-loaded MESOPAC in media simulating upper GIT and colon [Testing conditions: 0.1 N HCL + 1% SLS for gastric environment; phosphate buffer pH 6.5 + 1% SLS for small intestinal environment; phosphate buffer pH 7.4 + 1% SLS for colonic environment with and without β-mannanase and α-galactosidase; 30 mL with mini vessels and mini paddle, 50 rpm)*

A closer look at the individual categories, each segment alone, revealed that across all guar gum-to-loaded MESOPAC ratios, a noticeable difference can be seen between the presence and absence of enzymes in the colonic region. For example, the release jumped from 7.55% when no enzymes were present to 29.96% when subjected to the activity of two enzymes with 10:1 ratio. This difference was, however, less prominent with 3:1 loaded MESOPAC as the release was quite similar in the medium without enzyme compared to that with one enzyme (31.63% versus 29.27%, respectively). In general terms, this indicated the susceptibility of the formulation to enzymatic-induced drug release. But, one possible reason for the decreased susceptibility observed with 3:1 loaded-MESOPAC when investigated under the absence of enzymes or one enzyme is the small amount of guar gum present with respect to MESOPAC.

The amount of guar gum added might not be high enough for the enzyme to demonstrate its full range of activity in digesting the plug in a sense that could induce a noticeable difference in drug release between its absence and presence. In other words, when the enzyme's substrate is not abundant, the effect of plug digestion cannot be translated to an observable difference in release.

As a general principle, it is, however, important to note that the difference in release percentage of felodipine from guar gum-based MESOPAC between the different formulations within the colon was marginal. Surprisingly, the release percentages were confined to be within or around the 30% range upon the addition of two enzymes. The drug-loaded formulations at all coating ratios were able to retain microbial sensitivity and digestion-induced drug release within the colon but up to ~39% at most. A balance between minimal premature drug release and accelerated release in colonic environment is the ultimate goal of any colon-specific formulation. From **Figure 4.4**, it was evident that the 5:1 formulation achieved this balance, keeping drug release in upper GIT below 10% while showing moderate drug release in the colon. The other two ratios either showed lower release in the colon such as with 10:1 coated MESOPAC loaded with drug or exhibited higher upper GIT release as it was the case with 3:1 sample. The decision to only run 5:1 MESOPAC formulation in triplicate was justified by this balance to ensure the robustness of performance and to preserve the enzymes in hand. Yet, the absence of triplicate analysis with the others did not diminish the validity of the results as the figure still outlined key findings. But, it also raised concerns regarding the low overall drug release in the colon.

To address this dilemma, several options were explored. One key strategy to maximise the drug release within the colon was to optimise the conditions within the small volume dissolution setup such that the release profile becomes comparable to that of a standard compendial setting. During the process of drug development, dissolution testing is a routine requirement to assess product quality, where USP testing conditions and apparatuses are the preferred options (Scheubel et al., 2010). One of these testing conditions is the rotatable paddle fitted into a one-litre vessel, typically referred to as USP 2 method (Wang et al., 2018). Despite being universal and standardised, these widely recognised apparatuses have limitations. They usually demand large volumes of dissolution media and large amounts of materials and samples, which might be costly or may not be readily available during the early stages of product development (Klein & Shah, 2008). The shift to miniaturised vessels and paddle systems would then be reasonable to preserve the materials. For example, the use of miniaturised dissolution equipment was reported in cases where novel or low-dose molecules, low analytical sensitivity, or scarcity of materials hinder the practical analysis in the standardised large dissolution equipment (Scheubel et al., 2010; Wang et al., 2018). However,

an element to factor in is the variation in hydrodynamic conditions between the two settings. According to Klein & Shah (2008), it is important to maintain appropriate hydrodynamics when scaling down to the mini paddle setup to extend the reliability and reproducibility established with the large dissolution vessels, since hydrodynamics significantly affect the dissolution of the API (Klein & Shah, 2008). Therefore, the decision to use the miniaturised dissolution system in this chapter was driven by the amount of enzymes available in hand for simulating the colonic stage and by the cost as well as scarcity of the PROTAC molecule to be delivered to the colon. A similar attempt was made by Giusti (2021), who used the mini dissolution apparatus to preserve the enzymes used for colon targeting purposes. Scaling down to the mini paddle system was hence necessary yet consideration needed to be given to the hydrodynamic conditions.

In fact, compendial systems' configuration and dimensions vary slightly between suppliers, accounting for minor differences in release. Also, small volume dissolution apparatuses lack standardised performance verification tests (Klein & Shah, 2008; Scheubel et al., 2010). With that in mind, dissolution testing using the miniatured setup should be tailored to each investigation individually, and scaling down is more complex than expected (Scheubel et al., 2010). Hence, the dissolution profiles between the two settings might not be comparable unless a comparative analysis is performed to establish a correlation between the two (Klein & Shah, 2008). The low overall drug release observed earlier in the colonic region might actually be due to the adopted small dissolution vessel setup and the effect of stirring speeds on the release. Before proceeding with further colon-targeted dissolution studies, it became evident to investigate this and attempt to establish a correlation between the standardised and miniatured dissolution settings to achieve comparable drug release profiles. The aim was to identify the conditions, namely the speed of the rotating paddle, that would achieve similar drug release results between the two settings and that would maximise the release in the colon.

4.3.3.4. Establishing a Correlation in Drug Release Between Standard USP Paddle Apparatus and Small-volume Dissolution Vessels

The main reason behind the low overall colon release seen with previous trials was most likely ascribed to differences in hydrodynamics between the dissolution settings. One might also wonder whether MESOPAC is releasing the drug load in the first place. If the drug release from the carrier was originally incomplete, this is then another possible reason for the low overall release. To solve these controversies, dissolution studies of felodipine-loaded MESOPAC without the effect of guar gum were conducted in standard USP equipment. To compare the release percentages, dissolution studies were similarly performed using the miniaturised setup whilst varying the rotation speed to be at 50, 150, and 200 rpm. This

variation in speed was attempted to identify which rotational speed would achieve a similar performance to that of a standardised USP vessel. It is important to note that the same theoretical drug concentration was maintained between the two so that conditions were kept constant for comparative purposes. The dissolution profiles of felodipine-loaded MESOPAC in phosphate buffer pH 6.5 with 1% (w/v) SLS performed in large volume standardised vessels and in the miniaturised adaptations are presented in **Figure 4.5**.

Figure 4.5. *[redacted]*

The dissolution enhancement effect of MESOPAC for poorly soluble drugs can still be seen in both vessel settings, with dissolution of the drug within MESOPAC formulation surpassing that
of the raw form (p-value <0.05). The amount of drug released, however, varied depending on the type of the vessel. With raw felodipine, there was a significant difference between agitation speed of 50 rpm and 150 rpm in the miniaturised vessel setup (p-value <0.05), highlighting
the effect of speed on drug release. On the contrary, the release of raw drug was comparable between the two setups when a speed of 150 rpm was used in the small-volume setting (p-
value > 0.05). This indicated that a higher speed in the small vessel achieved a similar dissolution profile to that of a compendial setup when raw drug was analysed.
[following paragraph redacted]

It can be said that the release within the small vessel setup was highly dependent on the speed and was greatly influenced by hydrodynamic conditions. The incomplete release at paddle rotation of 50 rpm can be explained by a phenomenon referred to as "coning" that was observed upon visual inspection of the process, whereby materials accumulated at the bottom of the vessel just under the paddle in the form of a pile (Hellberg et al., 2021; Legace et al, 2004). **Figure 4.6** visually illustrates the coning phenomenon observed at low speeds in small volume vessels. In fact, coning becomes more prominent when a combination of poorly soluble drugs and low rotational speeds are present, which was the case with the previous investigations conducted herein (Hellberg et al., 2021). This phenomenon was a consequence of poor hydrodynamics that resulted in suboptimal agitation within the vessel, leading to incomplete dissolution and affecting the release profile (Hellberg et al., 2021; Legace et al., 2004).

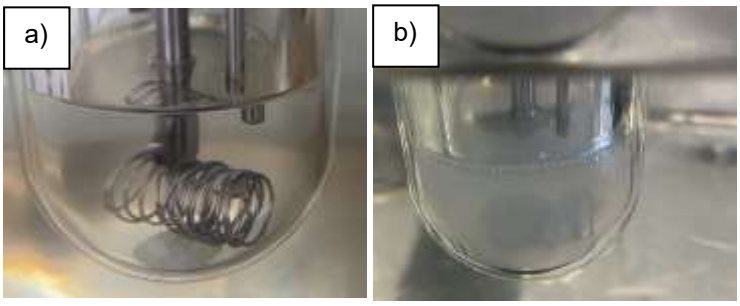

Figure 4.6. *a) Coning phenomenon observed with felodipine-loaded MESOPAC in small vessels with 50 rpm at 60 minutes into the test b) Absence of coning when the speed was adjusted to 150 rpm at 120 minutes*

One way to overcome the coning effect is to adjust the paddle rotation speed; increasing the speed generates greater turbulence within the vessel that provides enough force to distribute the powder more uniformly (Hellberg et al., 2021; Legace et al., 2004). The work presented by Klein (2006) clearly showcased the effect of coning on the release of several drugs. In all cases, a speed of 50 rpm in the miniaturised setup repeatedly revealed poor correlation with the large vessel profiles, accounting for lower rates of dissolution. An increment in the speed up to 75/100 rpm was needed with all tested drugs to match the release profiles obtained at 75 rpm with the standard compendial vessels (Klein, 2006). Similarly, Scheubel and co-workers (2010) concluded that the paddle speed is to be factored in when transferring

dissolution testing from compendial to small-volume vessels to ensure similarity in release. A speed of 125 rpm in the small-volume vessel was found to be equivalent to 50 rpm in standard equipment for immediate release tablets. Further supporting the research discussed above, Legace et al. (2004) reported high variability in results at a paddle speed of 50 rpm; when the speed was increased to 75 rpm, coning effect was eliminated leading to more robust findings. During the process of matching the release profiles between the two setups, **Figure 4.5** reveals that a paddle rotation speed of 50 rpm in the mini vessel adaptation was always inferior to that of the large vessel, with both the raw form and the loaded MESOPAC. This demonstrated minimal and highly variable release, which could be justified to some extent by the coning phenomenon. As the paddle speed was increased from 50 rpm to 150 and 200 rpm with the MESOPAC formulation, coning was eliminated, resulting in better hydrodynamics and improved reproducibility. This was evidenced by reduced variability, as indicated by narrower error bars. Although the increase in speed was meant to stretch the release as far as possible to meet that of the large-volume vessel, full overlap was not possible. The release data extrapolation was close enough but not fully superimposable, and further optimisation is required in the future.

Reflecting back to **Figure 4.4** that summarises the preliminary studies of physical blends of guar gum with MESOPAC, it seems by now that the low paddle speed of 50 rpm was responsible for low overall colon release that was capped at 39% at most regardless of the ratio used. Rather than just defaulting to the low speed often implemented with large-volume vessels, it became evident to adjust the speed to 150 rpm to achieve a profile that is as similar as possible to that of compendial setup. The increment to 150 rpm rather than 200 rpm was justified by the similarity between two speeds (p-value > 0.05) and further driven by literature, where researchers commonly adhered to 150 rpm at most (Hellberg et al., 2021; Klein, 2006; Klein & Shah, 2008; Scheubel et al., 2010). It was, thus, assumed that increasing the speed for colonic dissolution studies conducted in mini vessels to 150 rpm would result in enhanced distribution of the drug within the vessel, enough to discriminate between the effect of different guar gum ratios on drug release in a similar manner as would a compendial setup.

4.3.3.5. *In Vitro* Drug Release of Guar Gum-based MESOPAC Formulations for Colon-targeted Delivery

The *in vitro* dissolution of felodipine from MESOPAC physically blended with guar gum was resumed for colon targeting, with an adjusted paddle rotation speed as per the method development above (**section 4.3.3.4**). An agitation speed of 150 rpm was expected to achieve a release profile in simulated media utilising mini vessel close enough to that of a compendial setup. Three pre-determined ratios of guar gum-to-drug-loaded MESOPAC, which were 3:1, 5:1, and 10:1, respectively, were studied. The drug-loaded MESOPAC at different coating

ratios were studied in pH environments that simulate the upper GIT and colon. Medium with the latter was spiked with enzymes that tend to hydrolyse guar gum to allow drug release. The formulation was also studied in enzyme-free medium to serve as the control analysis. As a second supplementary control, felodipine-loaded MESOPAC without guar gum was studied in environments mimicking upper GIT and colon (**Appendix B**).

While the individual release percentages at different time points with the supplementary control (drug-loaded MESOPAC without guar gum) seemed highly variable, a general pattern that shows high felodipine release across all regions was noticed. This highlighted the role of guar gum in controlling the drug release, providing a targeted delivery to the colon.

It is, however, the variability within the data points of the supplementary control that needed to be addressed. The research conducted by Scheubel et al. (2010) proposed an explanation for such a variation. Their work clearly highlighted how formulations with different release mechanisms exhibit varying sensitivity to hydrodynamic conditions in miniaturised dissolution vessels.

According to Scheubel et al. (2010), immediate release formulations showed dependency on vessel hydrodynamics when compared to extended-release formulations. With the former, the dissolution rate is somewhat controlled by the rate of medium renewal around the dosage form, which is a consequence of optimal hydrodynamics. On the other hand, extended-release formulations are affected more by the formulation design or, in other words, the built-in mechanisms such as diffusion or erosion and are less likely to be limited by the renewal rate of medium surrounding it and vessel hydrodynamics (Scheubel et al., 2010).

MESOPAC displays a controlled release mechanism via diffusion from the pores and maintains this mechanism even after the addition of guar gum. So, both forms are classified as extended-release formulations. According to the discussion above, they should less likely be affected by the hydrodynamic conditions of the mini vessel. This stability was somewhat demonstrated with guar gum-containing samples and was reflected as consistent and reproducible release percentages (as discussed below). The release seemed to be dependent on diffusion from the pores, and the guar gum plug added an additional barrier. This diffusional complexity made the loaded MESOPAC formulation with guar gum highly dependent on diffusion through the pores and polysaccharide digestion instead of the surrounding hydrodynamic conditions. In contrast, despite being a form of controlled release, uncoated MESOPAC showed high variability in release data points. With the absence of the additional diffusional barrier of guar gum, the rate limiting step was likely diffusion from the pores only, which became more sensitive to the surrounding hydrodynamics in the small-volume setup. Diffusion, as a rate limiting step, was dominating but the deviation in release could be exacerbated by a greater degree of dependency on vessel hydrodynamics with the uncoated MESOPAC. Although both were less likely to depend on the rate of renewal of surrounding

media and hydrodynamic conditions for drug release compared to other types of formulations, one demonstrated greater sensitivity to the surrounding conditions in the miniaturised vessel compared to the other, accounting for the differences in reproducibility.

4.3.3.5.1. *In Vitro* Dissolution of Guar Gum-coated MESOPAC in Upper GIT

Figure 4.7 reveals the release data of felodipine from guar gum-coated MESOPAC at different ratios, medium conditions, and enzyme levels. Two general trends could be captured, whereby the release in upper GIT was minimal but increased in the colon upon the introduction of enzymes. It is desired for formulations targeted to the colon to ideally release less than 10% of the drug within the first five hours of the journey before reaching the colon (Kumar et al., 2020). In our work, the drug release in upper GIT was retarded and kept to a quite low level of <11% at all ratios, despite an increased agitational speed of 150 rpm. This indicated that the release was hindered by the swelling of guar gum as it got in contact with the dissolution medium. This swelling resulted in the formation of a viscous gel layer that retarded drug release, depending on the proportion of guar gum within the formulation and how quickly it hydrated (Krishnaiah et al., 2002).

Moreover, it was anticipated that the release percentages in the stomach and small intestine would be nearly similar across the enzymatic subdivisions of each ratio. This was due to their identical composition. Any difference in behaviour was anticipated to emerge only at later stages, when the effect of the enzyme became active. MESOPAC with guar gum achieved this equivalency across all ratios that is evident by the narrow error bars within each subdivision. Also, it achieved a suppressed release at an average of 10.06 ± 4.87%, 7.74 ± 2.67% and 5.52 ± 2.25% with 3:1, 5:1, and 10:1 MESOPAC formulations, respectively. Collectively, none of these values exceeded the generally accepted level that is to be maintained in upper GIT as stated earlier. In addition, increasing the proportion of guar gum within the formulation did not contribute to any difference in release in the upper GIT. This indicated that the formulations were able to withstand the journey in the upper GIT without releasing much of their drug load.

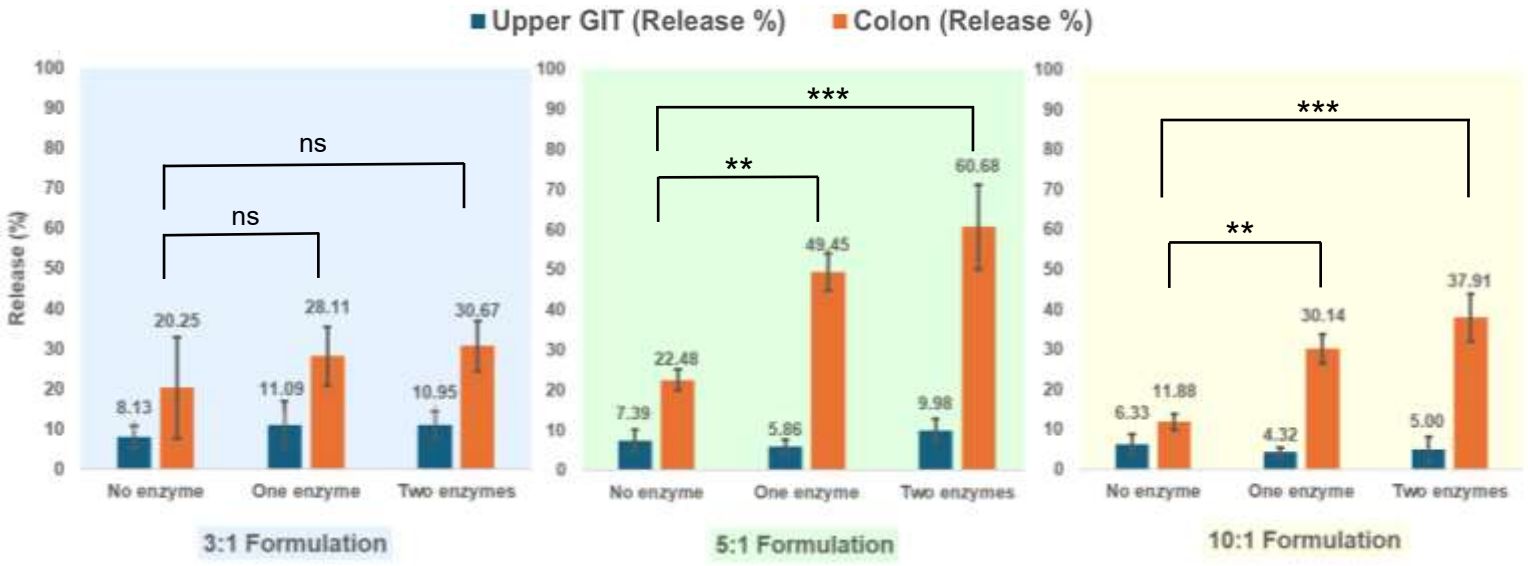

Figure 4.7. *Cumulative release percentages of felodipine from guar gum-based MESOPAC in media simulating the upper GIT and the colon with absence and presence of enzymes at guar gum-to-loaded MESOPAC ratios of 3:1, 5:1, and 10:1 (Data are presented as Mean ± SD. Testing conditions: 0.1 N HCL + 1% (w/v) SLS for gastric environment; phosphate buffer pH 6.5 + 1% (w/v) SLS for small intestinal environment; phosphate buffer pH 7.4 + 1% (w/v) SLS for colonic environment with and without β-mannanase and α-Galactosidase; 30 mL with miniaturised adapted version, 150 rpm) [ns= not significant; **= P-value <0.01; ***= P-value <0.001]*

4.3.3.5.2. *In Vitro* Dissolution of Guar Gum-coated MESOPAC in the Colon

Building upon the findings of upper GIT release, **Figure 4.7** also shows the colonic release of felodipine from MESOPAC coated with guar gum. Key trends that significantly impacted the colonic release emerged as a consequence of three factors. These factors were the paddle speed, enzymatic status of the medium, and ratio of guar gum-to-loaded MESOPAC.

a. Effect of Paddle Rotation Speed on Drug Release in the Colon

Earlier in this chapter, the release profiles of guar gum-based MESOPAC loaded with felodipine exhibited low drug release at the end of dissolution testing in the colon. This was ascribed to slow paddle rotation that necessitated increment to 150 rpm due to insufficient fluid flow at the bottom of the vessel. **Figure 4.4** shows the release percentages in the colon at 50 rpm while **Figure 4.7** presents those at 150 rpm. In general, a faster speed was associated with higher release for all ratios except for 3:1. For example, for the drug-loaded MESOPAC that is coated with guar gum at a 5:1 coating ratio, the release at the end of the colonic stage revealed an increase from 33.00 ± 6.11% at 50 rpm to 60.68 ± 10.57% at 150 rpm under the effect of two enzymes (p-value <0.05) (summarised in **Figure 4.8**). The higher release upon increasing the speed can be explained by the improved hydrodynamic mechanisms within mini vessels. Of all the velocities governing the flow of fluids, the circular

flow of the dissolution fluid around the vessel, also known as tangential velocity, dominates, displays the greatest effect on drug dissolution, and increases with increased rotation speed (Wang & Armenante, 2016; Wang et al., 2018). As a result, the fresh fluid moves around faster, which is critical for higher drug dissolution. Computational fluid dynamics have also shown direct relationship between agitation speed and surrounding fluid velocity; not only tangential velocity is influenced by higher agitation speed but also the “low-velocity region” at the bottom of the vessel. While this dead zone cannot be completely eliminated and is typically characterised by very minimal fluid flow, its diameter tends to decrease as the speed increases (Johansson et al., 2017; Mirza & Liu, 2005; Wang & Armenante, 2016; Wang et al., 2018). This reduction in diameter promotes better fluid interaction. Moreover, a higher speed accounts for higher strain around the dosage form (i.e. guar gum plug), which is responsible for a steeper velocity gradient and hence a faster mass transfer of dissolved drug between the medium and the dosage form (Wang & Armenante, 2016; Wang et al., 2018). Concerning the drug-loaded MESOPAC coated with guar gum at a 3:1 coating ratio, the reasons behind the variability in its performance and the unexpected outcomes are discussed further below, which mainly revolved around excessive sensitivity to hydrodynamic conditions because guar gum, at different proportions, forces formulations to behave differently under the same environment.

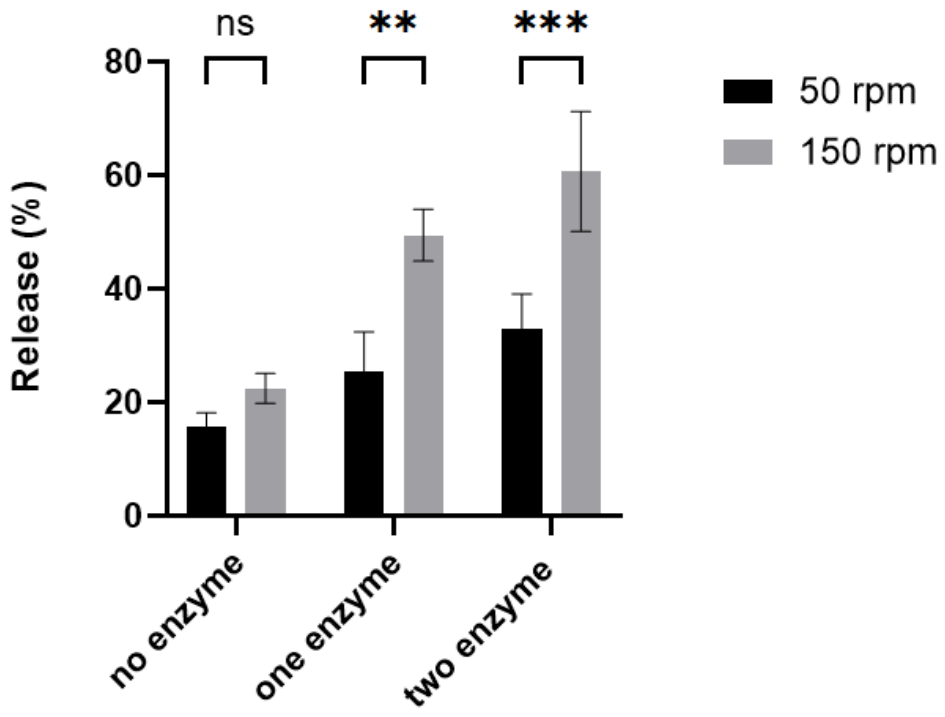

***Figure 4.8**. Felodipine release at the end of the colonic stage increases as the agitation speed is increased with the guar gum-coated drug-loaded MESOPAC at a 5:1 coating ratio upon the addition of enzymes [ns= not significant; **= P-value <0.01; ***= P-value <0.001]*

b. Effect of Guar Gum- hydrolysing Enzymes on Drug Release in the Colon

The performance of a guar gum-coated MESOPAC in the colon depends on the degradation of the swollen gum by bacterial enzymes in the colon. As enzymes were added to the media, the release was enhanced significantly (**Figure 4.7**). This pointed to the susceptibility of the formulation to the biodegradation of colonic enzymes. Generally, the effect of enzyme addition was noticeable with all ratios, with exception of the 3:1 samples. In the absence of enzymes, the release reached 22.48 ± 2.63% for the drug-loaded MESOPAC coated with guar gum at a 5:1 coating ratio, and 11.88 ± 2.04% for those at a 10:1 ratio by the end of the study. Upon the addition of two enzymes to the dissolution medium, the release jumped to 60.68 ± 10.57% and 37.91 ± 5.92% with 5:1 and 10:1 samples, respectively (p-value <0.05).

On the other hand, no significant difference ($p > 0.05$) in drug release was observed between the presence and absence of enzymes for drug-loaded MESOPAC coated with guar gum (5:1 ratio). One possible explanation might be that the amount of guar gum relative to MESOPAC was too low to act as a coat that creates a noticeable difference in release upon enzyme digestion. It might be even low enough for natural gum hydration to achieve a similar drug release to that of a medium with enzymes. This finding highlighted the importance of optimising the ratio of guar gum-to-drug-loaded MESOPAC to achieve the desired microbial susceptibility and drug release within the colon.

Figure 4.9 depicts the effect of enzyme addition on guar gum's plug at the end of the colonic stage upon hydration with dissolution medium (at a 5:1 ratio of guar gum-to-loaded MESOPAC). It can be seen that the swollen plug of guar gum remained intact in the absence of any enzymes, trapping the drug-loaded MESOPAC within its swollen matrix and impeding drug release. This correlated with the lower colonic drug release reported earlier in enzyme-free media when compared to enzyme-containing media. Upon the introduction of enzymes, the plug disintegrated into fragments, releasing the drug and MESOPAC particles into the dissolution medium. This was manifested as increased turbidity within the vessel and aligned with the higher release observed generally with the addition of enzymes.

In a similar attempt, Sawarkar et al. (2015) prepared colon-specific tablets containing 5-ASA that were coated with guar gum through compression coating at a ratio of 1:1. Only 3.45% of 5-ASA was detected during the first six hours of the study, representing the upper GIT. In colonic environment, nearly 80% of the drug was released, suggesting the ability of guar gum to protect the drug load until it is acted upon by enzymes in the colon. This susceptibility to degradation by enzymes was similarly demonstrated herein.

In another study by Chourasia and Jain (2004), the *in vitro* release of guar gum microspheres containing metronidazole was investigated. Drug release was retarded in upper GIT but was significantly enhanced reaching up to 96.24 ± 4.77% when rat caecal contents after six days of enzyme induction were introduced to the medium in contrast to 31.23 ± 1.49% when they

were absent. This further supported our work, suggesting susceptibility of guar gum as a coat for colonic delivery and reinforcing its degradative behaviour upon exposure to colonic enzymes.

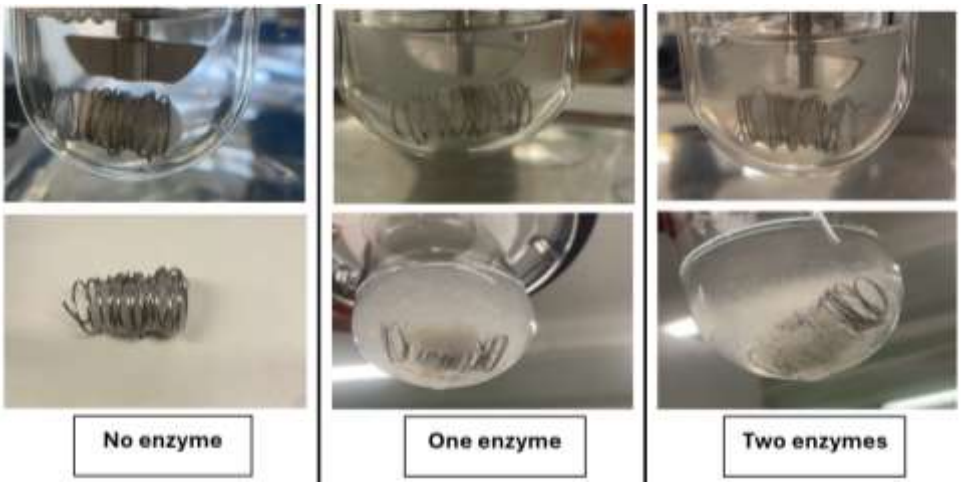

Figure 4.9. *The state of the swollen guar gum plug under the absence and presence of enzymes (Guar gum: drug-loaded MESOPAC at 5:1)*

c. Effect of the Ratio of Guar Gum-to-Drug-loaded MESOPAC on Drug Release in the Colon

It is highly important to account for the ratio of the guar gum in the physical blend of a colon-targeted delivery system. This is mainly driven by the significant effect that guar gum imparts to the formulation with regards to controlling drug release in the upper GIT and enzymatic susceptibility in the colon. The impact of the three guar gum-to-MESOPAC ratios on drug release was assessed herein, representing low, medium, and high guar gum content (**Figure 4.7**). The 10:1 coating ratio showed incomplete drug release, capped at 37.91 ± 5.92% in the presence of two enzymes. Although it showed susceptibility to degradation, the swollen plug was too thick for enzymes to penetrate and induce full drug release. **Figure 4.10** illustrates the thick gel layer that was formed with the 10:1 coating ratio and remained intact even after the full duration of the study, trapping the loaded-carrier particles. The release though in upper GIT had the lowest mean of all. Collectively, these findings can be ascribed to the high amount of guar gum present within the formulation that was beyond the optimal range for a balanced behaviour. It was anticipated that reducing the content of guar gum within the formulation would increase the percentage released in the colon because the gel barrier formed would be thinner, facilitating the enzymatic accessibility. This was indeed the case when guar gum content was reduced to 5:1 relative to felodipine-loaded MESOPAC. The release in the upper GIT was slightly higher than the 10:1 drug-loaded MESOPAC coated with guar gum but was still within the acceptable range. It was the release in the colon that showed a surge, reaching

60.68 ± 10.57% at the end of 18 hours in simulated colonic environment spiked with two enzymes. Such a finding implied that guar gum shows a ratio-dependent behaviour that is capable of forming coatings of varying structural integrity. The release of the drug can be modulated by the ratio of guar gum, as seen with the investigations carried herein.

However, the formulation with 3:1 coating ratio did not behave as expected and surprisingly displayed the lowest overall release in the colon, irrespective of the enzymatic status. The formulation at this ratio had the lowest amount of guar gum and should have possessed the highest drug release in colonic simulating media. This is because less guar gum produces a thinner gel layer, which expedites drug release and does not provide a tight control. However, this expected release profile was not observed. Instead, the drug-loaded MESOPAC coated with guar gum at 3:1 ratio exhibited the lowest colonic release among all tested ratios. Such an unexpected outcome could be possibly attributed to the hydrodynamics of small-volume dissolution testing. As suggested in **section 4.3.3.5**, different formulations exhibit varying sensitivities to the hydrodynamic conditions within a small vessel setup, depending on the rate-limiting step (Scheubel et al., 2010). That rate-limiting step controlling dissolution might be a simple diffusion process or a more complicated process that is predominantly dependent on hydrodynamic conditions. Besides the type of formulation that defines the release mechanism, formulations with built-in release controllers like guar gum display additional reduced sensitivity to the surrounding environment that is controlled by hydrodynamics and show more reproducible performance. In the case of 3:1 guar gum-coated MESOPAC, the amount of guar gum added was not sufficiently high enough to provide a gel matrix around MESOPAC that could provide a reliable dual-diffusion barrier. With this dual barrier not being rigid enough, the formulation became more prone to hydrodynamic conditions in the small volume vessels. As a result, those at a 3:1 coating ratio showed release percentages that were surprisingly low and variable with unpredictable profile. It behaved similarly to the control formulation without guar gum.

Meanwhile, the formulations containing higher guar gum-to-polymer ratios generated a robust gel plug that sufficiently controlled the release via diffusion and plug degradation. The release rate within these formulations (higher ratios) could be viewed as a function of formulation properties instead of being regulated by hydrodynamics of the miniaturised vessel. Consequently, the release profiles were less likely to be dependent on hydrodynamic conditions or to be affected by the renewal rate of the surrounding media. In fact, they were more reproducible, consistent, and reliable. The trends seen herein were corroborated by previous studies of the influence of different guar gum proportions within a polymeric blend on drug release (Momin & Pundarikakshudu, 2005), where low guar gum content was similarly responsible for premature drug release up to 40%. When the amount of guar gum incorporated was increased, better control of drug release in stomach and small intestine was achieved

with enzymatic action of colonic bacteria demonstrated in the colon, altogether allowing for a total drug release of 88.16%. However, as seen with the results in the present study, too high concentrations of guar gum within the blend led to the formation of highly dense plugs that were too rigid to be broken down by enzymes. This led to incomplete drug release over the intended duration of the study, supporting the importance of optimising the proportion of guar gum to achieve the desired balance between release hinderance in upper GIT and acceptable release in the colon (Momin & Pundarikakshudu, 2005).

Figure 4.10. *Intact gel plugs of guar gum remaining after 18 hours in colonic media, suggesting high amount of guar gum that cannot be degraded by enzymes*

d. Concluding Remarks on Drug Release from Guar Gum-based MESOPAC for Colon-targeted Delivery

From the dissolution testing of several guar gum-based formulations in environments simulating the upper GIT and the colon, it can be concluded that a high speed of 150 rpm in mini dissolution vessels addressed the challenge of incomplete release seen at lower speeds. Although it neither achieved full release nor the exact dissolution profile of a compendial setup, it accomplished a reasonable release towards the end of the colonic delivery period that was comparable to felodipine-loaded MESOPAC without the controlled effect of guar gum. Exact equivalency of release profiles with large-volume vessels and absolute drug release should be part of future work. At this stage, the presence of enzymes confirmed the susceptibility of the system for colonic degradation, accounting for high release compared to enzyme-free medium (p-value <0.05). The release was significantly enhanced upon the addition of two enzymes. It is noteworthy that the different ratios exhibited varying release profiles. Among them, the guar gum-coated drug-loaded particles at a 5:1 coating ratio showed the best overall performance. This included maximum colonic release, reproducible results, and acceptable early drug release. This ratio demonstrated the balance between maintaining the integrity of

the drug load in the upper GIT and promoting colon-specific release. Therefore, it was chosen as the optimal formulation for colon-targeted delivery of MESOPAC.

4.3.3.6. *In Vitro* Release of Guar Gum-based MESOPAC for Colon-targeted Delivery of a Model PROTAC Molecule

The collective work in this thesis introduces MESOPAC as a promising delivery technology that is capable of accommodating complex mid-sized molecules and addresses their delivery challenges, particularly poor solubility. It was necessary then to design a delivery system that not only overcomes the challenges of PROTACs but also achieves targeted efficiency and site-specific release.

With the colon becoming a favourable site for complex molecules due to the advantages mentioned earlier, it becomes evident to investigate the colonic targeting of guar gum-based MESOPAC that is loaded with a novel PROTAC molecule like MZ1.

As a control sample, MZ1-loaded MESOPAC without guar gum was studied in different GIT segments (**Appendix C**). Variability in release similar to that observed with felodipine-loaded MESOPAC was noted, which is explained thoroughly in **section 4.3.3.5.** Despite that, an overall trend persists, whereby MZ1's release in regions prior to the colon was too high. This indicated that the majority of the dose was released and highlights the need for guar gum to control the release until the formulation reaches the colon.

Meanwhile, **Figure 4.11** illustrates the gel plug behaviour of guar gum that was physically blended with MZ1 and MESOPAC at a ratio of 5:1 upon exposure to simulated media representing the different GIT segments. It can be seen that the gel plug remained intact by the end of the small intestinal phase but was fragmented upon exposure to enzyme, to allow drug release. Hence, the concept of enzyme-triggered drug release upon reaching the colon that was previously established with felodipine can be still adapted by next-generation molecules that possess challenging properties. As reported earlier, felodipine-loaded MESOPAC coated with guar gum at a 5:1 ratio (guar gum to formulation) demonstrated optimal performance in the presence of two enzymes. Given the success of this formulation, the 5:1 ratio under two enzymes, specifically, was selected for further investigation using MZ1 to evaluate whether similar behaviour could be achieved. According to **Figure 4.12**, MZ1's release in upper GIT was limited to 11.6 ± 0.93%. In contrast, the presence of endo-1,4 β-Mannanase and α-galactosidase that hydrolyse guar gum triggered the release of MZ1 in the colon, with 43.33 ± 8.01% being liberated at the end of the duration of the study (**Figure 4.12**). This site-specific release suggested that maximised therapeutic efficiency could be brought by combining complex drug delivery technologies and emerging cutting-edge molecules. This addresses the challenges associated with novel drugs and consequently improving their therapeutic outcomes. It also signified the wide applicability of the optimised MESOPAC

technology to accommodate a variety of molecules. Yet, one might argue that full release in the colon was not achieved with the PROTAC molecule. Higher release that is close to 100%, however, could be possible once hydrodynamic conditions within the small-volume dissolution setup are optimised as discussed in earlier sections. Delivering a model PROTAC molecule to the colon using mesoporous particles is a contribution that not only adds to the growing literature related to targeted therapy but also broadens the scope of colon-targeted drug delivery, in general, and PROTAC research, specifically.

Figure 4.11. *Intact plug of guar gum and MZ1-loaded MESOPAC in dissolution medium representing a) the stomach and b) the small intestine. Upon exposure to enzymes in colon, plug fragments into smaller pieces, resulting in drug release and vessel turbidity (c)*

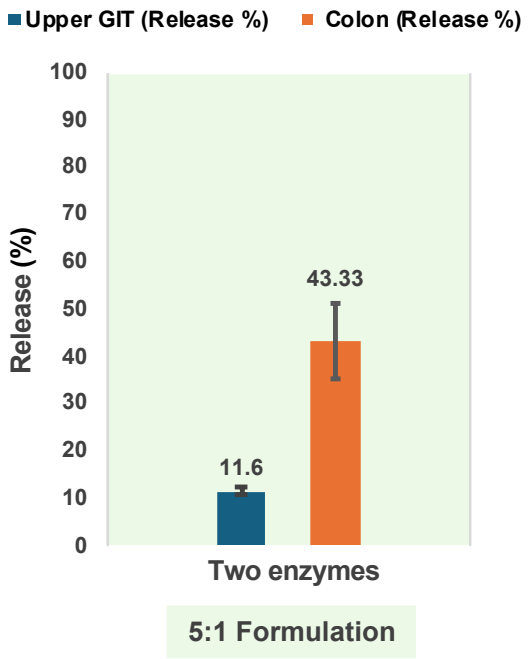

Figure 4.12. *Cumulative release percentages of MZ1 from guar gum-based MESOPAC in media simulating the upper GIT and the colon with the presence of two enzymes at guar gum-to-loaded MESOPAC ratio of 5:1 (Data are presented as Mean ± SD. Testing conditions: 0.1 N HCL + 0.3% (w/v) SLS for gastric environment; phosphate buffer pH 6.5 + 0.3% (w/v) SLS for small intestinal environment; phosphate buffer pH 7.4 + 0.3% (w/v) SLS for colonic environment with β-mannanase and α-Galactosidase; 30 mL with miniaturised adapted version, 150 rpm)*

4.4. Conclusion

Drug targeting to the colon gained interest over the past two decades due to the various advantages that the colon offers, making it an attractive site for delivery. These unique features of the colon were extensively exploited to maximise the therapeutic efficiency of delivery systems by minimising premature release in the upper GIT but ensuring drug release specifically within the colon. Yet, there remains a need to design colonic systems that can accommodate the newly developed molecules by utilising one of the colon's distinctive features, which is low proteolytic activity and reduced efflux transporters expression. Formulation designs based on polysaccharides that are selectively degraded by colonic microbiota seem promising; therefore, guar gum and pectin were investigated as potential coatings for colon-targeted delivery of MESOPAC.

Two main techniques, spray drying and physical blends, were adopted to create the colonic formulations with the selected polysaccharides. Regardless of the preparation technique, however, pectin demonstrated early drug release in the upper GIT, exceeding 41.32%. Guar gum, on the other hand, was more promising as it showed more controlled release when physically mixed with the drug-loaded carrier particles. The swellable gel network formed around MESOPAC upon the hydration of guar gum seemed to delay drug release and prevent the sweeping in of dissolution medium in the upper GIT until the formulation reaches the colon, where release was induced by enzymatic degradation of guar gum. For two of the three polymer-to-MESOPAC ratios tested, drug release profiles were reproducible and consistent with the intended release behavior. This reproducibility was attributed to the formation of a rigid gel network that was less likely to be affected by hydrodynamic conditions of the dissolution apparatus.

Hydrodynamics of dissolution medium in vessels was a factor influencing drug release behaviour, especially when small-volume dissolution vessels were in place to preserve the enzymes and API in hand. It was, however, necessary to adjust the operating parameters, namely the agitation speed, of the mini dissolution vessel to prevent the coning phenomenon, maximise release within the colonic region, and achieve a comparable release profile to that of the compendial, large-volume dissolution setup. Higher speed generally led to enhanced drug release.

The susceptibility of the formulation to colonic degradation was confirmed by the presence of enzymes as compared to their absence. Ultimately, guar gum-coated MESOPAC at a ratio of 5:1 was selected as the optimal delivery system for colonic targeting of PROTACs as it achieved the desired balance between low upper GIT drug release (~11%) and highly selective release in the colon (60.68 ± 10.57% with felodipine and 43.33 ± 8.01% with MZ1) when subjected to the activity of two enzymes in miniaturised vessels. MESOPAC holds a

great potential as a technology for colon-targeted delivery of both, small molecules and challenging mid-sized entities.

Chapter 5

Conclusion

5.1. Conclusion

Modern drug development is increasingly hindered by intractable protein targets that mediate the pathogenesis of several diseases including cancer. These targets are difficult to drug using traditional small molecules and require advanced molecules to enable their elimination. The past decade was, thus, characterised by increased scientific efforts to discover new targeted therapeutics such as PROTACs. Despite their unprecedented potential in inducing complete degradation of historically challenging targets by using the body's proteasomal machinery, PROTACs emerge with significant delivery challenges that hinder their clinical progression to the market. As they fall in a chemical space beyond the rule of five, PROTACs possess low solubility and permeability that result in an unfavourable bioavailability or pharmacokinetic profile. The pharmaceutical industry has identified the transformative potential of this novel modality and the need to design innovative technologies that address these challenges.

Current delivery platforms such as ASDs have been adapted to accommodate PROTAC molecules in literature, mainly to enhance their solubility. However, problems with excipient choice, scalability, and stability arise with ASDs. Mesoporous particles, thus, present an alternative novel amorphous formulation strategy to overcome the difficulties encountered with conventional ASDs. Mesoporous particles can be engineered e.g., via ultrasonic atomisation using spray drying to harbour a variety of molecules, ranging from small motifs to larger biologics and complex molecules. These carriers can enhance not only the physicochemical properties, such as the solubility, but also permeability if combined with targeting moieties that lead to optimal absorption site for a drug. Of all the target sites, the colon stands as an ideal site for delivery of a wide array of molecules, especially with advancements in targeted therapy driving the renewed interest in the colon. Hence, designing advanced delivery systems that respond to the distinct physiological features of the colonic environment creates opportunities for selective delivery of novel molecules.

[*Summary of Chapter Two redacted]*

Exploring the broad applicability of the optimised mesoporous particles that extends beyond small molecules to address complex delivery challenges associated with novel molecules was demonstrated in chapter three. Colorectal cancer is driven by a number of undruggable proteins, for which PROTACs, like MZ1, might be promising candidates to induce the degradation of these targets. MZ1, however, demonstrates poor solubility and permeability, which compromises its therapeutic potential and restricts its translation into clinical practice. Loading such a novel molecule into MESOPAC was a tough challenge, considering the limited literature and investigatory status of the molecule. Yet, spray drying revealed successful loading of MZ1 into MESOPAC at two different drug loads with acceptable yield. Solid content within the feed solution had the greatest impact on increasing the powder recovery when spray drying MZ1, with maximum yield of 52.8%. The success of the loading process was measured as a decrease in pore volume that indicated the occupation of the pores by MZ1. However, Raman spectroscopy revealed that MZ1 was mainly seen occupying the larger pores around the periphery of MESOPAC, a phenomenon that was attributed to limited diffusivity of MZ1 towards deeper pores due its large molecular size. This translated into flattened particles with an empty core. As a result, the network became susceptible to deflation as it cannot withstand the shear stress of the two-fluid nozzle employed in loading and solvent drying. Despite that, the ultimate goal of addressing the poor solubility of PROTACs by utilising mesoporous particles was established, with MZ1-loaded MESOPAC demonstrating superior dissolution

performance represented as a 4-fold increase in release compared to raw form at 30 minutes. In the present study, an advanced delivery technology was introduced as an alternative to the common platforms for solubility enhancement of PROTACs. Collectively, the findings of this chapter provided a proof-of-concept of how the integration of the appropriate delivery system can tackle the delivery challenges of PROTACs.

In chapter four, the colon was explored as a unique route for targeted delivery of small molecules and PROTACs using mesoporous particles. Its distinctive physiology makes it an ideal location for controlled delivery, with lower expression of efflux transporters and less hostile environment being a hotspot for delivering molecules susceptible to unfavourable degradation or uptake with other sites.

A formulation that aims to trigger the release of two molecules, felodipine or MZ1, upon reaching the colon but minimises early release in upper GIT was designed, utilising polysaccharides that are only digested by colonic enzymes secreted by the microflora. Pectin and guar gum were chosen as GRAS-listed polymers that could modulate the release of drugs to be colon-specific. Pectin was only able to retard the release in gastric environment but underwent dissolution in media simulating the small intestine. Therefore, it was not able to protect the drug load as more than 41.32% of felodipine was released prior to reaching the colon, regardless of the method of preparation. Its behaviour in acidic and alkaline environments is however highly dependent on its gelling behaviour, which is dictated by the type and structure of pectin involved. Pectin might be suitable for colonic targeting only if it is modified to reduce its solubility in media mimicking the small intestine.

Guar gum, on the other hand, was challenging to spray dry due its viscosity. Despite attempts to optimise the spray drying process, powder recovered was negligible, as the viscosity of the feed restricted further optimisation of parameters. Physical mixtures of guar-gum-to-drug-loaded MESOPAC at three different ratios were thought of as an alternative technique to spray drying. The mixture at 5:1 ratio demonstrated successful retardation of drug release in upper GIT to around ~11% with both, felodipine and MZ1. Upon exposure to enzymes in the colonic media, a surge in drug release was noticed, reaching 60.68 ± 10.57% with felodipine and 43.33 ± 8.01% with MZ1 when guar gum-to-loaded MESOPAC ratio was 5:1. The higher colonic release was attributed to the swellable gel network, which upon hydration, delays drug release and prevents the entry of dissolution medium in upper GIT until the formulation reaches the colon, and release is induced by enzymatic degradation of guar gum. Nevertheless, the incomplete release recorded with both drugs was likely due to suboptimal hydrodynamic conditions since small-volume dissolution vessels rather than compendial vessels were employed to study the *in vitro* dissolution performance of the colonic technology to preserve the enzymes and PROTAC. Attempts were made to improve the hydrodynamics

within the small vessels to achieve a correlation between the miniaturised system and the compendial large-volume vessels. It was noted that increasing the rotation speed of the mini paddle helps to overcome the phenomenon of coning that negatively influences the overall drug release. It also generates greater turbulence that drives the powder around, overcoming the overall low release seen in the colon at lower speeds. In addition to the speed, the ratio of guar gum-to-drug-loaded MESOPAC as well as the enzyme level affect the overall colonic drug release. Careful selection of these factors is necessary to maintain a balance between low upper GIT release and colonic selectivity. This would maximise the release in the large intestine such that it becomes comparable to that achieved in large-volume dissolution setup.

From a regulatory perspective, the development of a MZ1-loaded MESOPAC formulation coated with guar gum to the colon would likely follow the conventional new drug regulatory pathway. This is mainly because of the nature of PROTAC molecules that are not yet approved by FDA and the associated novelty of the delivery system. However, the use of well-established excipients that are GRAS-listed and are part of the food industry, such as guar gum, may facilitate a more streamlined approval process. The proposed carrier system is additionally based on CAB, which is a biodegradable material with an established safety profile. Compared to synthetic polymers or surfactants, the selected excipients offer a favourable safety and sustainability profile. Future steps would include preclinical evaluation of pharmacokinetics, toxicity, and stability of the final dosage form prior to clinical trials. In general, the colonic technology introduced in this chapter demonstrated a proof-of-concept of the ability of advanced mesoporous technologies to address the bioavailability challenges encountered by not only small molecules but also novel entities such as PROTACs to facilitate their selective delivery to the colon. Utilising the properties that MESOPAC and the colon, together, offer, controlled release of PROTACs within the colonic environment was established. This approach creates new opportunities for the colon as a promising site to deliver complex molecules.

5.2. Future Work

Further exploration of MESOPAC with other PROTAC molecules utilising different E3-ligases would expand the field of PROTAC delivery and demonstrate the capability of these molecules.

Future plans should consider thorough understanding and complete optimisation of the hydrodynamics between the miniaturised vessels and compendial setup. Moreover, because of the complexity of the human body, it would be more biologically relevant to extend beyond spiking media with enzymes to include rat caecal contents, bacterial cultures, or even comprehensive dynamic models that represent several regions of GIT with tight control over

parameters, only to capture the complexity of the GIT environment. There is also a need for in *vivo* assessment of the performance of the proposed colonic system in this thesis.

Future work can also focus on assessing the permeability of PROTACs. It is important to understand whether the poor permeability of PROTACs is enhanced after incorporation into MESOPAC and colonic targeting.

It is noteworthy to consider the scalability of the mesoporous carrier. Exploring the scaling up from research laboratories to industrial production is necessary to confirm that the process maintains its efficiency, and MESOPAC retains its morphology and functionality over large-scale processing.

Future studies should include testing the stability and functionality of MZ1 post-processing to ensure that the heat involved in spray drying does not compromise the PROTAC. This could involve analytical confirmation of structural integrity and retention of biological activity.

Moreover, assessing the chemical and physical stability of the PROTAC molecule within the finalised formulation during storage is necessary. Stability testing under ICH guidelines (i.e. long-term and accelerated testing) is recommended as part of future plans for regulatory development and scale-up.

5.3 Ethical and Sustainability Considerations

This study did not involve any animal or human subjects, and therefore no ethical approval was required. All laboratory procedures were conducted in accordance with safety protocols, including appropriate handling and disposal of chemicals and biologics.

From a sustainability perspective, the use of MESOPAC as a biodegradable carrier particle reduces environmental impact. Guar gum, a plant-derived polymer that is commonly used in food industry, was selected as a biocompatible coating material. Spray drying was performed with process optimisation to minimise material waste, which is an environmentally considerate approach. Future work involving *in vivo* evaluation (i.e. rat caecal contents) would be subject to ethical approval and relevant guidelines.

References

Abboud, K., Iacomini, M., Simas, F. & Cordeiro, L. (2020). High methoxyl pectin from the soluble dietary fiber of passion fruit peel forms weak gel without the requirement of sugar addition. *Carbohydrate Polymers*, **246**: 116616.

Akhgari, A., Farahmand, F., Afrasiabi, H., Sadeghi, F. & Vandamme, T. (2010). The effect of pectin on swelling and permeability characteristics of free films containing Eudragit RL and/or RS as a coating formulation aimed for colonic drug delivery. *DARU : Journal of Faculty of Pharmacy, Tehran University of Medical Sciences*, **18**(2): 91–96.

Albadarin, A., Potter, C., Davis, M., Iqbal, J., Korde, S., Pagire, S., Paradkar, A. & Walker, G. (2017). Development of stability-enhanced ternary solid dispersions via combinations of HPMCP and Soluplus® processed by hot melt extrusion. *International Journal of Pharmaceutics*, **532**(1): 603–611.

Albertini, B., Passerini, N. & Rodriguez, L. (2005). Evaluation of ultrasonic atomization as a new approach to prepare ionically cross-linked chitosan microparticles. *Journal of Pharmacy and Pharmacology*, **57**(7): 821–829.

Alhajj, N., O'Reilly, N. & Cathcart, H. (2021). Designing enhanced spray dried particles for inhalation: A review of the impact of excipients and processing parameters on particle properties. *Powder Technology*, **384**: 313-331.

Ali, J., Zgair, A., Hameed, G., Garnett, M., Roberts, C., Burley, J. & Gershkovich, P. (2019). Application of biorelevant saliva-based dissolution for optimisation of orally disintegrating formulations of felodipine. *International Journal of Pharmaceutics,* **555**: 228-236.

Al-Japairai, K., Almurisi, S., Mahmood, S., Madheswaran, T., Chatterjee, B., Sri, P., Mazlan, N., Al Hagbani, T. & Alheibshy, F. (2023). Strategies to improve the stability of amorphous solid dispersions in view of the hot melt extrusion (HME) method. *International Journal of Pharmaceutics*, **647**: 123536.

Al-Khattawi, A., Bayly, A., Phillips, A. & Wilson, D. (2018). The design and scale-up of spray dried particle delivery systems, *Expert Opinion on Drug Delivery*, **15**(1): 47–63.

Amidon, S., Brown, E. & Dave, S. (2015). Colon-targeted oral drug delivery systems: design trends and approaches. *AAPS PharmSciTech*: *An Official Journal of the American Association of Pharmaceutical Scientists*, **16**(4): 731-741.

Anane-Adjei, A., Jacobs, E., Nash, S., Askin, S., Soundararajan, R., Kyobula, M., Booth, J. & Campbell, A. (2022). Amorphous solid dispersions: Utilization and challenges in preclinical drug development within AstraZeneca. *International Journal of Pharmaceutics*, **614**: 121387.

Apprato, G., Poongavanam, V., Garcia Jimenez, D., Atilaw, Y., Erdelyi, M., Ermondi, G., Caron, G. & Kihlberg, J. (2024). Exploring the chemical space of orally bioavailable PROTACs. *Drug Discovery Today*, **29**(4): 103917.

Arias, D., Rodríguez, J., López, B. & Méndez, P. (2021. Evaluation of the physicochemical properties of pectin extracted from *Musa paradisiaca* banana peels at different pH conditions in the formation of nanoparticles. *Heliyon*, **7**(1): e06059.

Arumugham, T., Krishnamoorthy, R., AlYammahi, J., Hasan, S., & Banat, F. (2023). Spray dried date fruit extract with a maltodextrin/gum arabic binary blend carrier agent system: Process optimization and product quality. *International Journal of Biological Macromolecules*, **238**: 124340.

Ashford, M., Fell, J., Attwood, D., Sharma, H. & Woodhead, P. (1993). An evaluation of pectin as a carrier for drug targeting to the colon. *Journal of Controlled Release*, **26**(3): 213-220.

Avvaru, B., Patil, M., Gogate, P. & Pandit, A. (2006). Ultrasonic atomization: effect of liquid phase properties. *Ultrasonics*, **44**(2):146-58.

Awad, A., Madla, C., McCoubrey, L., Ferraro, F., Gavins, F., Buanz, A., Gaisford, S., Orlu, M., Siepmann, F., Siepmann, J. & Basit, A. (2022). Clinical translation of advanced colonic drug delivery technologies. *Advanced Drug Delivery Reviews*, **181**: 114076.

Barea, M. (2012). *An investigation into liposomal formulations for targeted drug delivery to the colon*. PhD thesis, University of Birmingham, Birmingham. Available at: https://etheses.bham.ac.uk//id/eprint/3430/1/Barea12PhD.pdf (Accessed: 19 January 2025).

Barrett, E., Joyner, L. & Halenda, P. (1951). The determination of pore volume and area distributions in porous substances. i. computations from nitrogen isotherms. *Journal of the American Chemical Society*, **73**(1): 373-380.

Basit A. (2005). Advances in Colonic Drug Delivery. *Drugs*, **65**(14):1991-2007.

Bavnhøj, G., Knopp, M., Madsen, M. & Löbmann, K. (2019). The role interplay between mesoporous silica pore volume and surface area and their effect on drug loading capacity. *International Journal of Pharmaceutics: X*, **1**: 100008.

BCC Publishing (2024). *Global Markets and Technologies for Advanced Drug Delivery Systems,* Boston. Available at: https://www.bccresearch.com/market-research/pharmaceuticals/advanced-drug-delivery-systems-tech-markets-report.html?srsltid=AfmBOorMnIbJltm5Bk7gv46vYNhVO26IqY1W2SOfwQvU-kYzrO8Vm_7c (Accessed: 15 January 2025).

BDD. [2020]. OralogiK [Online]. BDD-Pharma. Available from: https://www.bddpharma.com/oralogik (Accessed 19 Janauary 2025).

Behboudi-Jobbehdar, S., Soukoulis, C., Yonekura, L. & Fisk, I. (2013). Optimization of spray-drying process conditions for the production of maximally viable microencapsulated L. Acidophilus NCIMB 701748. *Drying Technology*, **31**(11): 1274–1283.

Békés, M., Langley, D. & Crews, C. (2022). PROTAC targeted protein degraders: the past is prologue. *National Reviews Drug Discovery*, **21**: 181–200.

Belbekhouche, S., Poostforooshan, J., Shaban, M., Ferrara, B., Alphonse, V., Cascone, I., Bousserrhine, N., Courty, J. & Weber, A. (2020). Fabrication of large pore mesoporous silica microspheres by salt-assisted spray-drying method for enhanced antibacterial activity and pancreatic cancer treatment. *International Journal of Pharmaceutics*, 590: 119930.

Berkland, C., Kim, K. & Pack, D. (2001). Fabrication of PLG microspheres with precisely controlled and monodisperse size distributions. *Journal of Controlled Release: Official Journal of the Controlled Release Society*, **73**(1): 59–74.

Berkland, C., King, M., Cox, A., Kim, K. & Pack, D. (2002). Precise control of PLG microsphere size provides enhanced control of drug release rate. *Journal of Controlled Release : Official Journal of the Controlled Release Society,* **82**(1), 137–147.

Bharti, C., Nagaich, U., Pal, A. & Gulati, N. (2015). Mesoporous silica nanoparticles in target drug delivery system: A review. *International Journal of Pharmaceutical Investigation*, **5**(3): 124-133.

Bigucci, F., Luppi, B., Monaco, L., Cerchiara, T. & Zecchi, V. (2010). Pectin-based microspheres for colon-specific delivery of vancomycin. *Journal of Pharmacy and Pharmacology*, **61**(1): 41-46.

Bittner, B. & Kissel, T. (2008). Ultrasonic atomization for spray drying: a versatile technique for the preparation of protein loaded biodegradable microspheres. *Journal of Microencapsulation*, **16**(3): 325-41.

Boel, E., Koekoekx, R., Dedroog, S., Babkin, I., Vetrano, M., Clasen, C. & Van den Mooter, G. (2020). Unraveling particle formation: from single droplet drying to spray drying and electrospraying. *Pharmaceutics*, **12**(7): 625.

Bose, A., Elyagoby, A. & Wong, T. (2014). Oral 5-fluorouracil colon-specific delivery through in vivo pellet coating for colon cancer and aberrant crypt foci treatment. *International Journal of Pharmaceutics*, **468**(1-2): 178–186.

Bricelj, A., Steinebach, C., Kuchta, R., Gütschow, M. & Sosič, I. (2021). E3 ligase ligands in successful PROTACs: an overview of syntheses and linker attachment points. *Frontiers in Chemistry*, **9**: 707317.

Brunauer, S., Emmett, P. & Teller, E. (1938). Adsorption of gases in multimolecular layers. *Journal of the American Chemical Society*, **60**(2): 309-319.

Buchi UK Ltd. (2025). *Spray Drying.* Available at: https://www.buchi.com/en/spray-drying (Accessed: 8 March 2025).

Burke, P., Klumb, L., Herberger, J., Nguyen, X., Harrell, R. & Zordich, M. (2004). Poly(lactide-co-glycolide) microsphere formulations of darbepoetin alfa: spray drying is an alternative to encapsulation by spray-freeze drying. *Pharmaceutical Research*, **21**(3): 500–506.

Burke, M., Park, J., Srinivasarao, M. & Khan, S. (2005). A novel enzymatic technique for limiting drug mobility in a hydrogel matrix. *Journal of Controlled Release,* **104**(1): 141–153.

Cai, D., Han, C., Liu, C., Ma, X., Qian, J., Zhou, J., Li, Y., Sun, Y., Zhang, C. & Zhu, W. (2020). Chitosan-capped enzyme-responsive hollow mesoporous silica nanoplatforms for colon-specific drug delivery. *Nanoscale Research Letters*, **15**:123.

Camacho-Lie, M., Antonio-Gutiérrez, O., López-Díaz, A., López-Malo, A. & Ramírez-Corona, N. (2023). Factors influencing droplet size in pneumatic and ultrasonic atomization and its application in food processing. *Discover Food*, **3**: 23.

Candia-Muñoz, N., Ramirez-Bunster, M., Vargas-Hernández, Y. & Gaete-Garretón, L. (2015). Ultrasonic spray drying vs high vacuum and microwaves technology for blueberries. *Physics Procedia,* **70**: 867-871.

Carrozza, D., Malavasi, G. & Ferrari, E. (2023). Very large pores mesoporous silica as new candidate for delivery of big therapeutics molecules, such as pharmaceutical peptides. *Materials*, **16**(11): 4151.

Cecchini, C., Pannilunghi, S., Tardy, S. & Scapozza, L. (2021). From Conception to Development: Investigating PROTACs Features for Improved Cell Permeability and Successful Protein Degradation. *Frontiers in chemistry*, **9**: 672267.

Chandel, D., Uppal, S., Mehta, S. & Shukla, G. (2020). Preparation and characterization of celecoxib entrapped guar gum nanoparticles targeted for oral drug delivery against colon cancer: an in-vitro study. *Journal of Drug Delivery and Therapeutics*, **10**(2-s): 14-21.

Chang, K. & Lin, J. (2000). Swelling behavior and the release of protein from chitosan–pectin composite particles. *Carbohydrate Polymers*, 43(2): 163-169.

Chen, H., Nguyen, N., Magtoto, C., Cobbold, S., Bidgood, G., Guzman, L., Richardson, L., Corbin, J., Au, A., Lechtenberg, B., Feltham, R., Sutherland, K., Grohmann, C., Nicholson, S. & Sleebs, B. (2023). Design and characterization of a heterobifunctional degrader of KEAP1. *Redox Biology*, **59**: 102552.

Chen, Y., Tandon, I., Heelan, W., Wang, Y., Tang, W. & Hu, Q. (2022). Proteolysis-targeting chimera (PROTAC) delivery system: advancing protein degraders towards clinical translation. *Chemical Society Reviews*, **51**(13): 5330–5350.

Cheow, W., Li, S. & Hadinoto, K. (2010). Spray drying formulation of hollow spherical aggregates of silica nanoparticles by experimental design. *Chemical Engineering Research and Design*, **88**(5–6): 673-685.

Chokshi, R., Zia, H., Sandhu, H., Shah, N. & Malick, W. (2007). Improving the dissolution rate of poorly water soluble drug by solid dispersion and solid solution: pros and cons. *Drug Delivery*, **14**(1): 33–45.

Chourasia, M. K., & Jain, S. K. (2004). Potential of guar gum microspheres for target specific drug release to colon. *Journal of Drug Targeting*, *12*(7), 435–442.

Christoforidou, T., Giasafaki, D., Andriotis, G., Bouropoulos, N., Theodoroula, N. F., Vizirianakis, S., Steriotis, T., Charalambopoulou, G. & Fatouros, G. (2021). Oral drug delivery systems based on ordered mesoporous silica nanoparticles for modulating the release of aprepitant. *International Journal of Molecular Sciences*, **22**(4): 1896.

Cimas, F., Niza, E., Juan, A., Noblejas-López, M., Bravo, I., Lara-Sanchez, A., Alonso-Moreno, C. & Ocaña, A. (2020). Controlled delivery of BET-PROTACS: in vitro evaluation of MZ1-loaded polymeric antibody conjugated nanoparticles in breast cancer. *Pharmaceutics*, **12**(10): 986.

D'Addio, S., Chan, J., Kwok, P., Prud'homme, R. & Chan, H. (2012). 'Spray freeze dried large porous particles for nano drug delivery by inhalation', in *Proceedings of the 2012 Respiratory Drug Delivery (RDD) Conference*, Phoenix, AZ, 13-17 May. Available at: https://core.ac.uk/download/pdf/37980433.pdf.

Das S. (2021). Pectin based multi-particulate carriers for colon-specific delivery of therapeutic agents. *International Journal of Pharmaceutics*, **605**:120814.

Dalmoro, A., d'Amore, M. & Barba, A. (2013). Droplet size prediction in the production of drug delivery microsystems by ultrasonic atomization. *Translational Medicine at UniSa*, **2**(7): 6-11.

Davis, S., Hardy, J. & Fara, J. (1986). Transit of pharmaceutical dosage forms through the small intestine. *Gut,* **27**: 886-892.

Dedroog, S., Pas, T., Vergauwen, B., Huygens, C. & Van den Mooter, G. (2020). Solid-state analysis of amorphous solid dispersions: Why DSC and XRPD may not be regarded as stand-alone techniques. *Journal of Pharmaceutical and Biomedical Analysis*, **178:** 112937.

Deshawar, D., Gupta, K. & Chokshi, P. (2020). Electrospinning of polymer solutions: An analysis of instability in a thinning jet with solvent evaporation. *Polymer*: **202**

Dong, Y., Ma, T., Xu, T., Feng, Z., Li, Y., Song, L., Yao, X., Ashby, C., & Hao, G. (2024). Characteristic roadmap of linker governs the rational design of PROTACs. *Acta Pharmaceutica Sinica. B*, **14**(10): 4266–4295.

Dortmund Data Bank. (2022). *Vapor-Liquid Equilibrium Data* [Online]. Accessed 23 January 2022. Available from: http://www.ddbst.com/en/EED/VLE/VLE%20Acetone%3BWater.php

Dranca, F. & Oroian, M. (2019). Optimization of pectin enzymatic extraction from *malus domestica* 'fălticeni' apple pomace with celluclast 1.5l. *Molecules,* **24**(11): 2158.

Duan, H., Lu, S., Gao, C., Bai, X., Qin, H., Wei, Y., Wu, X. & Liu, M. (2016). Mucoadhesive microparticulates based on polysaccharide for target dual drug delivery of 5-aminosalicylic acid and curcumin to inflamed colon. *Colloids and Surfaces b: Biointerfaces*, **145**: 510-519.

Eastman Chemical. (2021). *Eastman cellulose-based speciality polymers*, Accessed on 23 January 2022. https://www.eastman.com/Literature_Center/E/E325.pdf

Eijkelboom, N., Boven, A., Siemons, I., Wilms, P., Boom, R., Kohlus, R. & Schutyser, M. (2023). Particle structure development during spray drying from a single droplet to pilot-scale perspective. *Journal of Food Engineering*, **337**: 111222.

Einhorn-Stoll, U., Kunzek, H. & Dongowski, G. (2007). Thermal analysis of chemically and mechanically modified pectins, *Food Hydrocolloids*, **21**(7): 1101-1112.

Ekdahl, A., Mudie, D., Malewski, D., Amidon, G. & Goodwin, A. (2019). Effect of spray-dried particle morphology on mechanical and flow properties of felodipine in PVP VA amorphous solid dispersions. Journal of Pharmaceutical Sciences, 108 (11): 3657-3666.

Esposito, E., Roncarati, R., Cortesi, R., Cervellati, F. & Nastruzzi, C. (2000). Production of Eudragit microparticles by spray-drying technique: influence of experimental parameters on morphological and dimensional characteristics*. Pharmaceutical Development and Technology,* **5**(2): 267-78.

Evonik. [2020]. A commercially-proven colon targeted drug delivery system. Evonik. Available from: https://healthcare.evonik.com/en/drugdelivery/oral-drug-delivery/oral-drug-delivery-technologies/sustained-colonic-delivery (Accessed: 19 Janauary 2025).

Farzan, M., Roth, R., Schoelkopf, J., Huwyler, J. & Puchkov, M. (2023). The processes behind drug loading and release in porous drug delivery systems. *European Journal of Pharmaceutics and Biopharmaceutics*,**189**: 133–151.

Ferlay, J., Ervik, M., Lam, F., Laversanne, M., Colombet, M., Mery, L., Piñeros, M., Znaor, A., Soerjomataram, I., Bray, F. (2024). Global Cancer Observatory: Cancer Today. Lyon, France: International Agency for Research on Cancer. Available from: https://gco.iarc.who.int/today (Accessed: 1 July 2025).

Forde, G. & Friend, J. (2006). 'Production of biodegradable nano and micro particles via ultrasonic atomization for biopharmaceutical delivery', *Proceedings of the 2006 WSEAS International Conference on Cellular & Molecular Biology, Biophysics & Bioengineering*, Athens, Greece, 14-16 July, pp. 128-130.

Gallo, L., Llabot, J. M., Allemandi, D., Bucalá, V. & Piña, J. (2011). Influence of spray-drying operating conditions on Rhamnus purshiana (Cáscara sagrada) extract powder physical properties. *Powder Technology*, **208**(1): 205–214.

Gao, H., Sun, X. & Rao, Y. (2020). PROTAC technology: opportunities and challenges. *ACS Medicinal Chemistry Letters*, **11**(3): 237–240.

Gao, J., Jiang, X., Lei, S., Cheng, W., Lai, Y., Li, M., Yang, L., Liu, P., Chen, X., Huang, M., Yu, H., Xu, H. & Xu, Z. (2024). A region-confined PROTAC nanoplatform for spatiotemporally tunable protein degradation and enhanced cancer therapy. *Nature Communications*, **15**(1): 6608.

Garcia-Couce, J., Bada-Rivero, N., Hernandez, O., Nogueria, A., Caraccoilo, P., Abraham, G., Hernandez, J. & Peniche, C. (2019). Dexamethasone-loaded chitosan beads coated with a ph-dependent interpolymer complex for colon-specific drug delivery. *International Journal of Polymer Science,* 1-9.

Gliko-Kabir, I., Yagen, B., Baluom, M. & Rubinstein, A. (2000). Phosphated crosslinked guar for colon-specific drug delivery. II. In vitro and in vivo evaluation in the rat. *Journal of Controlled Release*, **63**(1-2): 129–134.

Goelo, V., Chaumun, M., Goncalves, A., Estevinho, B. & Rocha, F. (2020). Polysaccharide-based delivery systems for curcumin and turmeric powder encapsulation using a spray-drying process. *Powder Technology*, **370**: 137-146.

Goh, H., Heng, P. & Liew, C. (2018). Comparative evaluation of powder flow parameters with reference to particle size and shape. *International Journal of Pharmaceutics*, **547**(1-2): 133-141.

Gong, B., Zhang, W., Cong, W., Gu, Y., Ji, W., Yin, T., Zhou, H., Hu, H., Zhuang, J., Luo, Y., Liu, Y., Gao, J. & Yin, Y. (2024a). Systemic administration of neurotransmitter-derived lipidoids-PROTACs-DNA nanocomplex promotes Tau clearance and cognitive recovery for alzheimer's disease therapy. *Advanced Healthcare Materials*, **13**(32): e2400149.

Gong, T., Liu, X., Wang, X., Lu, Y. & Wang, X. (2024b). Applications of polysaccharides in enzyme-triggered oral colon-specific drug delivery systems: A review. *International Journal of Biological Macromolecules*, **275**(1): 133623.

González-Alvarez, M., Coll, C., Gonzalez-Alvarez, I., Giménez, C., Aznar, E., Martínez-Bisbal, M., Lozoya-Agulló, I., Bermejo, M., Martínez-Máñez, R. & Sancenón, F. (2017). Gated mesoporous silica nanocarriers for a "two-step" targeted system to colonic tissue. *Molecular Pharmaceutics*, **14**(12): 4442-4453.

Graham H. (2022). The mechanism of action and clinical value of PROTACs: A graphical review. *Cellular Signalling*, **99**: 110446.

Gui, Z., Zeng, Y., Xie, T., Chen, B., Wang, J., Wen, Y., Tan, T., Zou, T., Zhang, F. & Zhang, J. (2024). Cavitation is the determining mechanism for the atomization of high-viscosity liquid. *iScience*, **27**(6): 110071.

Guisti, F. (2021). 'Dissolution test strategies for colon-targeting drug products' [PowerPoint presentation]. *The COLOTAN 1stSymposium: Colon targeting of drugs: current state of the art.* Available at: https://colotan-etn.eu/wp-content/uploads/2021/06/F.-Giusti-_COLOTAN-2021.pdf (Accessed: 8 March 2025) .

Guo, Y., Zong, S., Pu, Y., Xu, B., Zhang, T. & Wang, B. (2018). Advances in pharmaceutical strategies enhancing the efficiencies of oral colon-targeted delivery systems in inflammatory bowel disease. *Molecules,* **23**: 1622.

Hanmantrao, M., Chaterjee, S., Kumar, R., Vishwas, S., Harish, V., Porwal, O., Alrouji, M., Alomeir, O., Alhajlah, S., Gulati, M., Gupta, G., Dua, K. & Singh, S. (2022). Development of Guar Gum-Pectin-Based Colon Targeted Solid Self-Nanoemulsifying Drug Delivery System of Xanthohumol. *Pharmaceutics*, **14**(11): 2384.

He, H., Li, F., Tang, R., Wu, N., Zhou, Y., Cao, Y., Wang, C., Wan, L., Zhou, Y., Zhuang, H. & Li, P. (2024) Ultrasound controllable release of proteolysis targeting chimeras for triple-negative breast cancer treatment. *Biomaterials Research*, **28**: 0064

He, H., Lu, Y., Qi, J., Zhu, Q., Chen, Z. & Wu, W. (2018). Adapting liposomes for oral drug delivery. *Acta Pharmaceutica Sinica. B*, **9**(1): 36–48.

He, Y. & Ho, C. (2015). Amorphous solid dispersions: utilization and challenges in drug discovery and development. *Journal of Pharmaceutical Sciences*, **104**(10): 3237–3258.

Hellberg, H., Westberg, A., Appelblad, P. & Mattsson, S. (2021). Evaluation of dissolution techniques for orally disintegrating mini-tablets. *Journal of Drug Delivery Science and Technology*, **61**: 102191.

Ho, J., Wang, H. & Forde, G. (2008). Process considerations related to the microencapsulation of plasmid DNA via ultrasonic atomization. *Biotechnology and Bioengineering*, **101**(1): 172–181.

Hofmann, N., Harms, M. & Mäder, K. (2024). ASDs of PROTACs: Spray-dried solid dispersions as enabling formulations. *International Journal of Pharmaceutics*, **650**: 123725.

Höhne, P., Mieller, B. & Rabe, T. (2020). Advancing spray granulation by ultrasound atomization. *International Journal of Applied Ceramic Technology,* **17**: 2212– 2219.

Hsieh, S., Huang, C., Lin, J. & Chen, Y. (2024). Spray cooling heat transfer of a two-fluid spray atomizer. ASME *Journal of Heat and Mass Transfer*, **146**(5): 052302.

Hu, Y., Zhou, J., Ye, F., Xiong, H., Peng, L., Zheng, Z., Xu, F., Cui, M., Wei, C., Wang, X., Wang, Z., Zhu, H., Lee, P., Zhou, M., Jiang, B. & Zhang, D. (2015). BRD4 inhibitor inhibits colorectal cancer growth and metastasis. *International Journal of Molecular Sciences*, **16**(1): 1928–1948.

Huang, J., Yao, Z., Li, B. & Ping, Y. (2023). Targeted delivery of PROTAC-based prodrug activated by bond-cleavage bioorthogonal chemistry for microneedle-assisted cancer therapy. *Journal of Controlled Release : Official Journal of the Controlled Release Society*, **361**: 270–279.

Hwang, S., Han, Y. & Gardner, D. J. (2023). Characterization of CNC nanoparticles prepared via ultrasonic-assisted spray drying and their application in composite films. *Nanomaterials (Basel)*, **13**(22): 2928.

International Conference on Harmonisation (ICH). (1997). *Q2B: Validation of analytical procedures*. U.S. Federal Register, **62**, 27463–27467.

IUPHAR/BPS Guide to PHARMACOLOGY (n.d.) *MZ1 (Ligand ID: 10728)*. Available at: https://www.guidetopharmacology.org/GRAC/LigandDisplayForward?ligandId=10728 (Accessed: 3 September 2025).

Intract Pharma [2020]. Soteria ®. Intract Pharma, Available from: https://www.intractpharma.com/fomulation-technologies/soteria/ (Accessed: 19 Janauary 2025).

Jacob, E., Borah, A., Jindal, A., Pillai, S., Yamamoto, Y., Maekawa, T. & Kumar, D. (2020). Synthesis and characterization of citrus-derived pectin nanoparticles based on their degree of esterification. *Journal of Materials Research*, **35**: 1514–1522.

Jelvehgari, M., Maghsoodi, M. & Nemati, H. (2010). Development of theophylline floating microballoons using cellulose acetate butyrate and/or Eudragit RL 100 polymers with different permeability characteristics. *Research in Pharmaceutical Sciences*, **5**(1):29-39.

Jiménez, D., Rossi Sebastiano, M., Vallaro, M., Mileo, V., Pizzirani, D., Moretti, E., Ermondi, G. & Caron, G. (2022). Designing soluble PROTACS: strategies and preliminary guidelines. *Journal of Medicinal Chemistry*, **65**(19): 12639–12649.

Jimenez, D., Rossi Sebastiano, M., Vallaro, M., Ermondi, G. & Caron, G. (2024). IMHB-mediated chameleonicity in drug design: A focus on structurally related PROTACS. *Journal of Medicinal Chemistry*, **67**(13): 11421–11434.

Jin, L., Ding, Y., Zhang, Y., Xu, X. & Cao, Q. (2016). A novel pH–enzyme-dependent mesalamine colon-specific delivery system. *Drug Design, Development, and Therapy*, **10**: 2021-2028.

Johansson, K., Plum, J., Mosleh, M., Madsen, C., Rades, T. & Müllertz, A. (2018). Characterization of the hydrodynamics in a miniaturized dissolution apparatus. *Journal of Pharmaceutical Sciences*, **107**(4): 1095–1103.

Joshi, B., Kaur, J., Khan, E., Vishwakarma, S., Kumar, A., Joshi, D., Kumar, A. & Joshi, A. (2023). Alginate-based 'nano-micro' hybrid matrices developed using ultrasonic atomization for Co-delivery of chemotherapeutic drugs against superficial tumors, *Journal of Drug Delivery Science and Technology*, **84**: 104532.

Katsuma, M., Watanabe, S., Kawai, H., Takemura, S., Masusda, Y. & Fukui, M. (2002). Studies on lactulose formulations for colon-specific drug delivery. *International Journal of Pharmaceutics*, **249**(1-2):33-43.

Kaur, R., Gulati, M. & Singh, S. (2017). Role of synbiotics in polysaccharide assisted colon targeted microspheres of mesalamine for the treatment of ulcerative colitis. *International Journal of Biological Macromolecules*, **95**: 438–450.

Kaushik, A., Kumar, A., Yu, C., Kuo, S., Liang, S., Singh, S., Wang, X., Wang, Y., Yen, C., Dai, X., Wei, D., Pan, C. & Shiue, Y. (2019). PCL–DOX microdroplets: an evaluation of the enhanced intracellular delivery of doxorubicin in metastatic cancer cells via in silico and in vitro approaches. *New Journal of Chemistry*, **43**: 12241-12256.

Khaire, R. & Gogate, P. (2020). Novel approaches based on ultrasound for spray drying of food and bioactive compounds. *Drying Technology*, **39**(12): 1832-1853.

Khotimchenko M. (2020). Pectin polymers for colon-targeted antitumor drug delivery. *International journal of biological macromolecules*, S0141-8130(20)33147-0.

Kim, D., Kim, Y., Tin, Y., Soe, M., Ko, B., Park, S., & Lee, J. (2021). Recent technologies for amorphization of poorly water-soluble drugs. *Pharmaceutics*, **13**(8): 1318.

Kim, H., Cheon, J., Lee, S., Min, J., Back, S., Song, J., Kim, D., Lim, S. & Han, H. (2020). Ternary nanocomposite carriers based on organic clay-lipid vesicles as an effective colon-targeted drug delivery system: preparation and in vitro/in vivo characterization. *Journal of Nanobiotechnology*, **18**(1): 17.

Klein, S. (2006). The mini paddle apparatus–a useful tool in the early developmental stage? experiences with immediate-release dosage forms. Dissolution Technologies, 6-11.

Klein, S. & Shah, V. (2008). A standardized mini paddle apparatus as an alternative to the standard paddle. *AAPS PharmSciTech*, **9**(4): 1179–1184.

Klein, T., Longhini, R., Bruschi, M. & de Mello, J. (2015). Microparticles containing guaraná extract obtained by spray-drying technique: development and characterization, *Revista Brasileira de Farmacognosia*, **25**(3): 292-300.

Krishnaiah, Y., Satyanarayana, S., Prasad, Y. & Rao, S. (1998). Evaluation of guar gum as a compression coat for drug targeting to colon. *International Journal of Pharmaceutics*, **171**(2): 137-146.

Krishnaiah, Y., Veer Raju, P., Kumar, B., Bhaskar, P. & Satyanarayana, V. (2001). Development of colon targeted drug delivery systems for mebendazole. *Journal of Controlled,* **77**(1-2): 87–95.

Krishnaiah, Y., Reddy, P., Satyanarayana, V. & Karthikeyan, R. (2002). Studies on the development of oral colon targeted drug delivery systems for metronidazole in the treatment of amoebiasis. *International Journal of Pharmaceutics*, **236**(1-2): 43–55.

Kumar, B., Kulanthaivel, S., Mondal, A., Mishra, S., Banerjee, B., Bhaumik, A., Banerjee, I. & Giri, S. (2017). Mesoporous silica nanoparticle-based enzyme responsive system for colon specific drug delivery through guar gum capping. *Colloids and Surfaces B: Biointerfaces*, **150**: 352-361.

Kumar, A., Gulati, M., Singh, S., Gowthamarajan, K., Prashar, R., Mankotia, D., Gupta, J., Banerjee, M., Sinha, S., Awasthi, A., Corrie, L., Kumar, R., Patni, P., Kumar, B., Pandey, N., Sadotra, M., Kumar, P., Kumar, R., Wadhwa, S. & Khursheed, R. (2020). Effect of co-administration of probiotics with guar gum, pectin and eudragit S100 based colon targeted mini tablets containing 5-Fluorouracil for site specific release. *Journal of Drug Delivery Science and Technology*, **60**.

Laier, C., Alstrøm, T., Bargholz, M., Sjøltov, P., Rades, T., Boisen, A. & Nielsen, L. (2019). Evaluation of the effects of spray drying parameters for producing cubosome powder precursors. *European Journal of Pharmaceutics and Biopharmaceutics*, **135**: 44-48.

Lang, R. (1962). Ultrasonic atomization of liquids. *The Journal of Acoustical Society of America,* **34** (1): 6–8.

Le, T. (2021). *Mesoporous materials for oral delivery of poorly soluble drugs*. PhD thesis. Aston University: UK.

Le, T., Elyafi, A., Mohammed, A. & Alkhattawi, A. (2019). Delivery of poorly soluble drugs via mesoporous silica: Impact of drug overloading on release and thermal profiles. *Pharmaceutics*, **11**(6): 269.

Lechanteur, A. & Evrard, B. (2020). Influence of composition and spray-drying process parameters on carrier-free dpi properties and behaviors in the lung: a review. *Pharmaceutics*, **12**(1): 55.

LeClair, D. A., Cranston, E. D., Xing, Z. & Thompson, M. (2016). Optimization of spray drying conditions for yield, particle size and biological activity of thermally stable viral vectors. *Pharmaceutical Research*, **33**(11): 2763–2776.

Lee, J., Lee, Y., Jung, Y., Park, J., Yoo, H., & Park, J. (2022). Discovery of E3 Ligase Ligands for Target Protein Degradation. *Molecules*, **27**(19): 6515.

Legace, M., Gravelle, L., Di Maso, M. & McClintock, S. (2004). Developing a discriminating dissolution procedure for a dual active pharmaceutical product with unique solubility characteristics. *Dissolution Technologies,* 13-17.

Legako, J. & Dunford, N. (2010). Effect of spray nozzle design on fish oil-whey protein microcapsule properties. *Journal of Food Science*, **1**(75): 394-400.

Li, K. & Crews, C. (2022). PROTACs: past, present and future. *Chemical Society Reviews*, **51**(12): 5214–5236.

Li, T., Wan, B., Jog, R., Costa, A. & Burgess, D. (2022). Pectin microparticles for peptide delivery: Optimization of spray drying processing. *International Journal of Pharmaceutics*, **613:** 121384.

Liang, Y., Nandakumar, K. & Cheng, K. (2020). Design and pharmaceutical applications of proteolysis-targeting chimeric molecules. *Biochemical Pharmacology*, **182**: 114211.

Lim, V., Peh, K. & Sahudin, S. (2013). Synthesis, characterisation, and evaluation of a cross-linked disulphide amide-anhydride-containing polymer based on cysteine for colonic drug delivery. *International Journal of Molecular Science*, **14**: 24670-24691.

Lin, C. & Gentry, J. (2003). Spray drying drop morphology: experimental study. *Aerosol Science and Technology*, **37**(1): 15-32.

Liu, Y., Yang, J., Wang, T., Luo, M., Chen, Y., Chen, C., Ronai, Z., Zhou, Y., Ruppin, E. & Han, L. (2023). Expanding PROTACtable genome universe of E3 ligases. *Nature Communications*, **14**(1): 6509.

Liu, W., Deng, Z., Zhang, Y., Zhu, X., Huang, J., Zhang, H. & Zhu, J. (2024). Decoding powder flowability: Machine learning pioneers the analysis of particle-size distribution effects. *Powder Technology,* **435**: 119407.

Lu, L., Chen, G., Qiu, Y., Li, M., Liu, D., Hu., D., Gu., X. & Xiao, Z. (2016). Nanoparticle-based oral delivery systems for colon targeting: principles and design strategies. *Science Bulletin*, **61**(9): 670-681.

M, A. & Gogate, P. (2024). Improved synthesis of metformin hydrochloride-sodium alginate (MH-NaALG) microspheres using ultrasonic spray drying. *Heliyon*, **10**(6): e28205.

Ma, J., Fang, L., Sun, Z., Li, M., Fan, T., Xiang, G. & Ma, X. (2024). Folate-PEG-protac micelles for enhancing tumor-specific targeting proteolysis in vivo. *Advanced Healthcare Materials*, **13**(20): e2400109.

Ma, S., Ji, J., Tong, Y., Zhu, Y., Dou, J., Zhang, X., Xu, S., Zhu, T., Xu, X., You, Q. & Jiang, Z. (2022). Non-small molecule PROTACs (NSM-PROTACs): Protein degradation kaleidoscope. *Acta Pharmaceutica Sinica. B*, **12**(7): 2990–3005.

Madan, J., Ahuja, V., Dua, K., Samajdar, S., Ramchandra, M. & Giri, S. (2022). PROTACS: current trends in protein degradation by proteolysis-targeting chimeras. *BioDrugs*, **36**: 609–623.

Mäkilä, E., Ferreira, M., Kivelä, H., Niemi, S., Correia, A., Shahbazi, M., Kauppila, J., Hirvonen, J., Santos, H., & Salonen, J. (2014). Confinement effects on drugs in thermally hydrocarbonized porous silicon. *Langmuir: the ACS Journal of Surfaces and Colloids*, **30**(8): 2196–2205.

Manna, S., Karmakar, S., Sen, O., Sinha, P., Jana, S., & Jana, S. (2024). Recent updates on guar gum derivatives in colon specific drug delivery. *Carbohydrate polymers*, *334*, 122009.

Marcellinaro, R., Spoletini, D., Grieco, M., Avella, P., Cappuccio, M., Troiano, R., Lisi, G., Garbarino, G. & Carlini, M. (2023). Colorectal cancer: current updates and future perspectives. *Journal of Clinical Medicine*, **13**(1): 40.

Mareczek, L., Mueller, L., Halstenberg, L., Geiger, T., Walz, M., Zheng, M. & Hausch, F. (2024). Use of poly (vinyl alcohol) in spray-dried dispersions: enhancing solubility and stability of proteolysis targeting chimeras. *Pharmaceutics*, **16**(7): 924.

Marie, A., Tourbin, M., Robisson, A., Ablitzer, C. & Frances, C. (2022). Wet size measurements for the evaluation of the deagglomeration behaviour of spray-dried alumina powders in suspension. *Ceramics International*, **48**(6): 7926-7936.

Martín-Acosta, P. & Xiao, X. (2021). PROTACs to address the challenges facing small molecule inhibitors. *European Journal of Medicinal Chemistry*, **210**: 112993.

Maury, M., Murphy, K., Kumar, S., Shi, L. & Lee, G. (2005). Effects of process variables on the powder yield of spray-dried trehalose on a laboratory spray-dryer. *European Journal of Pharmaceutics and Biopharmaceutics*, **59**(3): 565–573.

McCoubrey, L., Favaron, A., Awad, A., Orlu, M., Gaisford, S. & Basit, A. (2023). Colonic drug delivery: Formulating the next generation of colon-targeted therapeutics. *Journal of Controlled Release*, **353:** 1107–1126.

Meere, M., Pontrelli, G. & McGinty, S. (2019). Modelling phase separation in amorphous solid dispersions. *Acta Biomaterialia*, **94**: 410–424.

Mehrabi, M., Gardy, J., Talebi, F., Farshchi, A., Hassanpour, A. & Bayly, A. (2023). An investigation of the effect of powder flowability on the powder spreading in additive manufacturing. *Powder Technology*, **413**: 117997.

Microspray. (2022). *What is ultrasonic cavitation?* [Online]. [Accessed 2 January 2022]. Available from: https://microspray.com/ultrasonic-atomization-cavitation

Minko T. (2020). Nanoformulation of BRD4-Degrading PROTAC: improving druggability to target the 'undruggable' MYC in pancreatic cancer. *Trends in Pharmacological Sciences*, **41**(10): 684–686.

Mirza, T., Joshi, Y., Liu, Q. & Vivilecchia, R. (2005). Evaluation of dissolution hydrodynamics in the usp, peak™ and flat-bottom vessels using different solubility drugs. *Dissolution Technologies,* **1**: 11-16.

Momin, M. & Pundarikakshudu, K. (2005). Optimization and pharmacotechnical evaluation of compression-coated colon-specific drug delivery system of triphala using factorial design. *Drug Development Research,* **65.**

Moon, Y., Jeon, S., Shim, M. & Kim, K. (2023). Cancer-specific delivery of proteolysis-targeting chimeras (PROTACs) and their application to cancer immunotherapy. *Pharmaceutics*, **15**(2): 411.

Moutaharrik, S., Palugan, L., Cerea, M., Meroni, G., Casagni, E., Roda, G., Martino, P., Gazzaniga, A., Maroni, A. & Foppoli, A. (2024) Colon Drug Delivery Systems Based on Swellable and Microbially Degradable High-Methoxyl Pectin: Coating Process and In Vitro Performance. *Pharmaceutics*, **16**(4): 508.

Naeem, M., Choi, M., Cao, J., Lee, Y., Ikram, M., Yoon, S., Lee, J., Moon, H., Kim, M., Jung, Y. & Yoo, J. (2015). Colon-targeted delivery of budesonide using dual pH- and time-dependent polymeric nanoparticles for colitis therapy. *Drug Design, Development, and Therapy,* **9**: 3789-3799.

Naeem, M., Bae, J., Oshi, M., Kim, M., Moon, H., Lee, B., Im, E., Jung, Y. & Yoo, J. (2018). Colon-targeted delivery of cyclosporine A using dual-functional Eudragit® FS30D/PLGA nanoparticles ameliorates murine experimental colitis. *International Journal of Nanomedicine*, **13**: 1225–1240.

Naidu, H., Kahraman, O. & Feng, H. (2022). Novel applications of ultrasonic atomization in the manufacturing of fine chemicals, pharmaceuticals, and medical devices. *Ultrasonics Sonochemistry*, **86**:105984.

Nandiyanto, D., Ogi, T., Wang, W., Gardon, L. & Okuyama, K. (2019). Template-assisted spray-drying method for the fabrication of porous particles with tunable structures*. Advanced Powder Technology*, **30**(12): 2908-2924.

Narala, S., Nyavanandi, D., Mandati, P., Youssef, A., Alzahrani, A., Kolimi, P., Zhang, F. & Repka, M. (2023). Preparation and *in vitro* evaluation of hot-melt extruded pectin-based pellets containing ketoprofen for colon targeting. *Internationa Jjournal of Pharmaceutics: X*, **5**: 100156.

Nathani, A., Aare, M., Sun, L., Bagde, A., Li, Y., Rishi, A. & Singh, M. (2024). Unlocking the potential of camel milk-derived exosomes as novel delivery systems: enhanced bioavailability of ARV-825 PROTAC for cancer therapy. *Pharmaceutics*, **16**(8): 1070.

Neklesa, T., Winkler, J. & Crews, C. (2017). Targeted protein degradation by PROTACs. *Pharmacology & therapeutics*, **174**: 138–144.

Ng, Y., Yusuf, S., Chiu, H. & Lim, V. (2020). Redox-sensitive linear and cross-linked cystamine-based polymers for colon-targeted drug delivery: design, synthesis, and characterization. *Pharmaceutics*, **12**(5): 461.

Nguyen, M., Tran, P. & Tran, T. (2019). A single-layer film coating for colon-targeted oral delivery. *International Journal of Pharmaceutics,* **559**: 402-409.

Nguyen, T., Hirano, T., Chamida, R., Septiani, E., Nguyen, N. & Ogi, T. (2024). Porous pectin particle formation utilizing spray drying with a three-fluid nozzle. *Powder Technology*, **440**: 119782.

Nii, S. (2016) 'Ultrasonic Atomization', in *Handbook of Ultrasonics and Sonochemistry*. Singapore: Springer. Available at: https://doi.org/10.1007/978-981-287-278-4_7.

Oliveira, G., Ferrari, P., Carvalho, L. & Evangelista, R. (2010). Chitosan–pectin multiparticulate systems associated with enteric polymers for colonic drug delivery. *Carbohydrate Polymers*, **82**(3): 1004-1009.

Opnme, [2025]. BET PROTAC-MZ1 [Online]. Boehringer Ingelheim International. Available from: https://www.opnme.com/molecules/bet-mz-1 [Accessed 8 March 2025].

Otto, C., Schmidt, S., Kastner, C., Denk, S., Kettler, J., Müller, N., Germer, C., Wolf, E., Gallant, P. & Wiegering, A. (2019). Targeting bromodomain-containing protein 4 (BRD4) inhibits MYC expression in colorectal cancer cells. *Neoplasia*, **21**(11): 1110–1120.

Ousset, A., Chirico, R., Robin, F., Schubert, M., Somville, P. & Dodou, K. (2018). A novel protocol using small-scale spray-drying for the efficient screening of solid dispersions in early drug development and formulation, as a straight pathway from screening to manufacturing stages. *Pharmaceuticals*, **11**(3): 81.

Paiva, S. & Crews, C. (2019). Targeted protein degradation: elements of PROTAC design. *Current Opinion in Chemical Biology*, **50:** 111–119.

Panão, M. (2022). Ultrasonic atomization: new spray characterization approaches. *Fluids*, **7**(1): 29.

Prasad, Y., Krishnaiah, Y. & Satyanarayana, S. (1998). In vitro evaluation of guar gum as a carrier for colon-specific drug delivery. *Journal of Controlled Release : Official Journal of the Controlled Release Society*, **51**(2-3): 281–287.

Perkušić, M., Nižić Nodilo, L., Ugrina, I., Špoljarić, D., Jakobušić Brala, C., Pepić, I., Lovrić, J., Matijašić, G., Gretić, M., Zadravec, D., Kalogjera, L. & Hafner, A. (2022). Tailoring functional spray-dried powder platform for efficient donepezil nose-to-brain delivery. *International Journal of Pharmaceutics*, **624**: 122038.

Permal, R., Chang, W., Chen, T., Seale, B., Hamid, N. & Kam, R. (2020). Optimising the spray drying of avocado wastewater and use of the powder as a food preservative for preventing lipid peroxidation. *Foods*, **9**: 1187.

Philip, A. & Philip, B. (2010). Colon targeted drug delivery systems: a review on primary and novel approaches. *Oman Medical Journal*, **25**(2):70-7.

Pichlak, M., Sobierajski, T., Błażewska, K. & Gendaszewska-Darmach, E. (2023). Targeting reversible post-translational modifications with PROTACs: a focus on enzymes modifying protein lysine and arginine residues. *Journal of Enzyme Inhibition and Medicinal Chemistry*, **38**(1): 2254012.

Pike, A., Williamson, B., Harlfinger, S., Martin, S. & McGinnity, D. (2020). Optimising proteolysis-targeting chimeras (PROTACs) for oral drug delivery: a drug metabolism and pharmacokinetics perspective. *Drug Discovery Today*, **25**(10): 793–1800.

Poeiras, G. (2018). *Impact of spray drying nozzle and chamber design on powders properties* (Master's thesis). Técnico Lisboa. Available at:

https://scholar.tecnico.ulisboa.pt/records/6ICqWFEpA8QcgVfEblcdXijAKDqpRnYlmtmz?lang=en (Accessed: 15 January 2025).

Poostforooshan, J., Belbekhouche, S., Shaban, M., Alphonse, V., Habert, D., Bousserrhine, N., Courty, J. & Weber, A. (2020). Aerosol-assisted synthesis of tailor-made hollow mesoporous silica microspheres for controlled release of antibacterial and anticancer agents. *ACS Applied Materials & Interfaces*, **12(**6): 6885-6898.

Poozesh, S. & Bilgili, E. (2019). Scale-up of pharmaceutical spray drying using scale-up rules: A review. *International Journal of Pharmaceutics*, **562**: 271–292.

Pöstges, F., Kayser, K., Appelhaus, J., Monschke, M., Gütschow, M., Steinebach, C. & Wagner, K. G. (2023). Solubility enhanced formulation approaches to overcome oral delivery obstacles of PROTACS. *Pharmaceutics*, **15**(1):156.

Prabaharan M. (2011). Prospective of guar gum and its derivatives as controlled drug delivery systems. *International Journal of Biological Macromolecules*, **49**(2): 117–124.

Pradhan, S. (2011). Multiparticulate combined approaches for colon specific drug delivery. *International Journal of Biomedical Research*, **2**(9): 476-485.

Prasanth, V., Jayaprakash, R. & Mathew, S. (2012). Colon specific drug delivery systems: A review on various pharmaceutical approaches. *Journal of Applied Pharmaceutical Science*, **2**(1):163-169.

Priyadarshi, A., Shahrani, S., Choma, T., Zrodowski, L., Qin, L., Leung, C., Clark, S., Fezzaa, K., Mi, J., Lee, P., Eskin, D. & Tzanakis, L. (2024). New insights into the mechanism of ultrasonic atomization for the production of metal powders in additive manufacturing, *Additive Manufacturing*, **83**: 104033.

Qi, S., Dong, J., Xu, Z., Cheng, X., Zhang, W. & Qin, J. (2021). PROPTAC: an effective targeted protein degradation strategy for cancer therapy. *Frontiers in Pharmacology*, **12:** 692574.

Radhakrishna, M., Grimaldi, J., Belfort, G. & Kumar, S. (2013). Stability of proteins inside a hydrophobic cavity. *Langmuir: the ACS Journal of Surfaces and Colloids*, **29**(28): 8922–8928.

Rajan, R. & Pandit, A. (2001). Correlations to predict droplet size in ultrasonic atomisation. *Ultrasonics*, **39**(4): 235–255.

Ramisetty, K., Pandit, A. & Gogate, P. (2013). Investigations into ultrasound induced atomization. *Ultrasonics Sonochemistry*, **20**(1): 254-264.

Ravichandran, K., Palaniraj, R., Saw, N., Gabr, A., Ahmed, A., Knorr, D. & Smetanska, I. (2014). Effects of different encapsulation agents and drying process on stability of betalains extract. *Journal of Food Science and Technology*, **51**(9): 2216–2221.

Rentería-Ortega, M., Colín-Alvarez, M., Gaona-Sánchez, V., Chalapud, M., García-Hernández, A., León-Espinosa, E., Valdespino-León, M., Serrano-Villa, F. & Calderón-Domínguez, G. (2023). characterization and applications of the pectin extracted from the peel of *passiflora tripartita* var. *mollissima*. *Membranes*, **13**(9): 797.

Ribeiro, L., Alcântara, A., Darder, M., Aranda, P., Araújo-Moreira, F. & Ruiz-Hitzky, E. (2014). Pectin-coated chitosan-LDH bionanocomposite beads as potential systems for colon-targeted drug delivery. *International Jjournal of Pharmaceutics*, **463**(1): 1–9.

Ribeiro, S., Almeida, R., Batista, L., Lima, J., Sarinho, A., Nascimento, A. & Lisboa, H. (2024). Investigation of guar gum and xanthan gum influence on essential thyme oil emulsion properties and encapsulation release using modeling tools. *Foods (Basel, Switzerland)*, **13**(6): 816.

Rodriguez, L., Passerini, N., Cavallari, C., Cini, M., Sancin, P. & Fini, A. (1999). Description and preliminary evaluation of a new ultrasonic atomizer for spray-congealing processes. *International Journal of Pharmaceutics*, **183**(2): 133–143.

Ruano, P., Lazo Delgado, L., Picco, S., Palacios, J., Schieda, J., Flores, P. & Mingrone, L. (2020). Extraction and characterization of pectins from peels of Criolla oranges (Citrus sinensis): Experimental reviews. In M. Masuelli (Ed.), Pectins - Extraction, purification, characterization and applications. IntechOpen. https://doi.org/10.5772/intechopen.88944

Rubinstein, A., Radai, R., Ezra, M., Pathak, S. & Rokem, J. (1993). In vitro evaluation of calcium pectinate: a potential colon-specific drug delivery carrier. *Pharmaceutical Research*, **10**(2): 258–263.

Rubinstein, A., Tirosh, B., Baluom, M., Nassar, T., David, A., Radai, R., Gliko-Kabir, I. & Friedman, A. (1997). The rationale for peptide drug delivery to the colon and the potential of polymeric carriers as effective tools. *Journal of Controlled Release*, **46**(1–2): 59-73.

Rutherford, K. & McManus, K. (2024). PROTACs: current and future potential as a precision medicine strategy to combat cancer. *Molecular Cancer Therapeutics*, **23**(4): 454–463.

Said, N., Olawuyi, I. & Lee, W. (2023). Pectin hydrogels: gel-forming behaviors, mechanisms, and food applications. *Gels,* **9**(9): 732.

Salum, P., Berktas, S., Bas, D., Cam, M. & Erbay, Z. (2023). Optimization of spray drying conditions for improved physical properties in the production of enzyme-modified cheese powder. *Journal of Food Science*, **88**: 244–258.

Sarabandi, K., Peighambardoust, S., Sadeghi Mahoonak, A. & Samaei, S. (2018). Effect of different carriers on microstructure and physical characteristics of spray dried apple juice concentrate. *Journal of Food Science and Technology*, **55**(8): 3098–3109.

Saraswat, A., Patki, M., Fu, Y., Barot, S., Dukhande, V. & Patel, K. (2020). Nanoformulation of proteolysis targeting chimera targeting 'undruggable' *c-Myc* for the treatment of pancreatic cancer. *Nanomedicine*, **15**(18): 1761–1777.

Saraswat, A., Vemana, H., Dukhande, V. & Patel, K. (2022). Galactose-decorated liver tumor-specific nanoliposomes incorporating selective BRD4-targeted PROTAC for hepatocellular carcinoma therapy. *Heliyon*, **8**(1): e08702.

Saraswat, A., Vemana, H., Dukhande, V. & Patel, K. (2024). Novel gene therapy for drug-resistant melanoma: Synergistic combination of PTEN plasmid and BRD4 PROTAC-loaded lipid nanocarriers. *Molecular Therapy. Nucleic Acids*: **35**(3):102292.

Scheubel, E., Lindenberg, M., Beyssac, E. & Cardot, J. (2010). Small volume dissolution testing as a powerful method during pharmaceutical development. *Pharmaceutics*, **2**(4): 351–363.

Schittny, A., Huwyler, J. & Puchkov, M. (2020). Mechanisms of increased bioavailability through amorphous solid dispersions: a review. *Drug Delivery*, **27**(1): 110-127.

Seeli, D. & Prabaharan, M. (2016). Guar gum succinate as a carrier for colon-specific drug delivery. *International Journal of Biological Macromolecules*, **84**: 10–15.

Shah, N., Sharma, O., Mehta, T. Amin, A. (2016). Design of experiment approach for formulating multi-unit colon-targeted drug delivery system: in vitro and in vivo studies. *Drug Development and Industrial Pharmacy,* **42**(5): 825-835.

Sharma, G., Sharma, S., Kumar, A., Al-Muhtaseb, A., Naushad, M., Ghfar, A., Mola, G. & Stadler, F. (2018). Guar gum and its composites as potential materials for diverse applications: A review. *Carbohydrate Polymers*, **199**: 534–545.

Shyale, S., Chowdary, K., Krishnaiah, Y. & Bhat, N. (2006). Pharmacokinetic evaluation and studies on the clinical efficacy of guar gum-–based oral drug delivery systems of albendazole and albendazole-β-cyclodextrin for colon-targeting in human volunteers. *Drug Development Research*, **67**: 154-165.

Shen, X., Yu, D., Zhu, L., Branford-White, C., White, K. & Chatterton, N. (2011). Electrospun diclofenac sodium loaded Eudragit® L 100-55 nanofibers for colon-targeted drug delivery. *International Journal of Pharmaceutics*, **408**: 200-207.

Shepard, K., Adam, M., Morgen,M., Mudie, D., Regan, D., Baumann, J. & Vodak, D. (2020) Impact of process parameters on particle morphology and filament formation in spray dried Eudragit L100 polymer*. Powder Technology*, **362**: 221-230

Shepard, T. (2011). *Bubble size effect on effervescent atomization*. PhD thesis. University of Minnesota: USA.

Siles-Sánchez, M., García-Ponsoda, P., Fernandez-Jalao, I., Jaime, L. & Santoyo, S. (2024). Development of pectin particles as a colon-targeted marjoram phenolic compound delivery system. *Foods*, **13**(2): 188.

Silva, I., Gurruchaga, M. & Goñi, I. (2009). Physical blends of starch graft copolymers as matrices for colon targeting drug delivery systems. *Carbohydrate Polymers*, **76**(4): 593-601.

Sincere, N., Anand, K., Ashique, S., Yang, J. & You, C. (2023). PROTACs: Emerging targeted protein degradation approaches for advanced druggable strategies. *Molecules,* **28**(10): 4014.

Singh, A. & Van den Mooter, G. (2016). Spray drying formulation of amorphous solid dispersions. *Advanced Drug Delivery Reviews*, **100**: 27–50.

Sinha, R. & Kumria, R. (2001). Polysaccharides in colon-specific drug delivery. *International Journal of Pharmaceutics,* **224**: 19-38.

Slegers, S., Linzas, M., Drijkoningen, J., D'Haen, J., Reddy, N. & Deferme, W. (2017). Surface Roughness Reduction of Additive Manufactured Products by Applying a Functional Coating Using Ultrasonic Spray Coating. *Coatings*, **7**(12): 208.

Sobierajski, T., Małolepsza, J., Pichlak, M., Gendaszewska-Darmach, E. & Błażewska, K. M. (2024). The impact of E3 ligase choice on PROTAC effectiveness in protein kinase degradation. *Drug Discovery Today*, **29**(7): 104032.

Solomos, M., Punia, A., Saboo, S., John, C., Boyce, C., Chin, A., Taggart, R., Smith, D., Lamm, M. & Schenck, L. (2023). Evaluating spray drying and co-precipitation as manufacturing

processes for amorphous solid dispersions of a low Tg API. *Journal of Pharmaceutical Sciences*, **12**(8): 2087-2096.

Šoltys, M., Kovačík, P., Dammer, O., Beránek, J. & Štěpánek, F. (2019). Effect of solvent selection on drug loading and amorphisation in mesoporous silica particles. *International Journal of Pharmaceutics*, **555**: 19-27.

Song, Y.-L., Cheng, C.-H., Reddy, M. & Islam, M. (2021). Simulation of onset of the capillary surface wave in the ultrasonic atomizer. *Micromachines*, **12**(10): 1146.

Sriamornsak, P. & Nunthanid, J. (1998). Calcium pectinate gel beads for controlled release drug delivery: I. Preparation and in vitro release studies. *International Journal of Pharmaceutics*, **160**(2): 207-212.

Sukri, N., Hashib, S., Rahman, N., Hasfalina, C. & Abdulsalam, M. (2018). Effect of maltodextrin concentration and slurry temperature on pineapple powder using ultrasonic spray dryer. *Food Research*, **2**(6): 582 – 586.

Sun, X., Gao, H., Yang, Y., He, M., Wu, Y., Song, Y., Tong, Y. & Rao, Y. (2019). PROTACs: great opportunities for academia and industry. *Signal Transduction and Targeted Therapy*, **4**: 64.

Sawarkar, S., Deshpande, S., Bajaj, A. & Nikam, V. (2015). In Vivo evaluation of 5-ASA colon-specific tablets using experimental-induced colitis rat animal model. *AAPS PharmSciTech*, **16**(6): 1445–1454.

Talebi, F., Haydari, Z., Salehi, H., Mehrabi, M., Gardy, J., Bradley, M., Bayly, A. & Hassanpour, A. (2024). Spreadability of powders for additive manufacturing: A critical review of metrics and characterisation methods, *Particuology*, **93**: 211-234.

Tan, S., Jiang, T., Ebrahimi, A. & Langrish, T. (2018). Effect of spray-drying temperature on the formation of flower-like lactose for griseofulvin loading. *European Journal of Pharmaceutical Sciences*, **111**: 534-539.

Tang, R., Wang, Z., Xiang, S., Wang, L., Yu, Y., Wang, Q., Deng, Q., Hou, T. & Sun, H. (2023). Uncovering the kinetic characteristics and degradation preference of protac systems with advanced theoretical analyses. *Journal of the American Chemical Society,* **3**(6): 1775–1789.

Tay, J., Chua, X., Ang, C., Subramanian, G., Tan, S., Lin, E., Wu, W., Goh, K. & Lim, K. (2021). Effects of spray-drying inlet temperature on the production of high-quality native rice starch. *Processes,* **9**: 1557.

Telang, A. & Thorat, B. (2010). Optimization of process parameters for spray drying of fermented soy milk. *Drying Technology*, **28**(12): 1445-1456.

Thananukul, K., Kaewsaneha, C., Opaprakasit, P., Lebaz, N., Errachid, A. & Elaissari, A. (2021). Smart gating porous particles as new carriers for drug delivery. *Advanced Drug Delivery Review*s, **174**: 425-446.

Tian, B., Liu, S., Wu, S., Lu, W., Wang, D., Jin, L., Hu, B., Li, K., Wang, Z. & Quan, Z. (2017). pH-responsive poly (acrylic acid)-gated mesoporous silica and its application in oral colon targeted drug delivery for doxorubicin. *Colloids and Surfaces B: Biointerfaces,* **154**: 287-296.

Tontul, I. & Topuz, A. (2017). Spray-drying of fruit and vegetable juices: Effect of drying conditions on the product yield and physical properties. *Trends in Food Science & Technology*, **63**: 91-102.

Tripathi, J., Ambolikar, R., Gupta, S., Jain, D., Bahadur, J. & Variyar, P. (2019). Methylation of guar gum for improving mechanical and barrier properties of biodegradable packaging films. *Scientific Reports*, **9**(1): 14505.

Tripathi, J., Ambolikar, R., Gupta, S. (2022) .Methylated radiation depolymerized Guar gum- a novel wall material for flavour encapsulation. *Food Chemistry Advances*,**1**: 100102.

Troup, R., Fallan, C. & Baud, M. (2020). Current strategies for the design of PROTAC linkers: a critical review. *Exploration of Targeted Anti-tumor Therapy*, **1**(5): 273–312.

Tsapis, N., Dufresne, E., Sinha, S., Riera, C., Hutchinson, J., Mahadevan, L. & Weitz, D. (2005). Onset of buckling in drying droplets of colloidal suspensions. *Physical Review Letters*, **94**(1): 018302.

Turan, F., Cengiz, A. & Kahyaoglu, T. (2015). Evaluation of ultrasonic nozzle with spray-drying as a novel method for the microencapsulation of blueberry's bioactive compounds. *Innovative Food Science & Emerging Technologies*, **32**: 136-145.

Turan, F., Cengiz, A., Sandıkçı, D., Dervisoglu, M. & Kahyaoglu, T. (2016). Influence of an ultrasonic nozzle in spray-drying and storage on the properties of blueberry powder and microcapsules. *Journal of the Science of Food and Agriculture*, **96**: 4062-4076.

Turan, F., & Kahyaoglu, T. (2020). The effect of ultrasonic spray nozzle on carbohydrate and protein based coating materials for blueberry extract microencapsulation. *Journal of the Science of Food and Agriculture*, **101**(1):120-130.

Turkoglu, M. & Ugurlu, T. (2002). In vitro evaluation of pectin-HPMC compression coated 5-aminosalicylic acid tablets for colonic delivery. *European Journal of Pharmaceutics and Biopharmaceutics,* **53**(1): 65–73.

Ukmar, T., Godec, A., Planinšek, O., Kaučič, V., Mali, G. & Gaberšček, M. (2011). The phase (trans)formation and physical state of a model drug in mesoscopic confinement. *Physical Chemistry Chemical Physics : Pccp*, **13**(35): 16046–16054.

Ultrasonic Controller Operating Manual. (2014). *Ultrasonic controller* BÜCHI. Accessed on 23 January 2022. https://www.anamed.com.tr/UserFiles/Documents/Ultrasonic_Controller_OM_en_B_LR_0.pdf

United States Pharmacopoeia (USP). (2024). United States Pharmacopoeia Convention, Inc., Rockville, MD.

Vaidya, A., Jain, A., Khare, P., Agrawal, R. & Jain, S. (2009). Metronidazole loaded pectin microspheres for colon targeting. *Journal of Pharmaceutical Sciences*, **98**(11): 4229–4236.

Varum, F., Freire, A., Fadda, H., Bravo, R. & Basit, A. (2020)**.** A dual pH and microbiota-triggered coating (Phloral™) for fail-safe colonic drug release. *International Journal of Pharmaceutics*, **583**.

Vass, P., Démuth, B., Hirsch, E., Nagy, B., Andersen, S., Vigh, T., Verreck, G., Csontos, I., Nagy, Z. & Marosi, G. (2019). Drying technology strategies for colon-targeted oral delivery of biopharmaceuticals. *Journal of Controlled Release,* **296**: 162-178.

Vehring, R., Foss, W. & Lechuga-Ballesteros, D. (2007). Particle formation in spray drying, *Journal of Aerosol Science*, **38**(7): 728-746.

Vemula, S. & Veerareddy, P. (2012). Development, evaluation and pharmacokinetics of time-dependent ketorolac tromethamine tablets. *Expert Opinion on Drug Delivery*, **10**(1): 33-45.

Vemula, S. & Bontha, V. (2013). Colon targeted guar gum compression coated tablets of flurbiprofen: formulation, development, and pharmacokinetics. *BioMed Research International*, 287919.

Vemula, S. (2015). Formulation and pharmacokinetics of colon-specific double-compression coated mini-tablets: Chronopharmaceutical delivery of ketorolac tromethamine. *International Journal of Pharmaceutics*, **491**: 35-41.

Wakerly, Z., Fell, J., Attwood, D. & Parkins, D. (1996). Pectin/ethylcellulose film coating formulations for colonic drug delivery. *Pharmaceutical Research*, **13**(8): 1210–1212.

Wakerly, Z., Fell, J., Attwood, D. & Parkins, D. (1997). Studies on drug release from pectin/ethylcellulose film-coated tablets: A potential colonic delivery system. *International Journal of Pharmaceutics*, **153**(2): 219-224.

Wang, B. & Armenante, P. (2016). Experimental and computational determination of the hydrodynamics of mini vessel dissolution testing systems. *International Journal of Pharmaceutics*, **510**(1): 336–349.

Wang, B., Bredael, G. & Armenante, P. (2018). Computational hydrodynamic comparison of a mini vessel and a USP 2 dissolution testing system to predict the dynamic operating conditions for similarity of dissolution performance. *International Journal of Pharmaceutics*, **539(**1-2): 112–130.

Wang, B., Liu, F., Xiang, J., He, Y., Zhang, Z., Cheng, Z., Liu, W. & Tan, S. (2021). A critical review of spray-dried amorphous pharmaceuticals: Synthesis, analysis and application. *International Journal of Pharmaceutics*, **594:** 120165.

Wang, S., Meng, Y., Li, J., Liu, J., Liu, Z. & Li, D. (2020). A novel and simple oral colon-specific drug delivery system based on the pectin/modified nano-carbon sphere nanocomposite gel films. *International Journal of Biological Macromolecules*, **157**: 170-176.

Wang, X., Chen, Q. & Lü, X. (2014). Pectin extracted from apple pomace and citrus peel by subcritical water. *Food Hydrocolloids*, **38**: 129-137.

Wang, X., Su, L., Niu, C., Li, X., Wang, R., Li, B., Liu, S. & Xu, Y. (2024). Targeted degradation of KRAS protein in non-small cell lung cancer: Therapeutic strategies using liposomal PROTACs with enhanced cellular uptake and pharmacokinetic profiles. *Drug Development Research*, **85**(5): e22241.

Wang, Y., Lan, L., Wang, M., Zhang, J., Gao, Y., Shi, L. & Sun, L. (2023). PROTACS: A technology with a gold rush-like atmosphere. *European Journal of Medicinal Chemistry*, **247**: 115037.

Wei, H., Qing, D., De-Ying, C., Bai, X. & Fanli-Fang (2007). Pectin/Ethylcellulose as film coatings for colon-specific drug delivery: preparation and in vitro evaluation using 5-fluorouracil pellets. *PDA Journal of Pharmaceutical Science and Technology*, **61**(2): 121–130.

Wen, Y., Gallego, M., Nielsen, L., Jorgensen, L., Everland, H., Møller, E. & Nielsen, H. (2011). Biodegradable nanocomposite microparticles as drug delivering injectable cell scaffolds, *Journal of Controlled Release*, **156**(1): 11-20.

Weng, Y., Li, Y., Chen, X., Song, H. & Zhao, C. X. (2024). Encapsulation of enzymes in food industry using spray drying: recent advances and process scale-ups. *Critical Reviews in Food Science and Nutrition*, **64**(22): 7941–7958.

Wong, D., Larrabee, S., Clifford, K., Tremblay, J. & Friend, D. (1997) USP dissolution apparatus iii (reciprocating cylinder) for screening of guar-based colonic delivery formulations. *Journal of Controlled Release*, **47**(2): 173-179.

Wu, C., Bi, C., Kim, G., Yang, Z., Li, S., Dai, T., Wu, X., Tan, J., He, N. & Li, S. (2025). Oral colon-targeted responsive chitosan/pectin-based nanoparticles propels the application of tofacitinib in colitis therapy. *Scientific Reports, **15.***

Würfel, H. & Heinze, T. (2025). Acidic dimethyl sulfoxide: A solvent system for the fast dissolution of pectin derivatives suitable for subsequent modification. *Carbohydrate Polymers,* **348**(Pt B): 122872.

Xie, H. & Zhang, C. (2024). Potential of the nanoplatform and PROTAC interface to achieve targeted protein degradation through the Ubiquitin-Proteasome system. *European Journal of Medicinal Chemistry*, **267**: 116168.

Xu, M., Yun, Y., Li, C., Ruan, Y., Muraoka, O., Xie, W. & Sun, X. (2024). Radiation responsive PROTAC nanoparticles for tumor-specific proteolysis enhanced radiotherapy. *Journal of Materials Chemistry. B*, **12**(13): 3240–3248.

Yan, S., Zhang, G., Luo, W., Xu, M., Peng, R., Du, Z., Liu, Y., Bai, Z., Xiao, X. & Qin, S. (2024). PROTAC technology: From drug development to probe technology for target deconvolution. *European Journal of Medicinal Chemistry*, **276**: 16725.

Yang, W., Saboo, S., Zhou, L., Askin, S. & Bak, A. (2024). Early evaluation of opportunities in oral delivery of PROTACs to overcome their molecular challenges. *Drug Discovery Today*, **29**(2): 103865.

Yellela, S., S, S. & YV, R.(2009). Guar gum-based colon-specific drug delivery systems for the treatment of inflammatory bowel diseases. *Inflammatory Bowel Diseases*, **15**(suppl_2): S56.

Yeo, Y. & Park, K. (2004). A new microencapsulation method using an ultrasonic atomizer based on interfacial solvent exchange. *Journal of Controlled Release: Official Journal of the Controlled Release Society*, **100**(3): 379–388.

Yiming, M. & Allan, C. (2014). Designing colon-specific delivery systems for anticancer drug-loaded nanoparticles: an evaluation of alginate carriers. *Journal of Biomedical Materials Research,* **102**(9): 3167-3176.

Yin, M., Yuan, K., Lv, Z., Yuan, Y., Feng, X. & Wu, Q. (2024). Novel lanthanum-based fluorescent drug-loaded microspheres for tracing and inhibition of the hepg2 cells line. *Journal of Macromolecular Science, Part B*, **63**(11): 1203–1214.

Zafar, S., Sayed, E., Rana, S., Rasekh, M., Onaiwu, E., Nazari, K., Kucuk, I., Fatouros, D., Arshad, M. & Ahmad, Z. (2024). Particulate atomisation design methods for the development and engineering of advanced drug delivery systems: A review. *International Journal of Pharmaceutics*, **666**: 124771.

Zengerle, M., Chan, K. & Ciulli, A. (2015). Selective small molecule induced degradation of the bet bromodomain protein BRD4. *ACS Chemical Biology*, **10**(8): 1770–1777.

Zhang, H., Li, M., Li, J., Agrawal, A., Hui, H. & Liu, D. (2022a). Superiority of mesoporous silica-based amorphous formulations over spray-dried solid dispersions *Pharmaceutics*, **14**(2): 428.

Zhang, H., Fan, Z., Peng, D., Huang, C., Wu, X. & Sun, F. (2024). Tuning the hydrophobic performance and thermal stability of pectin film by acetic anhydride esterification. International Journal of Biological Macromolecules, **276**(Pt 1): 133746.

Zhang, H., Wu, H., Wang, L., Gao, Y., Galarza, L., Zhao, Y., Wang, Z., Gao, L. & Han, J. (2025a). Preparation and characterization of ASDs improves the solubility and dissolution performance of a PROTAC drug. *Journal of Drug Delivery Science and Technology*, 106837.

Zhang, T., & Youan, B. B. (2010). Analysis of process parameters affecting spray-dried oily core nanocapsules using factorial design. *AAPS PharmSciTech*, **11**(3): 1422–1431.

Zhang, W., Jin, Y., Wang, J., Gu, M., Wang, Y., Zhang, X., Zhang, Y., Yu, W., Liu, Y., Yuan, W. & Su, J. (2025b). Co-delivery of PROTAC and siRNA via novel liposomes for the treatment of malignant tumors. *Journal of Colloid and Interface Science*, **678**(Pt A): 896–907.

Zhang, X., Guo, X., Zhuo, R., Tao, Y., Liang, W., Yang, R., Chen, Y., Cao, H., Jia, S., Yu, J., Liao, X., Li, X., Fang, F., Li, G., Wu, D., Xu, Y., Li, Z., Pan, J. & Wang, J. (2022b). BRD4 inhibitor MZ1 exerts anti-cancer effects by targeting MYCN and MAPK signaling in neuroblastoma. *Biochemical and Biophysical Research Communications*, **604**: 63–69.

Zhou, M., Shen, L., Lin, X., Hong, Y. & Feng, Y. (2017) Design and pharmaceutical applications of porous particles. *RCS Advances*, **7**(63): 29490-39501.

Zhou, Q., Wu, W., Jia, K., Qi, G., Sun, X. & Li, P. (2022). Design and characterization of PROTAC degraders specific to protein N-terminal methyltransferase 1. *European Journal of Medicinal Chemistry*, **244**: 114830.

Zhou, X., Zhang, S., Huebner, W., Ownby, P. & Gu, H. (2001). Effect of the solvent on the particle morphology of spray dried PMMA. *Journal of Materials Science*, **36**: 3759-3768.

Zhu, J., Zhong, L., Chen, W., Song, Y., Qian, Z., Cao, X., Huang, Q., Zhang, B., Chen, H. & Chen, W (2019). Preparation and characterization of pectin/chitosan beads containing porous starch embedded with doxorubicin hydrochloride: A novel and simple colon targeted drug delivery system. *Food Hydrocolloids*, **95**: 562-570.

Appendices

Appendix A. *[redacted]*

***Figure A.1**. [redacted]*

Appendix B. *In Vitro* Dissolution of Felodipine-loaded MESOPAC as a Control Sample

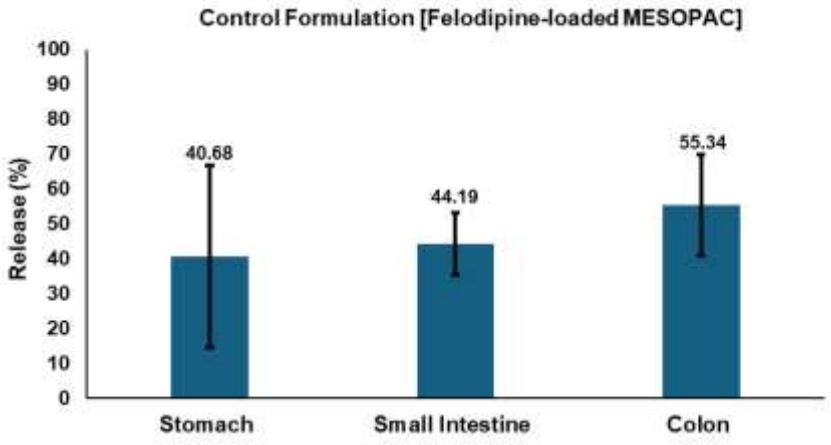

Figure B.1. *Release percentages of felodipine from MESOPAC without guar gum in media simulating the different segments of the GIT: 0.1N HCL + 1% (w/v) SLS to represent the gastric environment, phosphate buffer pH 6.5 + 1% (w/v) SLS to represent the small intestine, and phosphate buffer pH 7.4 + 1% (w/v) SLS to represent enzyme-free colonic conditions [Test conditions: 150 rpm in small-volume dissolution apparatus; separate capsule for each phase]*

Appendix C. *In Vitro* Dissolution of MZ1-loaded MESOPAC as a Control Sample

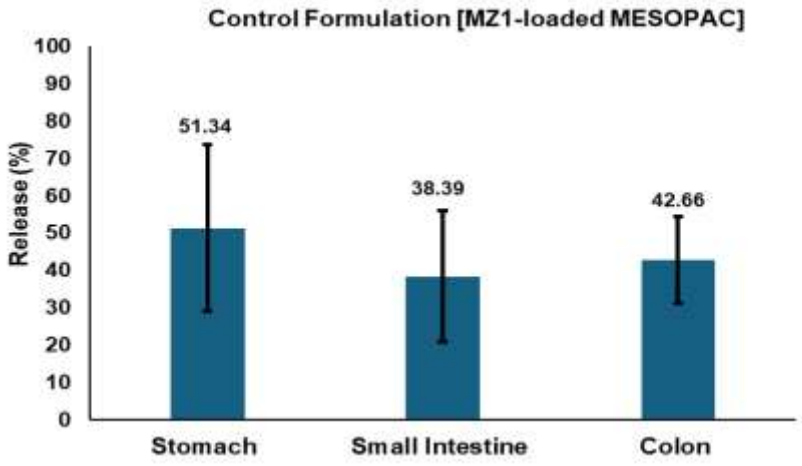

Figure C.1. *Release percentages of MZ1 from MESOPAC without guar gum in media simulating the different segments of the GIT: 0.1N HCL + 1% (w/v) SLS to represent the gastric environment, phosphate buffer pH 6.5 + 1% (w/v) SLS to represent the small intestine, and phosphate buffer pH 7.4 + 1% (w/v) SLS to represent enzyme-free colonic conditions [Test conditions: 150 rpm in small-volume dissolution apparatus; separate capsule for each phase]*